

BJR

Breast
Imaging

Research papers from *BJR*



MAMMOMAT Revelation

InSpect integrated specimen scanner for faster biopsies



InSpect technology works to improve biopsy workflows, shortening compression time whilst allowing samples to be checked directly at the system.

- Additional specimen X-ray system is not needed saving you space and money
- Get your specimens imaged in less than 20 seconds
- Stay with your patient during the entire examination

Available for Stereotactic Biopsy and 50° Wide-Angle Breast Biopsy on the MAMMOMAT Revelation.



50° Wide-Angle Biopsy

Target accuracy of ± 1 mm based on 50° wide-angle tomosynthesis

One-Click Targeting

Automatic movement to defined target



For further information contact
joanne.barry@siemens-healthineers.com

siemens-healthineers.co.uk/revelation

Contents

Advertorial

Mammography in snapshots: then and now
Siemens Healthineers

Commentaries

How we provided appropriate breast imaging practices in the epicentre of the COVID-19 outbreak in Italy

F Pesapane, S Penco, A Rotili, L Nicosia, A Bozzini, C Trentin, V Dominelli, F Priolo, M Farina, I Marinucci, S Meroni, F Abbate, L Meneghetti, A Latronico, M Pizzamiglio and E Cassano

<https://doi.org/10.1259/bjr.20200679>

Breast cancer screening in average-risk women: towards personalized screening

A G V Bitencourt, C Rossi Saccarelli, C Kuhl and E A Morris

<https://doi.org/10.1259/bjr.20190660>

Review

Microcalcification on mammography: approaches to interpretation and biopsy

L Wilkinson, V Thomas and N Sharma

<https://doi.org/10.1259/bjr.20160594>

Full Papers

Evaluation of a new image reconstruction method for digital breast tomosynthesis: effects on the visibility of breast lesions and breast density

J Krammer, S Zolotarev, I Hillman, K Karalis, D Stsepankou, V Vengrinovich, J Hesser and T M Svahn

<https://doi.org/10.1259/bjr.20190345>

Compression forces used in the Norwegian Breast Cancer Screening Program

G G Waade, N Moshina, S Sebuødegård, P Hogg and S Hofvind

<https://doi.org/10.1259/bjr.20160770>

Added value of contrast-enhanced mammography in assessment of breast asymmetries

R Wessam, M M M Gomaa, M A Fouad, S M Mokhtar and Y M Tohamey

<https://doi.org/10.1259/bjr.20180245>

Conspicuity of suspicious breast lesions on contrast enhanced breast CT compared to digital breast tomosynthesis and mammography

S Aminololama-Shakeri, C K. Abbey, J E López, A M Hernandez, P Gazi, J M Boone and K K Lindfors

<https://doi.org/10.1259/bjr.20181034>

Detection of noncalcified breast cancer in patients with extremely dense breasts using digital breast tomosynthesis compared with full-field digital mammography

A Yi, J M Chang, S U Shin, A J Chu, N Cho, D-Y Noh and W K Moon

<https://doi.org/10.1259/bjr.20180101>

Diagnostic value of halo sign in young women (aged 45 to 49 years) in a breast screening programme with synthesized 2D mammography

M P Sánchez-Camacho González-Carrato, C Romero Castellano, P M Aguilar Angulo, L M Cruz Hernández, M Sánchez Casado, J Ruiz Martín, I Fraile Alonso, J M Pinto Varela, V Martínez-Vizcaíno

<https://doi.org/10.1259/bjr.20180444>

Quantitative analysis of enhanced malignant and benign lesions on contrast-enhanced spectral mammography

C-Y Deng, Y-H Juan, Y-C Cheung, Y-C Lin, Y-F Lo, G G Lin, S-C Chen and S-H Ng

<https://doi.org/10.1259/bjr.20170605>

Radiation risk of breast screening in England with digital mammography

L M Warren, D R Dance and K C Young

<https://doi.org/10.1259/bjr.20150897>

BJR

BJR is the international research journal of the British Institute of Radiology and is the oldest scientific journal in the field of radiology and related sciences.

An international, multi-disciplinary journal, *BJR* covers the clinical and technical aspects of medical imaging, radiotherapy, oncology, medical physics, radiobiology and the underpinning sciences. *BJR* is essential reading for radiologists, medical physicists, radiation oncologists, radiotherapists, radiographers and radiobiologists.

At Siemens Healthineers, our mission is to enable healthcare providers to increase value by empowering them on their journey towards expanding precision medicine, transforming care delivery, and improving patient experience, all enabled by digitalising healthcare.

An estimated five million patients worldwide everyday benefit from our innovative technologies and services in the areas of diagnostic and therapeutic imaging, laboratory diagnostics and molecular medicine as well as digital health and enterprise services.

We're a leading medical technology company with over 120 years of experience and 18,500 patents globally. With over 50,000 employees in more than 70 countries, we'll continue to innovate and shape the future of healthcare.

For more information and latest product line, please visit www.siemens-healthineers.co.uk

Mammography in snapshots: then and now

One-in-seven UK women will be diagnosed with breast cancer during their lifetime. Screening for breast cancer and catching the disease early, is crucial¹.

Siemens first introduced equipment which could be used to image the breast in 1957 to aid in the diagnosis of breast cancer, and the National Breast Screening Programme began in 1988. Although the technology behind breast cancer diagnosis and prevention has changed dramatically over time, some barriers to screening attendance still exist.

The Mammography Team at Siemens Healthineers GB&I, take a look back through the archives and comment on how evolutions in technology have impacted mammography, how society has adapted, and how cultural barriers have influenced uptake along the way...

THEN snapshot: not the 'done thing'

Stage in time: **1957**

Technology in use: **Analogue mammography**

Featured image: **Siemens Tridoros 4 X-ray generator with mammocones**

Life for women was very different in 1957 compared to today, with many choosing to prioritise their home and family life. According to research, during this time 13,398 men obtained degrees in comparison with just 3,939 women². The average age of a first-time mother was 25 in 1957, compared to 29 currently³. This illustrates how the UK has changed culturally over time.

"Mammography was in its early stages in 1957, and innovations like the Siemens Tridoros 4 X-ray generator with mammocones offered break-through technology. Breast cancer is talked about a lot more openly today than in the past, when treatment of breast cancer was more aggressive, and the number of women willing to address the issue of breast cancer risk was low. We've heard stories of women ignoring breast lumps, simply because talking or sharing, even with a partner, just wasn't the done thing."



NOW snapshot: seeking a more open dialogue

Stage in time: **2018**

Technology in use: **MAMMOMAT Revelation with HD Tomosynthesis**

Featured image: **The Real Full Monty: Ladies Night (Credit: ITV)**

Fast-forward to today and, although statistics show there is still work to be done (the UK lags behind the European target rate for 75% screening attendance), many women in the UK are now more comfortable talking about breast cancer.



Recent TV performances, such as the Real Full Monty: Ladies Night, which was aired by ITV in March 2018 to a massive 5.5m viewers, are helping to generate a more open dialogue. However, in some UK communities, there are still significant barriers to tackling breast cancer, with studies showing that Black and Minority Ethnic women (BME) have a particularly low uptake of the national breast screening programme, for example⁴.

“Culturally, the UK is a very different place now, but there is still work to be done to encourage some communities to engage with the issue of breast cancer. Outreach programmes are really important for both minority ethnic groups and also rural communities, where women may struggle to travel. Naturally, some women will want to bring a chaperone with them too, it is important to accommodate different requirements.”

THEN snapshot: submerged in a new method

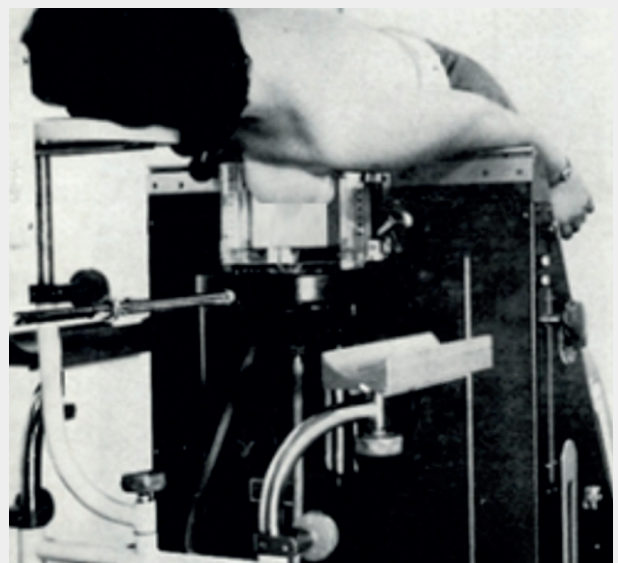
Stage in time: **1964**

Technology in use: **Isodense technique**

Featured image: **Fluidograph made by Siemens-Reiniger-Werke**

By the 1960s, examination methods to diagnose and prevent breast cancer had begun to develop and by 1964 the isodense technique was introduced. The new technique involved submerging the breast in alcohol, and the Siemens Fluidograph was one of the first to use this new method.

“Fluidography was an early attempt to even the breast thickness – something that is still a challenge to the present day. Comfort (or rather a concern about discomfort) is one of the key reasons why some women do not attend screening and so we are still constantly striving to improve this situation.”



NOW snapshot: reinventing the experience

Stage in time: **2018**

Technology in use: **MAMMOMAT Revelation with HD Tomosynthesis**

Featured image: **MAMMOMAT Revelation with HD Tomosynthesis**



“For a long time, mammography has not been considered a pleasant experience for some women – and looking at some of the old images it is easy to see why!

“Technology has evolved dramatically over the years, and continues to do so, meaning that the process has now completely changed. The experience varies for everyone and while a mammogram will perhaps never be completely comfortable, the latest innovations are quicker, more accurate, and are designed with the patient in mind.”

The MAMMOMAT Revelation with HD Tomosynthesis has the very latest technology in breast imaging and has been designed to make mammography a less daunting experience for patients. The system has features such as soft compression paddles and is able to complete a highly accurate image within a few minutes, meaning a mammogram can be performed quicker than ever before.

THEN snapshot: screening at a lower dose

Stage in time: **1988**

Technology in use: **Analogue mammography with reduced radiation**

Featured image: **MAMMOMAT 2**

From the 1980s onwards, mammography started to become more patient-centric. There was an emphasis on making the process quicker for the patient, and new developments also started to acquire the images using a lower dose of radiation, meaning a reduction in risk to patients.

“Innovation had started to accelerate, and the equipment began to look more familiar to the systems used today. With the patient in mind, lower dose levels made mammography a safer form of examination, the design and features of the machines had also started to incorporate ways of making the overall experience more agreeable.”



NOW snapshot: so much to do and so little time

Stage in time: 2020

Technology in use: **MAMMOMAT Revelation with 50° Wide-Angle Tomosynthesis**
Featured image: **InHealth visit the Mobile Digital Mammography Unit during its tour of the UK and Ireland**

Women today lead busy and demanding lives. In 2017 more women achieved university places than men⁵, and in 2016, an estimated 163 million women were starting or running new businesses in 74 economies around the world⁶. For those working in London, they spend an average 72.8 minutes a day just to get to work⁷.

“With so much to do in so little time, it’s important that healthcare slots into women’s busy schedules without too much inconvenience caused. Getting women to attend screening is the key; from there we can provide the latest technology to catch cancer early.

“Being aware of the pressures women in today’s society are under is vital and finding new ways to engage with a wider group of women remains important. Installing mobile units in helpful locations like supermarket car parks, is just one way of ensuring that screening is made as accessible as possible”.



The constant challenge in the evolution of mammography technology, is adapting to change

As we have seen, women’s expectations and lifestyles have altered a lot since the 1950s, and they have also changed significantly since breast cancer screening was first introduced 30 years ago.

Screening currently diagnoses about 10,000 cases of breast cancer annually, and since 1988 has saved many lives by early detection of breast cancer.

Crucial to its success is continued innovation. No matter what cultural background women may have, or where in the country they may live, mammography within the NHS strives to accommodate differences in lifestyle requirements and perspectives. Advancing technology is the tool that has provided us with the ability to expand precision medicine, transform care delivery and improve the patient experience.

For more information on the Siemens Healthineers MAMMOMAT Revelation with 50° Wide-Angle Tomosynthesis see **www.siemens-healthineers.co.uk/revelation**

¹<http://www.cancerresearchuk.org/health-professional/cancer-statistics/statistics-by-cancer-type/breast-cancer#heading-Zero>

²1950 statistics from: researchbriefings.files.parliament.uk/documents/SN04252/SN04252.pdf

³<https://www.ons.gov.uk/peoplepopulationandcommunity/birthsdeathsandmarriages/livebirths/datasets/birthsbyparentscharacteristics>

⁴<https://diversityhealthcare.imedpub.com/exploring-factors-contributing-to-low-uptake-of-the-nhs-breast-cancer-screening-program-meamong-black-african-women-in-the-UK.php?aid=19994>

⁵<https://www.independent.co.uk/news/education/education-news/record-numbers-of-women-gender-gap-men-going-on-to-university-applications-ucas-a-level-results-a7916266.html>

⁶<https://www.prowess.org.uk/facts>

⁷<http://www.dailymail.co.uk/news/article-232243/London-commute-Workers-spend-75-minutes-day-getting-work-worse-women.html>

Received:
04 June 2020

Revised:
11 August 2020

Accepted:
18 August 2020

© 2020 The Authors. Published by the British Institute of Radiology under the terms of the Creative Commons Attribution 4.0 Unported License <http://creativecommons.org/licenses/by/4.0/>, which permits unrestricted use, distribution and reproduction in any medium, provided the original author and source are credited.

Cite this article as:

Pesapane F, Penco S, Rotili A, Nicosia L, Bozzini A, Trentin C, et al. How we provided appropriate breast imaging practices in the epicentre of the COVID-19 outbreak in Italy. *Br J Radiol* 2020; **93**: 20200679.

COMMENTARY

How we provided appropriate breast imaging practices in the epicentre of the COVID-19 outbreak in Italy

FILIPPO PESAPANE, MD, SILVIA PENCO, MD, ANNA ROTILI, MD, LUCA NICOSIA, MD, ANNA BOZZINI, MD, CHIARA TRENTIN, MD, VALERIA DOMINELLI, MD, FRANCESCA PRIOLO, MD, MARIAGIORGIA FARINA, MD, IRENE MARINUCCI, MD, STEFANO MERONI, MD, FRANCESCA ABBATE, MD, LORENZA MENEGHETTI, MD, ANTUONO LATRONICO, MD, MARIA PIZZAMIGLIO, MD and ENRICO CASSANO, MD

Breast Imaging Division, IEO European Institute of Oncology IRCCS, Milan, Italy

Address correspondence to: Dr Filippo Pesapane
E-mail: filippo.pesapane@ieo.it

ABSTRACT

Italy has one of the highest COVID-19 clinical burdens in the world and Lombardy region accounts for more than half of the deaths of the country. Since COVID-19 is a novel disease, early impactful decisions are often based on experience of referral centres.

We report the re-organisation which our institute (IEO, European Institute of Oncology), a cancer referral centre in Lombardy, went through to make our breast-imaging division pandemic-proof. Using personal-protective-equipment and innovative protocols, we provided essential breast-imaging procedures during COVID-19 pandemic without compromising cancer outcomes.

The emergency management and infection-control-measures implemented in our division protected both the patients and the staff, making this experience useful for other radiology departments dealing with the pandemic.

INTRODUCTION

Since the severe acute respiratory syndrome coronavirus 2 (SARS-CoV-2) was first identified in Wuhan (Hubei Province, China) in December 2019,¹ it has spread globally resulting in the ongoing coronavirus pandemic. As of 3 June 2020, more than 6.38 million cases of patients with such novel coronavirus disease (COVID-19) had been reported in more than 188 countries and territories, resulting in more than 380,000 deaths and more than 2.73 million hospitalisation.² Until 3 June 2020, Italy had currently 39,893 active cases, one of the highest in the world.² Overall, at the time of writing, there have been 233,515 confirmed cases and 33,530 deaths (a rate of 555 deaths per million population).³ However, due to the limited number of tests performed, the real number of infected people in Italy, as in other countries, was estimated to be higher than the official count.⁴ Lombardy, an area of 23,844 square kilometres (9,206 sq. mi) with 10 million people, is the most populous, the richest and most productive region in the country and one of the top regions in Europe under the same criteria,⁵ and has 89,205 confirmed cases and 16,145 deaths of COVID-19, representing, as on 3 June 2020, the most hard-hit part in all Italy, and probably all over the world.⁶

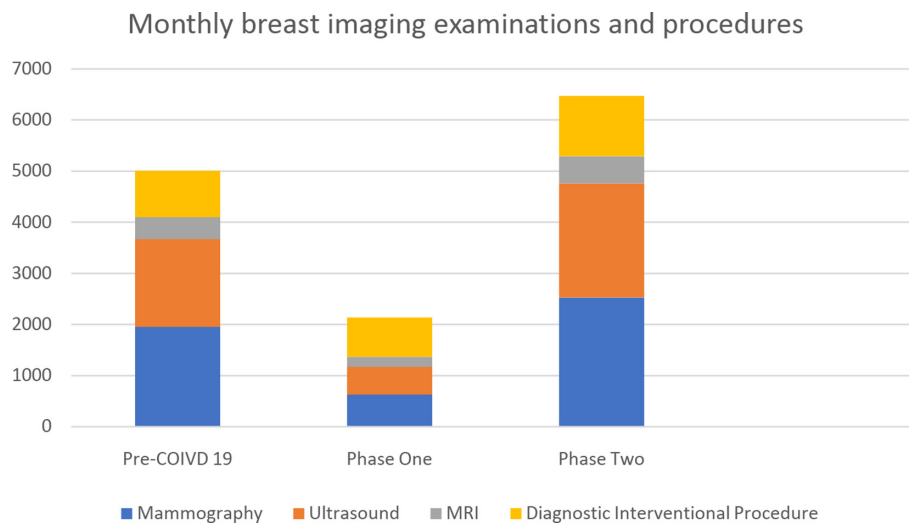
We discuss the re-organisation at an unprecedented scale of a breast-imaging division of our institute IEO, European Institute of Oncology), a cancer referral centre with high patient volume, located in Lombardy.

As the most common manifestation of COVID-19 is pneumonia,¹ radiology units have been directly involved from the beginning of this emergency providing lung imaging assessment. At the same time, diagnostic imaging facilities must maintain in all phases of such pandemic, the standard radiologic support for cancer patients, including patients who needed to execute regular follow-up.⁷ To guarantee the appropriate safety standard, dedicated procedures are required to protect both the staff members and patients. Therefore, a reconfiguration of radiology units with the application of strict infection control procedures is essential as well as the establishment of protocols to manage subjects with suspected COVID-19 infection.

DISCUSSION

Italy was the first European nation adopting strict lockdown measures with the so-called “Phase 1” starting on 8 March and which have been in force for 55 days. Italy entered the so-called “Phase 2” of the COVID-19 emergency on 4

Figure 1. Distribution of breast-imaging examinations and diagnostic interventional procedures by month in a period before COVID-19 and during Phase 1 and Phase 2 in our institute.



May 2020, with the start of the gradual lifting of the lockdown measures.⁸

With more than 65,000 breast imaging examinations and procedures provided in 2019, our breast-imaging division is one of the most important referral centre in Europe for breast cancer care.^{9,10} From the beginning of COVID-19 crisis, our goal was to continue to provide optimal care to breast cancer patients while reducing infective risk to patients and to staff.

During Phase 1, Lombardy's government made a differentiation between elective and non-deferrable examinations/procedures to optimize the available healthcare resources, defining which patients could be treated, namely only emergency and oncologic patients.¹¹ Accordingly, we stopped routine mammography and ultrasound screenings, as well as MRI examinations which were deferrable, but did not cancel appointments for patients with time-sensitive imaging needs. Specifically, we reported a decrease of 68% of both mammography and ultrasound (from 1950/month to 625/month and from 1720/month to 544/month, respectively) and of 52% of breast MRI (from 430/month to 195/month) (Figure 1).

Most of the interventional diagnostic procedures (such percutaneous ultrasound, stereotactic and MRI-guided biopsies) continued as normal in our centre, with a reported decrease of only 15% (from 910/month to 772/month) during Phase 1 (Figure 1).

Although deciding which patients deserve an examination is not always dependent on a list of predefined criteria, we are a team of 15 breast-dedicated radiologists and, in such extreme circumstances, we had to trust our expertise to select which patients to see, approaching this challenging task with diligence and vigilance. The main principle to decide whether to post-pone an off-patients' examination is to find the right balance between risks (namely, a delay of diagnosis and treatment) and advantages

(namely, to avoid being infected or to infect in-patients). Accordingly, our team of radiologists evaluated day-by-day the clinical history of all patients who had a booking in our unit: radiologists examined patient's medical records or, when there were not available, directly contacted patients by phone. Generally, we strongly suggested to patients with flu-like symptoms, even if mild, and with immunodeficiency disorders to delay their appointments. On the other hand, the parameters that were considered for not post-to maintaining the scheduled examination appointment, as COVID-19 had shown to be more lethal in the elderly, their familiarity for breast cancer, their current treatment (e.g. immunotherapy) and the long time elapsed since the last breast-imaging examination.

Accordingly, in Phase 1 of COVID-19 pandemic we have made no significant changes in our diagnostic procedure workflows although we re-organised our department workflow to limit the risk of transmission between patients, and between patients and staff.

Radiologists, technical radiologists and nurses were trained to consider all the patients as potentially COVID-19 positive regardless of their symptoms and they underwent training for proper donning/doffing of PPE, namely hair cap, goggles for eye protection, disposable long sleeve fluid-resistant gown, disposable gloves, with coverage over gown cuffs, and a filtering face piece mask (FFP2) over goggles.¹² Since COVID-19 is demonstrated to transmit also by touching contaminated surfaces/items, after each exam, the ultrasound probes and the mammography machine are cleaned with 1000 mg l⁻¹ chlorine-containing disinfectant.¹³ Moreover, our unit obtained a backup call team to serve as the "clean team" for grabbing supplies and taking over after a procedure on a COVID positive/under investigation patient.

As mentioned above, during Phase 1, the number of radiological examinations decreased, due to both the cancellation

of non-urgent visits and the fear of the population of visiting hospitals, which were considered a potential source of contagion. With fewer patients to see, radiologists and residents changed their work routines, using work time to make progress on research topics or to participate in webinars or to learn about trending topics. Such research activities were not formally restructured, and no tracking was implemented because the managers of our unit fully respected the personal way of dealing with such troubled and unusual times. Despite a lack of formal monitoring, our team showed a great sense of responsibility and all radiologists, when not engaged in clinical activity, devoted themselves to the study and/or to research activities with great seriousness, compatibly with the different predisposition to research and their personal impediments. Finally, some breast-imaging employees also have volunteered to be deployed to other areas if they have the necessary skills and experience. During Phase 1, 4 out of 25 radiologists and around 25% of staff (both radiologists and other healthcare employees) of our division, especially those with young children, decided to go on a 2-weeks paid leave, funded in part by our institute and in part by the Government. Unfortunately, remote working was not possible due to both the nature of our job (which includes performing ultrasound exams or communicating bad news to oncological patients), and the technical limitations of our institute which does not have the appropriate technology to allow performance from home of some of our activities (*e.g.* reading of mammography or MRI).

In Phase 2, Lombardy government allowed our centre to open again to elective (*i.e.* deferrable) examinations, including the follow-up imaging exams which are crucial for breast cancer patients.¹⁴ Therefore, each radiologist, with the help of administration staff, is contacting the patients that were postponed, selecting which patients to see first in accordance with the criteria listed above, and all the staff is planning to work extended (from 8 am until 7 pm instead of 4 pm) and weekend hours (one Saturday every 3 weeks for each radiologist) to address the growing backlog of patients. We expect to recover all the patients we previously postponed within 3 months, in order not to defer the breast cancer patients' follow-up beyond 90 days from their expected date. So far, the volume of patients in the first 2 months of Phase 2 is estimated to be around 30% more (from 10,020 to 12,950 a total of diagnostic and interventional procedures) than the 2-months before of the outbreak of COVID-19 in Italy, namely January and February (Figure 1).

Additional protections for radiologists and other staff members are continually enforced: all staff members and all the patients now must wear masks (surgical mask or FFP2) inside our centre. The same PPE used in Phase 1 are used by radiologists when they cannot guarantee the 1-metre distance from the patient for more than 15 min. This essentially means that that hair cap, goggles for eye protection, disposable long sleeve fluid-resistant gown, gloves and FFP2 mask are still mandatory for breast ultrasound.

All machines (mammography and MR scans) and their parts (ultrasound probes) are still cleaned by radiologist technician with 1000 mg l⁻¹ chlorine-containing disinfectant¹³ after each examination.

In addition, facilities have added social distancing measures, such as limiting the number of chairs in waiting rooms, allowing access only to patients (companions can only access in case of real need), and scheduling appointments 30 min apart or on alternate days.

While in Phase 1, outpatients were screened for COVID-19 through questionnaires and temperature checks before entering our centre, temperature of patients and staff are now screened twice: first in the lobby and again at the breast imaging front desk, in both cases by a professional health worker. All patients are informed that, in the presence of fever, cough and/or flu-like symptoms, one medical doctor of our institute will evaluate the possibility to admit or refuse patients.

Finally, all in-patients undergo the reverse transcription polymerase chain reaction test performed on respiratory samples obtained by a nasopharyngeal swab the day before their hospitalisation. The ultimate aim at our centre is to test even asymptomatic outpatients: although our healthcare system cannot currently afford such amount of testing, our centre uses its own funds to reach this result, as it seems to be the most effective way to provide the appropriate safety standard for cancer patients.¹⁵

In conclusion, how radiology divisions respond to any infectious disease outbreak is determined primarily by the estimated risk of cross-infection to the staff and other patients.⁷ When the risk is high, as in the current case of COVID-19 infection, strict control infection protocols need to be applied to reduce the spread of the disease. Notably, in our breast imaging division, no incidents between non-infected and infected patients have been documented so far, and there has been only few cases of COVID-19 infection of healthcare workers in our department. By sharing our experience, with the reconfiguration of our breast-imaging division in a cancer referral centre located in one of the most important outbreak of COVID-19 in the world, we offer a roadmap for proceeding and we aim to mobilise the global research community to generate the data that are critically needed to offer the best possible care to breast cancer patients in this pandemic and during potential future emergencies of this kind.

CONTRIBUTORS

(1) Conception and design: Dr. Filippo Pesapane, Dr. Enrico Cassano, (2) Administrative support: Dr. Enrico Cassano, (3) Provision of study materials or patients: All Authors, (4) Collection and assembly of data: All Authors, (5) Data analysis and interpretation: All Authors, (6) Manuscript writing: All authors, (7) Final approval of manuscript: All authors.

REFERENCES

- Huang C, Wang Y, Li X, Ren L, Zhao J, Hu Y, et al. Clinical features of patients infected with 2019 novel coronavirus in Wuhan, China. *Lancet* 2020; **395**: 497–506. doi: [https://doi.org/10.1016/S0140-6736\(20\)30183-5](https://doi.org/10.1016/S0140-6736(20)30183-5)
- ArcGIS Johns Hopkins University.COVID-19 Dashboard by the Center for Systems Science and Engineering (CSSE) at Johns Hopkins University (JHU). 2020. Available from: <https://gisanddata.maps.arcgis.com/apps/opsdashboard/index.html#/bda7594740fd40299423467b48e9ecf6> [03 June 2020].
- Worldometer. Coronavirus cases: Reported Cases and Deaths by Country. 2020. Available from: <https://www.worldometers.info/coronavirus/#countries> [03 June 2020].
- Lau H, Khosrawipour V, Kocbach P, Mikolajczyk A, Ichii H, Schubert J, et al. Internationally lost COVID-19 cases. *J Microbiol Immunol Infect* 2020; **53**: 454–8. doi: <https://doi.org/10.1016/j.jmii.2020.03.013>
- Commission E. Regional GDP per inhabitant in the EU27 GDP per inhabitant in 2006 ranged from 25% of the EU27 average in Nord-Est in Romania to 336% in Inner London. 2009. Available from: https://ec.europa.eu/commission/presscorner/detail/en/STAT_09_23.
- Odone A, Delmonte D, Scognamiglio T, Signorelli C. COVID-19 deaths in Lombardy, Italy: data in context. *Lancet Public Health*; 2020.
- Huang Z, Zhao S, Li Z, Chen W, Zhao L, Deng L, et al. The battle against coronavirus disease 2019 (COVID-19): emergency management and infection control in a radiology department. *J Am Coll Radiol* 2020;.
- Torri E, Sbrogiò LG, Rosa ED, Cinquetti S, Francia F, Ferro A. Italian public health response to the COVID-19 pandemic: case report from the field, insights and challenges for the Department of prevention. *Int J Environ Res Public Health* 2020; **17**: 3666. doi: <https://doi.org/10.3390/ijerph17103666>
- Cairns L. Twenty years of activity at the European Institute of oncology, Milan, Italy. *Ecancermedicalscience* 2014; **8**: ed37. doi: <https://doi.org/10.3332/ecancer.2014.ed37>
- Penco S, Rotili A, Pesapane F, Trentin C, Dominelli V, Faggian A, et al. Mri-Guided vacuum-assisted breast biopsy: experience of a single tertiary referral cancer centre and prospects for the future. *Med Oncol* 2020; **37**: 36. doi: <https://doi.org/10.1007/s12032-020-01358-w>
- Decreto N. 3351 “DISPOSIZIONI INTEGRATIVE IN ATTUAZIONE DELLA DGR N. XI/2906 DELL’8/03/2020 PER L’ORGANIZZAZIONE DELLA RETE OSPEDALIERA IN ORDINE ALL’EMERGENZA EPIDEMIOLOGICA DA COVID – 19”; 2020.
- Kooraki S, Hosseiny M, Myers L, Gholamrezanezhad A. Coronavirus (COVID-19) outbreak: what the Department of radiology should know. *J Am Coll Radiol* 2020; **17**: 447–51. doi: <https://doi.org/10.1016/j.jacr.2020.02.008>
- Mirza SK, Tragon TR, Fukui MB, Hartman MS, Hartman AL. Microbiology for radiologists: how to minimize infection transmission in the radiology department. *Radiographics* 2015; **35**: 1231–44. doi: <https://doi.org/10.1148/rg.2015140034>
- Lombardia R. Coronavirus: riorganizzazione delle attività di ricovero e ambulatoriali. 2020. Available from: <https://www.regione.lombardia.it/wps/portal/istituzionale/HP/DettaglioRedazionale/servizi-e-informazioni/cittadini/salute-e-prevenzione/coronavirus/sospensione-attivita-ambulatoriali> [03 June 2020].
- van de Haar J, Hoes LR, Coles CE, Seamon K, Fröhling S, Jäger D, et al. Caring for patients with cancer in the COVID-19 era. *Nat Med* 2020; **26**: 665–71. doi: <https://doi.org/10.1038/s41591-020-0874-8>

Received:
26 July 2019

Revised:
06 September 2019

Accepted:
16 September 2019

<https://doi.org/10.1259/bjr.20190660>

Cite this article as:

Bitencourt AGV, Rossi Saccarelli C, Kuhl C, Morris EA. Breast cancer screening in average-risk women: towards personalized screening. *Br J Radiol* 2019; **92**: 20190660.

COMMENTARY

Breast cancer screening in average-risk women: towards personalized screening

^{1,2}ALMIR GV BITENCOURT, MD, PhD, ^{1,3}CAROLINA ROSSI SACCARELLI, MD, ⁴CHRISTIANE KUHL, MD, PhD and ¹ELIZABETH A MORRIS, MD

¹Department of Radiology, Breast Imaging Service, Memorial Sloan Kettering Cancer Center, New York, NY, USA,

²Department of Imaging, A.C. Camargo Cancer Center, São Paulo, SP, Brazil

³Department of Radiology, Hospital Sírio-Libanês, São Paulo, SP, Brazil

⁴Department of Diagnostic and Interventional Radiology, University Hospital Aachen, RWTH Aachen University, Aachen, Germany

Address correspondence to: Elizabeth A Morris

E-mail: morrise@mskcc.org

The authors Almir GV Bitencourt and Carolina Rossi Saccarelli contributed equally to the work.

ABSTRACT

Breast cancer screening is widely recognized for reducing breast cancer mortality. The objective in screening is to diagnose asymptomatic early stage disease, thereby improving treatment efficacy. Screening recommendations have been widely debated over the past years and controversies remain regarding the optimal screening frequency, age to start screening, and age to end screening. While there are no new trials, follow-up information of randomized controlled trials has become available. The American College of Physicians recently issued a new guidance statement on screening for breast cancer in average-risk women, with similar recommendations to the U.S. Preventive Services Task Force and to European guidelines. However, these guidelines differ from those of other American specialty societies. The variations reflect differences in the organizations' values, the metrics used to evaluate screening results, and the differences in healthcare organization (individualized or state-organized healthcare). False-positive rates and overdiagnosis of biologically insignificant cancer are perceived as the most important potential harms associated with mammographic screening; however, there is limited evidence on their actual consequences. Most specialty societies agree that physicians should offer mammographic screening at age 40 years for average-risk women and discuss its benefits and potential harms to achieve a personalized screening strategy through a shared decision-making process.

INTRODUCTION

Breast cancer screening is widely recognized for reducing breast cancer mortality. The objective in screening is to diagnose asymptomatic early-stage disease, thereby improving treatment efficacy. Despite the consensus regarding the benefits of screening, controversy remains regarding the optimal screening frequency, age to start screening, and age to end screening.^{1,2}

CURRENT GUIDELINES

Recently, the American College of Physicians (ACP) issued a new guidance statement on breast cancer screening in average-risk women.³ In summary, ACP recommends biennial mammography for women aged 50–74 years, that clinicians discuss the potential benefits and harms of screening with women aged 40–49 years, and that screening is discontinued for women over 74 years or with a life expectancy less than 10 years.

These recommendations are similar to those of the U.S. Preventive Services Task Force (USPSTF), published in 2016.⁴ However, other American specialty societies such as the American College of Radiology (ACR), American Cancer Society (ACS), and National Comprehensive Cancer Network (NCCN) agree that screening should be performed annually in average-risk women beginning at age 40 years.^{1,5} These variations reflect the differences in values between the organizations and correspondingly the specific metrics and relative weight of the metrics used to evaluate mammographic screening results. The ACP and USPSTF evaluate the cost-effectiveness of screening based on the reduction of mortality as well as the perceived harms. Meanwhile, medical specialty societies that are directly involved in the management of breast cancer patients assess other benefits of screening besides reduced mortality, such as fewer aggressive treatments through early detection, reduction of morbidity associated with advanced stages

Table 1. Recommendations for breast cancer screening in average-risk women

	ACR	NCCN	ACS	ACP, USPSTF	EUSOBI	ESMO
Age to initiate (years)	40	40	45; offer at 40–44	50; individualize at 40–49	50; Consider also 40–49	50; Consider also 40–49
Screening interval	Annual	Annual	Annual for 40–54; biennial or annual >55	Biennial	Biennial for 50–69; Annual for 40–49	Annual or biennial for 50–69
Age to end	Not yet established; Continue if life expectancy >5–7 years	Not yet established; Continue if life expectancy ≥10 years	Continue if life expectancy ≥10 years	74	69; Consider also 70–74	69; Consider also 70–74

ACP, American College of Physicians; ACR, American College of Radiology; ACS, American Cancer Society; ESMO, European Society of Medical Oncology; EUSOBI, European Society of Breast Imaging; NCCN, National Comprehensive Cancer Network; USPSTF, U.S Preventive Services Task Force.

of the disease, and years of life lost to breast cancer. Annual screening appears to result in fewer deaths from breast cancer, especially in younger women, although it does lead to higher costs associated with additional recalls and invasive procedures.⁵ However, where each organization determines where to draw the line between what is acceptable or not varies.

In Europe, each country has differently organized breast cancer screening programs. Most of the European programs suggest biennial screening from 50 to 70 years. These practices are in line with the recommendations of the European Society of Breast Imaging (EUSOBI). EUSOBI recommends biennial mammography screening for women aged 50–69 years and also suggests the extension of mammography screening for women aged 40–49 years and 70–75 years, annually and biennially, respectively.⁶ Of note, the United Kingdom National Health Service offers screening every 3 years for women aged 50–70 years, although some subspecialty societies recommend more frequent screening, *i.e.* the Royal College of Radiologists suggests that a 2-year interval would be more appropriate.⁷ The European Society for Medical Oncology (ESMO) recommends annual or biennial screening mammography in women aged 50–69 years and suggests that regular mammography may also be performed in women aged 40–49 years and 70–74 years, although noting that the evidence of benefit is less well established.⁸ Table 1 summarizes the recommendations of the most important societies for breast cancer screening in average-risk women.

POTENTIAL HARMS OF SCREENING MAMMOGRAPHY

When discussing the criticisms of screening mammography, it is important to note the larger perspective and thus the main context for the criticisms: is the perspective a societal one with state-organized national screening programs where cost-effectiveness or economic aspects are likely to be emphasized; or is the perspective a patient-centered one with individualized health-care where medical and psychological implications of screening are likely to be emphasized?

The most important potential harms associated with mammographic screening are false-positive diagnosis and overdiagnosis, leading to economic and medical implications.

False-positive recalls lead to increased costs of screening, thus reducing the benefit-to-cost ratio, because it leads to additional imaging and invasive procedures and can increase screening-associated morbidity. In general, recall rates tend to be higher in opportunistic screening than in organized screening programs where specified (low) recall rates are enforced. Screening with improved radiographic breast imaging methods such as digital breast tomosynthesis (DBT) can reduce false-positive recalls, especially in younger⁹ women; however, DBT is not yet widely used for population-based screening and reduced costs due to reduced false-positive calls are counter-weighted by increased costs for equipment and radiologist reading of DBT studies. From a medical or individual perspective, the potential harms related to false-positive results might be overestimated; usually less than 5% of all false-positive recalls result in invasive procedures. A recent meta-analysis has shown that women value the possibility of an earlier diagnosis over the risks of a false-positive result, and they understand that false-positive diagnoses are an unavoidable part of radiologists' attempts to find breast cancer as early as possible.¹⁰

Overdiagnosis is defined as the detection of a biologically insignificant cancer that would not reduce an individual's well-being and life expectancy in the absence of screening. Estimates of its magnitude are unreliable.⁷ Even now, with recent advances in molecular biology, it is not possible to identify tumours that do not progress to clinically significant disease. Overdiagnosis is related to age; in a woman in her 40s or 50s, overdiagnosis is rare; however, in a woman in her 80s, it becomes an issue.¹¹ Therefore, overdiagnosis should not be a factor to decide when to start screening or how often screening should be performed. Delaying the onset or increasing the screening interval will raise the rate of overdiagnosed cancers and retard the diagnosis of rapid-growing and more biologically aggressive cancers, leading to underdiagnosis. The devastating consequences of a late diagnosis should also be recognized, especially for young women, who are the most adversely affected by the years of life lost due to the disease. Although the adverse effects of overdiagnosis can be relieved by providing patient information and proper management, the lethal consequences of underdiagnosis cannot be mitigated.¹²

RISK ASSESSMENT AND RISK-ADAPTED SCREENING

The ACR has issued new guidelines recommending that breast cancer risk assessment should be performed in all women at the age of 30 years to guide counselling regarding surveillance, genetic testing, and risk reduction treatments.¹³ For screening purposes, a woman is considered at average risk if she does not have a personal history of breast cancer, strong family history of breast cancer, high-risk predisposition syndromes or genetic mutations, and no history of thoracic radiation therapy before the age of 30 years.¹⁴ Risk assessment can be performed with validated statistical tools, such as the Gail, Claus, Tyrer–Cuzick, BRCAPRO, and BOADICEA models; a woman with 15% or less lifetime risk of breast cancer is considered as average risk. Women with higher than average risk should undergo different screening strategies, *i.e.* supplemental imaging modalities such as MRI or ultrasound.^{13,15}

Risk assessment models have been validated in specific populations based on different variables including classical risk factors such as age, first- and second-degree family history, and personal medical and reproductive history.¹⁶ These models are usually not applicable to women with hereditary cancer syndromes; thus, using guidelines to determine if a patient is a candidate for genetic counselling and possibly genetic testing are essential components to a comprehensive breast cancer screening program.¹⁶ Additionally, polygenic risk scores based on low penetrance single nucleotide polymorphisms (SNPs) will probably play an important role in breast cancer risk assessment in the future.¹⁷ It is also important to note that mathematical risk assessment models vary in their ability to accurately incorporate risk associated with the presence of high-risk lesions in prior biopsies, such as atypical ductal hyperplasia and lobular neoplasia, and that most of these models do not include mammographic density assessment, which is an independent risk factor for breast cancer.¹⁸ Recently, deep learning models using mammographic images demonstrated the potential to substantially improve risk discrimination compared with an established breast cancer risk model that includes breast density.¹⁹ These findings reinforce the need to develop more individualized and accurate risk assessment tools that include classical risk factors, genetic assessment, and image features.

The American College of Obstetricians and Gynecologists (ACOG) guidelines, published in 2017, stated that average-risk women should be offered screening mammography at age 40 years and that the screening strategy should be made through a shared decision-making process between patient and physician.²⁰ In this context, it is important that the information provided to women about the benefits and potential harms of screening should be available in a transparent and objective way so they can make informed decisions. Because high breast density is a known risk factor for breast cancer and will reduce the diagnostic accuracy of mammography, density reporting laws in the United States support the awareness of this condition and supplemental screening for these women. The implementation of risk-adapted breast screening strategies incorporating breast density could further refine the risk assessment process in average-risk women. Based on risk stratification, women may be offered screening with an individually adjusted starting age and different imaging modalities. Because annual screening appears to provide additional benefit over biennial screening, particularly in younger women, the ACS recommends that women should be offered the opportunity to begin annual screening at age 40 years and that women aged 55 years and older should transition to biennial screening or could continue screening annually.

CONCLUSION

The differences between guidelines and recommendations are the relative value that different groups place on the perceived harms of screening. Despite the different recommendations, most agree that mammographic screening should be offered at age 40 years for average-risk women and that the benefits and potential harms should be discussed to achieve a personalized screening strategy through a shared decision-making process.

ACKNOWLEDGMENT

This work was partially supported by the NIH/NCI Cancer Center Support Grant (P30 CA008748) and the Breast Cancer Research Foundation.

COMPETING INTERESTS

Elizabeth A. Morris has received a grant for Grail, Inc. for research work not related to the present commentary.

REFERENCES

1. Lee CS, Moy L, Friedewald SM, Sickles EA, Monticciolo DL. Harmonizing breast cancer screening recommendations: metrics and accountability. *AJR Am J Roentgenol* 2018; **210**: 241–5. doi: <https://doi.org/10.2214/AJR.17.18704>
2. Tabár L, Vitak B, Chen TH-H, Yen AM-F, Cohen A, Tot T, et al. Swedish two-county trial: impact of mammographic screening on breast cancer mortality during 3 decades. *Radiology* 2011; **260**: 658–63. doi: <https://doi.org/10.1148/radiol.11110469>
3. Qaseem A, Lin JS, Mustafa RA, Horwitch CA, Wilt TJ, .for the Clinical Guidelines Committee of the American College of Physicians Screening for breast cancer in average-risk women: a guidance statement from the American College of physicians. *Ann Intern Med* 2019; **170**: 547. doi: <https://doi.org/10.7326/M18-2147>
4. Siu AL, .U.S. Preventive Services Task Force Screening for breast cancer: U.S. preventive services Task force recommendation statement. *Ann Intern Med* 2016; **164**: 279. doi: <https://doi.org/10.7326/M15-2886>
5. Helvie MA, Bevers TB. Screening mammography for average-risk women: the controversy and NCCN's position. *J Natl Compr Canc Netw* 2018; **16**: 1398–404. doi: <https://doi.org/10.6004/jnccn.2018.7081>
6. Sardanelli F, Aase HS, Álvarez M, et al. Position paper on screening for breast cancer by the European Society of breast imaging (EUSOBI) and 30 National breast radiology bodies from Austria, Belgium,

- Bosnia and Herzegovina, Bulgaria, Croatia, Czech Republic, Denmark, Estonia, Finland, France, G. *Eur Radiol* 2017; **27**: 2737–43.
7. Marmot MG, Altman DG, Cameron DA, Dewar JA, Thompson SG, Wilcox M, et al. The benefits and harms of breast cancer screening: an independent review. *Lancet* 2012; **380**: 1778–86. doi: [https://doi.org/10.1016/S0140-6736\(12\)61611-0](https://doi.org/10.1016/S0140-6736(12)61611-0)
 8. Cardoso F, Kyriakides S, Ohno S, et al. Early breast cancer: ESMO clinical practice guidelines for diagnosis, treatment and follow-up. *Ann Oncol* 2019.
 9. Conant EF, Barlow WE, Herschorn SD, Weaver DL, Beaber EF, Tosteson ANA, et al. Association of digital breast Tomosynthesis vs digital mammography with cancer detection and recall rates by age and breast density. *JAMA Oncol* 2019; **5**: 635. doi: <https://doi.org/10.1001/jamaoncol.2018.7078>
 10. Mathioudakis AG, Salakari M, Pylkkanen L, Saz-Parkinson Z, Bramesfeld A, Deandrea S, et al. Systematic review on women's values and preferences concerning breast cancer screening and diagnostic services. *Psychooncology* 2019; **28**: 939–47. doi: <https://doi.org/10.1002/pon.5041>
 11. Hendrick RE. Obligate overdiagnosis due to mammographic screening: a direct estimate for U.S. women. *Radiology* 2018; **287**: 391–7. doi: <https://doi.org/10.1148/radiol.2017171622>
 12. Kuhl CK. Underdiagnosis is the main challenge in breast cancer screening. *Lancet Oncol* 2015; **2019**: 6–7.
 13. Monticciolo DL, Newell MS, Moy L, Niell B, Monsees B, Sickles EA. Breast Cancer Screening in Women at Higher-Than-Average Risk: Recommendations From the ACR. *Journal of the American College of Radiology* 2018; **15**: 408–14. doi: <https://doi.org/10.1016/j.jacr.2017.11.034>
 14. Oeffinger KC, Fontham ETH, Etzioni R, et al. Breast cancer screening for women at average risk: 2015 guideline update from the American cancer Society. *JAMA - J Am Med Assoc* 2015; **314**: 1599–614.
 15. Mann RM, Kuhl CK, Moy L. Contrast-Enhanced MRI for breast cancer screening. *J Magn Reson Imaging* 2019; **16**. Barke LD, Freivogel ME. Breast cancer risk assessment models and high-risk screening. *Radiol Clin North Am* 2017; **55**: 457–74. doi: <https://doi.org/10.1016/j.rcl.2016.12.013>
 17. Wood ME, Farina NH, Ahern TP, Cuke ME, Stein JL, Stein GS, et al. Towards a more precise and individualized assessment of breast cancer risk. *Aging* 2019; **11**: 1305–16. doi: <https://doi.org/10.18632/aging.101803>
 18. Lee CI, Chen LE, Elmore JG. Risk-based breast cancer screening: implications of breast density. *Med Clin North Am* 2017; **101**: 725–41.
 19. Yala A, Lehman C, Schuster T, Portnoi T, Barzilay R. A deep learning mammography-based model for improved breast cancer risk prediction. *Radiology* 2019; **292**: 60–6. doi: <https://doi.org/10.1148/radiol.2019182716>
 20. The American College of obstetricians and Gynecologists. breast cancer risk assessment and screening in average-risk women. *ACOG Pract Bull* 2017; **179**: 1–16.

Cite this article as:

Wilkinson L, Thomas V, Sharma N. Microcalcification on mammography: approaches to interpretation and biopsy. *Br J Radiol* 2017; **90**: 20160594.

REVIEW ARTICLE

Microcalcification on mammography: approaches to interpretation and biopsy

LOUISE WILKINSON, BMBCh, FRCR, VAL THOMAS, MBBS, FRCPath and NISHA SHARMA, MBChB, FRCR

¹Department of Breast Imaging, St Georges Hospital, Tooting, London

²Department of Pathology, St Georges Hospital, Tooting, London

³Breast Unit, Leeds Teaching Hospital NHS Trust, Leeds, UK

Address correspondence to: Dr Louise S Wilkinson

E-mail: louise.wilkinson@stgeorges.nhs.uk

ABSTRACT

This article discusses the significance of microcalcifications on mammography and the changes in technology that have influenced management; it also describes a pragmatic approach to investigation of microcalcification in a UK screening programme.

BACKGROUND AND PREVALENCE OF MICROCALCIFICATIONS

Microcalcifications result from the deposition of calcium oxalate and calcium phosphate within the breast tissue. The mechanism by which calcium deposition occurs is not clearly understood; it may be an active cellular process, or an effect of cellular degeneration. Calcification deposits are found within the ductal system, the breast acini, stroma and vessels, mainly as calcium oxalate and calcium phosphate.

Calcium oxalate is produced by apocrine cells in the breast. The crystals are usually colourless and may be difficult to see on routine histopathology without polarization. They are mainly related to benign cystic change, but can also be seen in association with breast cancer. Calcium oxalate cannot be metabolized by mammalian cells and there is emerging evidence that exposure to high levels of oxalate may affect epithelial cells by triggering cellular and genetic changes.¹

Calcium phosphate, usually in the form of calcium hydroxyapatite (similar to the form of calcium laid down in bone during skeletal growth²), is more easily recognized in histopathology as it stains purple with haematoxylin and eosin. It is more commonly associated with malignant lesions than calcium oxalate.³ Magnesium-substituted hydroxyapatite has also been reported.⁴ There is evidence that a change in levels and calcium carbonate content of hydroxyapatite may influence breast cancer cell growth.⁵

Radiographic microcalcification was first described in 1913 by Albert Salomon, a surgeon in Berlin. He imaged over 3000 surgical specimens describing the association of microcalcifications with breast cancer, demonstrated tumour spread to the lymph nodes and postulated that there were different types of breast cancer.⁶

Mammography developed as a speciality through the late 1950s and 1960s, with the first screening equipment introduced in the late 1960s.⁷ Improvements in technology with low kilovoltage, high-definition screen/film combinations and magnification views allowed the diagnosis of preclinical breast cancer. In 1986, Sickles⁸ proposed an interpretation scheme for microcalcifications utilizing a structured approach of classification into “benign” (requiring no further intervention), “probably benign” (managed by periodic mammography) and “suggestive of malignancy” (requiring biopsy).

The advent of organized screening during the late 1980s led to an increase in the detection of microcalcifications and, as a result, an increase in the detection of ductal carcinoma *in situ* (DCIS). The age-standardized incidence of DCIS in the UK has increased from around 3 per 100,000 before the advent of the National Health Service Breast Screening Programme (NHSBSP) to 23 per 100,000 in 2013. It continues to increase with the introduction of digital mammography and the UK national trial assessing the effect of increasing the age range of females invited for screening.⁹

There is no routinely published data from the UK national screening programmes describing the radiological features prompting further assessment, but data from other national screening programmes are available. This indicates that the recall rate for calcifications ranges from 0.4 to 2% of females screened. Investigation of mammographic microcalcification results in a diagnosis of malignancy in up to 0.3% of females screened (Table 1).

Changes due to evolving technology—imaging

Triple assessment by clinical examination, imaging and biopsy remains the fundamental approach to breast diagnosis. The conversion to digital mammography has increased the conspicuity of microcalcification on mammography and the introduction of increasingly sophisticated biopsy techniques has facilitated tissue diagnosis.

Analogue mammography used high-resolution film/screen combinations, which were designed for optimal spatial and contrast resolution at low dose. Computed radiography has been used as an interim step for cost reasons, but digital mammography is now widely used. Digital mammography employs post-processing of the image to enhance the appearance of microcalcifications: the comparative data from the Netherlands in Table 1 demonstrate an increase in calcium detection with the change to digital imaging. Computer-aided diagnosis algorithms can further increase the detection of microcalcifications, but do not improve cancer detection in a screening setting when mammograms are double-read.¹⁴ Magnification views can be used to enhance the morphology of calcifications. Digital breast tomosynthesis does not substantially improve the interpretation of microcalcifications.¹⁵

Changes due to evolving technology—localization techniques

Microcalcification on mammography is relatively non-specific, and non-operative diagnosis by image-guided needle sample is essential. In the early days, localization was performed using craniocaudal and lateral mammograms with a localization compression grid. Early stereotactic approaches using two-angled views to give a three-dimensional coordinate for needle placement were hampered by the delays of analogue film processing and patient movement.¹⁶ The breakthrough into small-field digital technology was a spin-off of the Hubble Space Telescope in the mid-1990s, when a joint project between National Aeronautics and Space Administration and Scientific Imaging Technologies developed a new charged-couple device.¹⁷ The technology allowed a high resolution, wide dynamic range and low light sensitivity, shortening exposure time while preserving image quality, resulting in the LORAD Stereo Guided Breast Biopsy System. This has been incorporated into two approaches to stereotactic guided biopsy; it can be performed on dedicated equipment in the prone position that may be more comfortable for the patient and reduces the risk of fainting, but does not provide a conventional mammography facility. Alternatively, biopsy may be performed with the patient seated or recumbent using an add-on device to an upright mammography machine.

More recently, tomosynthesis-guided biopsy technology has become available; this is reported to be quicker and more effective for sampling low-contrast soft-tissue lesions because it requires less repositioning. However, a recent technology evaluation on behalf of the NHSBSP indicated that a stereotactic approach was preferred over tomosynthesis-guided biopsy for soft microcalcifications.¹⁸

Table 1. Published data on investigation of microcalcifications in population screening programmes

Comparative screening data	Germany (Wiegel 2010 ¹⁰)	United States (Glynn 2011 ¹¹)		Netherlands (Bluekens 2012 ¹²)		Australia (Farshid 2014 ¹³)
Screening interval	Biennial	Not stated? Annual		Biennial		Biennial
Modality	Digital	Analogue	Digital (Years 1 and 2)	Analogue	Digital	Not stated
Number screened ^a	24,067	32,600	19,282	1,045,978	152,515	1494,809
Recall rate (%)	7.5	6.0	8.5	1.5	2.4	4.6
Cancer detection rate (%)	1.0	0.33	0.55	0.52	0.6	0.52
Assessment data for calcifications ^b						
Recall for calcifications	1.7%	0.79%	1.82%	0.20%	0.67%	0.42% had biopsy for calc
DCIS from calcifications	0.20%			0.04%	0.09%	
% of women diagnosed with malignancy from calcifications	0.32%	0.12%	0.20%			0.15%
PPV of biopsy of calcification	36%	41.1%	22.6%			35.8%

DCIS, ductal carcinoma *in situ*; PPV, positive-predictive value.

^aProportion of initial and subsequent attenders may differ between cohorts.

^bRates are estimated from numbers of lesions/cancers and number of women screened.

Changes due to evolving technology—biopsy devices

At the advent of the NHSBSP in 1988, needle sampling was performed by fine needle aspiration cytology to achieve pre-operative diagnosis. Cytological analysis of fine needle specimens is a specialized technique requiring particular expertise on the part of the operator and the cytologist. It is difficult to assess sample adequacy at the time of procedure, and cytology cannot distinguish between non-invasive and invasive malignancy. NHSBSP guidance (2001) indicates a median absolute sensitivity of cytology of 57%—just over half the carcinomas identified had pre-operative malignant cytology.¹⁹

In 1994, Parker et al²⁰ published data on the outcomes of 6152 core biopsies from 20 institutions, concluding that 14-G core breast biopsy is a reproducible and reliable alternative to surgical biopsy. This became the percutaneous biopsy method of choice, used as a reference for subsequent developments.

The shortcomings of 14-G biopsies led to the introduction of larger cores assisted by vacuum to ensure retrieval, which also allowed multiple samples to be collected with a single percutaneous introduction.^{21,22} Such devices range from 7–12 G and can be used to remove tissue volumes equivalent to the weight of a surgical specimen. This allows the pathologist considerably more tissue for analysis improving diagnostic accuracy, but requires additional processing and reporting time to ensure the sample has been sufficiently scrutinized.

RADIOLOGICAL IDENTIFICATION AND INTERPRETATION OF MICROCALCIFICATION

Microcalcifications are seen on many mammograms and there are well-described patterns that help to distinguish benign from potentially malignant changes. The Breast Imaging-Reporting and Data System lexicon supports consistency in nomenclature and provides descriptions to discriminate between benign and malignant changes.²³ Approaches to interpretation include appreciation of the extent, morphology and distribution of the calcifications. The Royal College of Radiologists Breast Group has described a five-point scale to communicate the level of suspicion (Table 2).²⁴ Review of prior mammograms to assess interval change is critical, although malignant calcifications may occasionally show minimal change in appearance over several years.²⁵

The primary feature of calcifications that prompts further analysis is clustering (>5 calcifications in a square centimetre)

Table 2. The Royal College of Radiologists Breast Group Classification for Breast Imaging²⁴

Mammographic grade	Description
M1	Normal
M2	Benign
M3	Indeterminate/probably benign
M4	Suspicious of malignancy
M5	Highly suspicious of malignancy

Figure 1 illustrates characteristic appearances of benign and malignant calcification. (Figure 1).

Features that suggest benign change include:

- multiple similar clusters in more than one quadrant in one or both breasts
- uniformity of the individual flecks
- lack of interval change.

Features that indicate further evaluation is required include:

- pleomorphism (variability in shape, size and density)
- linear and branching forms
- segmental distribution within a lobe of the breast
- interval change.

The characteristic morphological features of calcification are less reliable in small clusters and just under 50% of DCIS calcification clusters contain punctate calcifications.²⁵

Microcalcifications associated with a mass lesion should be reviewed carefully. Some patterns are clearly benign (such as popcorn calcification in a fibroadenoma), but malignant change may arise in any area of breast tissue and it is possible, for example, to find DCIS colonizing a fibroadenoma.

If microcalcifications cannot reasonably be assumed to be benign, the appearance is classified as indeterminate to malignant (M3, M4 and M5) and further evaluation is required. Magnification views may be used to demonstrate the morphology more clearly and display very fine calcifications not visible on routine mammography. Lateral mammograms are useful to display the layering of calcifications in the dependent aspect of microcysts, eliminating the need for biopsy. MRI may be used for further evaluation of calcifications²⁶ and has potential to improve specificity by reliably identifying benign change, reducing the number of cases requiring biopsy.

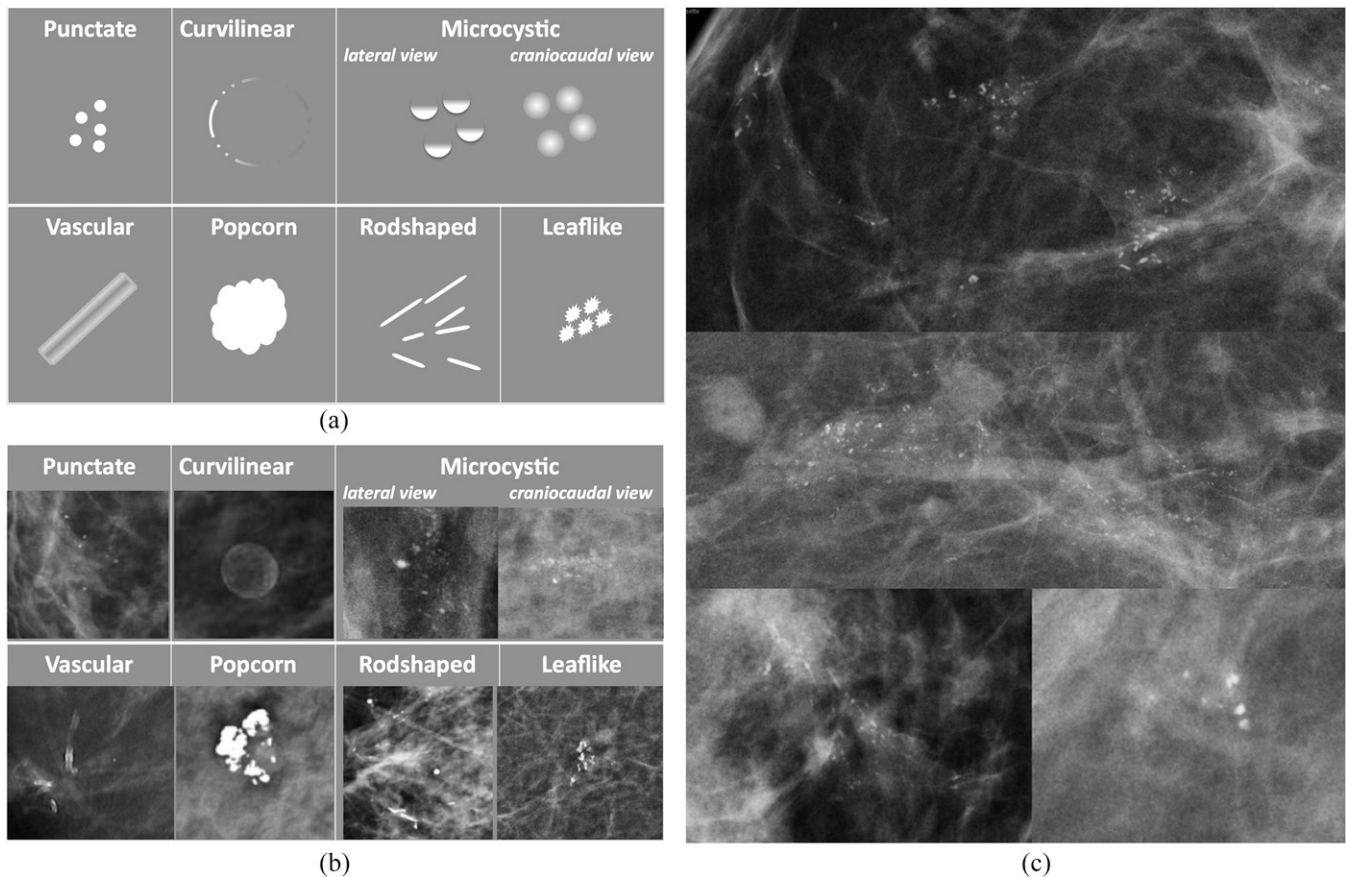
Any calcification that is not clearly benign should be considered for biopsy.

LOCALIZATION TECHNIQUE AND SAMPLING DEVICE

Biopsy is recommended when further imaging of calcification has not shown that changes are clearly benign. In general, calcification is biopsied using a stereotactic approach, or increasingly tomography, for localization. This requires a team approach to enable accurate positioning and recognition of the mammographic lesion. It is important to understand the geometry of the localization device to ensure precise needle placement.

When appropriate, biopsy can be performed using ultrasound. Successful identification of calcification on ultrasound relies on accurate localization of the cluster in the correct quadrant, distance from the nipple and depth below the skin surface. Calcification tends to be more conspicuous if there is any change in the adjacent soft tissue, and ultrasound-guided biopsy of calcification therefore may have a higher yield of malignancy than mammographic imaging.^{27,28} The size of the biopsy needle varies with local protocols; some practitioners favour a large

Figure 1. (a) Patterns of calcification associated with a benign change; (b) examples of calcification associated with a benign change; and (c) examples of malignant calcification.



vacuum-assisted sample and others prefer a 14-G sample, with vacuum-assisted biopsy (VAB) for selected cases.

The accuracy of 14-G biopsy depends on the size of the microcalcification cluster, the volume of the representative tissue obtained and the nature of the pathology. Today, there is a range of automated needles available commercially. Most studies describe the use of 14-G needles with a long throw (around 2 cm); a smaller gauge or shorter throw provides less tissue for analysis, which reduces the accuracy of the biopsy. The needles are single use, either for use with a reusable biopsy device or a fully disposable needle. The reusable device usually has a more rigorous spring, but can become contaminated with blood tracking back up the needle and therefore should be sterilized between procedures. The fully disposable devices are marginally more costly and are available in a range of gauge and throw. Some needles have a single action of advancing the inner stylet with sample trough, followed by the outer cutting cannula. Others, which allow initial advancement of the stylet followed by advancement of the cutting cannula, aid more precise needle placement in the case of small lesions or minimal tissue depth. All require multiple insertions to retrieve multiple samples and may only obtain scanty samples in dense or fibrous breast tissues.

Immediate specimen radiography is invaluable to assess the adequacy of the specimen—multiple calcifications are essential,

preferably in more than one core, depending on the extent of calcification on the mammogram. At least five flecks of calcification should be seen or flecks in three separate cores to ensure that the sample is representative.²⁹ It is important to ensure that calcification seen on specimen radiography correlates to the size and morphology of the calcification on mammography. A 14-G needle sample may be confidently used to establish a benign diagnosis such as microcystic or fibroadenomatoid change, or a malignant diagnosis of invasive cancer, but underestimates the nature of disease in approximately 27% of cases when DCIS and indeterminate lesions such as atypia are present.³⁰

Much of the current literature on percutaneous biopsy of the breast describes outcomes of large sample volumes obtained through a vacuum-assisted needle. This has the advantage of reaching a definitive diagnosis with a single procedure, the duration of the procedure is reduced as the needle is introduced only once and the samples are large in volume. Haemostasis may take longer, but there is no significant difference in complication rates and the procedure is well tolerated by patients.³¹

Although vacuum-assisted large core biopsy has many benefits, the cost of consumables is substantially greater than 14-G biopsy. In most instances, a 14-G biopsy will be sufficient to make the diagnosis, and even small clusters may be successfully sampled if sufficient care is taken over localization. It is not

essential to leave a marker clip *in situ* if calcium remains visible after biopsy, although an ultrasound visible marker makes it easier to identify the biopsy area when surgery is anticipated. Exceptions include very small or scattered clusters, when VAB is preferred in the first instance. In 2016, the cost of a 14-G needle and needle guides is approximately £20. A vacuum needle requires a dedicated vacuum system and marker clip placement is considered essential. The cost of a vacuum needle, guides and marker clip is around £300. In addition, the increase in work for the pathologist is considerable, as the greater volume of tissue may mean that it is difficult to identify small clusters of calcification and that more levels of multiple blocks need to be examined.

THE ROLE OF THE PATHOLOGIST IN INTERPRETATION OF BIOPSIES

Accurate diagnosis of microcalcifications depends on effective collaboration between the radiologist and pathologist. It is important that the radiologist understands the process of sample preparation. The specimen and request should be fully labelled, including adequate information regarding the nature of the lesion sampled. The radiologists should comment on the presence of calcification and give their opinion of the likely pathology: the pathologist should have access to the specimen radiograph. Segregating the samples containing calcification is useful after VAB so that subsequent levelling can be concentrated on the relevant material. Adequate fixation is necessary and larger volume samples take longer to fix. At embedding, despite the use of heated forceps, it is possible for tiny fragments of biopsy to be conveyed into subsequent samples. In this event, the pathologist may see fragments of irrelevant tissue separate from the main sample, which rarely present a diagnostic dilemma. This effect can be minimized by ensuring that breast biopsies are interspersed with non-breast samples during embedding. The samples are embedded in wax and the block is then rough-cut until the sample is apparent. Occasionally, tissues discarded during this process may include the relevant calcification.

Successive levels are then cut for staining. Current guidance indicates a minimum of 3 levels; a 0.004-mm level is cut, then 10 levels are cut and discarded, the next level is preserved and 10 further levels discarded. This means that approximately 10% of the first 0.13 mm of the block is available for review. A 14-G core biopsy is approximately 1.6-mm thick; so, the first three levels represent <10% of the specimen. Further levels are necessary if the calcification is not visible. In practice, it is more efficient to cut six levels in the first instance and review, before cutting further levels if required. A 9-G vacuum sample is approximately 3.6-mm thick and three levels constitute <4% of the tissue volume. For reference, microcalcifications are demonstrated on mammography at 0.1 mm or larger and cancer cells are approximately 0.03 mm.

The sections are routinely stained with haematoxylin and eosin. Additional staining, including immunohistochemistry, may be used to assist in diagnosis.³²

The pathological entities that are associated with microcalcification have been well described in the NHSBSP

Table 3. Pathology identified on percutaneous breast biopsy

Benign proliferative change (B2)
Fibroadenoma
Fibrocystic change
Sclerosing adenosis
Columnar cell change
Indeterminate lesions (B3)
Atypical ductal proliferation (AEDIP)
<i>In situ</i> lobular neoplasia, including lobular carcinoma <i>in situ</i> and atypical lobular hyperplasia (ILN)
Papilloma
Radial scar
Mucinous lesions
Non-invasive cancer (B5a)
Ductal carcinoma in situ (DCIS) and intracystic carcinoma
Pleomorphic lobular carcinoma <i>in situ</i>
Invasive cancer (B5b)
Invasive ductal carcinoma
Invasive lobular carcinoma
Special type including papillary, tubular and mucinous carcinomas

AEDIP, atypical epithelial ductal proliferation; DCIS, ductal carcinoma *in situ*.

Cancer which extends <1mm outside the duct wall is classified as microinvasive (B5c).

guidance.³³ Some commonly encountered entities are included in Table 3.

There is a spectrum of benign changes described, which may be associated with epithelial proliferation with or without atypia. A variety of lesions are classified as “indeterminate”, some because they show atypical morphology and others such as radial scar, papilloma and mucinous lesions because they may be associated with malignancy and are deemed inadequately sampled until completely removed. The diagnosis and management of indeterminate lesions will be discussed in a subsequent review. The distinction between atypia and low-grade *in situ* carcinoma depends on the extent of changes. If the abnormality measures >2 mm, or more than one duct system is involved, the lesion is best described as low-grade DCIS rather than atypia. In these circumstances, a larger volume of tissue at pre-operative diagnosis supports more accurate assessment by the pathologist.

THE IMPACT OF INVESTIGATING MICROCALCIFICATION

Calcification represents a challenge in both perception and interpretation. Small clusters of calcification are easy to miss and difficult to interpret. An aggressive approach to recall and investigation may result in high rates of benign biopsies, but reducing the number of females recalled is likely to mean some significant changes are not investigated. The benefit of biopsy is early diagnosis, meaning treatment can be easier and more effective, with a mortality benefit. The balance of overdiagnosis

and overtreatment are difficult to model but were described for the NHSBSP in 2012.³⁴ Some of the challenges of choosing an approach that balances risk and benefit are discussed below.

The rate of microcalcification and DCIS identified at screening depends on the age of the population and the frequency of screening. It is therefore difficult to establish baseline expected levels for assessment and rate of cancer diagnosis from calcifications.

Farshid *et al*³⁵ published a series of 2545 cases investigated between 1992 and 2007, where microcalcification without soft-tissue change was biopsied. Almost half (47.7%) of the cases were graded as indeterminate, 28.3% cases as suspicious and 24.0% cases as highly suspicious. After assessment, 47.9% of cases were malignant, 4.8% cases were indeterminate (including atypia) and 47.3% cases were benign. Less than one-third (30.9%) of DCIS was low grade, and the features predicting higher grade included radiological suspicion, extent and the presence of a palpable mass.

National audit data for UK screening units in 2014–15 indicate that the rate of diagnosis of DCIS ranges from 0.5 to 3.1 cases per 1000 females screened (average 1.8).³⁶ It is likely that this variation is due to different thresholds for biopsy. Maintaining a high threshold for sampling microcalcifications will reduce the number of females recalled and subjected to needle sampling. This minimizes unnecessary stress and discomfort in many cases and reduces the potential for overdiagnosis of low-grade DCIS and indeterminate lesions that are treated but may never affect a female in her lifetime. However, this is at the cost of missing some cases of both DCIS and invasive cancer, which may present at the next screen or as an interval cancer.

A recent analysis of data for over 5 million females screened between 2003 and 2007 investigated the relationship between the detection of DCIS and subsequent diagnosis of interval cancer in the UK. This showed that the average frequency of DCIS detected at screening was 1.6 per 1000 females screened (unit range: 0.54–3.56 per 1000 females screened). There was a significant negative association of screen-detected DCIS cases with the rate of invasive interval cancer; for every three cases of DCIS diagnosed, there was one less interval cancer.³⁷

Microcalcification was seen more frequently in cancers that were identified by only one of two readers than in cancers detected by both readers in a screening environment.³⁸ Reviews of imaging of females presenting with screen-detected and interval cancers show that approximately 30% of cancers were missed on the prior mammogram. Further analysis of the cases with findings on previous imaging showed that 18% of cases showed microcalcifications with digital mammography and 32% of cases showed microcalcifications with screen/film mammography.³⁹ Warren *et al*⁴⁰ reviewed 193 cases where cancer was diagnosed after assessment and found that microcalcifications were more likely to have been inadequately assessed than other lesions. A review of the prior mammograms of females with DCIS showed abnormality in 22% of cases.⁴¹ The calcification morphology on the prior mammogram was more indeterminate, indicating that a lower threshold for sampling indeterminate calcifications would increase the diagnosis of early DCIS.

In light of the discussion regarding overdiagnosis and overtreatment, alternatives to surgical excision for low-grade lesions are being considered. The LORIS trial (a trial comparing surgery with active monitoring for low risk DCIS) has been designed to test the efficacy of vacuum-assisted excision and regular surveillance for low-grade DCIS.⁴²

The appearance and effect of treating screen-detected DCIS is being recorded by the Sloane Project, a UK-wide prospective audit of screen-detected DCIS and atypical hyperplasias of the breast.⁴³ The Sloane Project began collecting data in 2003–4, including information about pre-operative findings as well as the management of DCIS. It has identified variation in the use of post-operative radiotherapy, oestrogen receptor measurement and surveillance protocols in the UK. Of interest to radiologists, the Sloane Project has demonstrated that typical calcifications in DCIS change with size of lesion. Casting calcifications are typical of larger areas of DCIS, including low grade, but small clusters of punctate or granular calcifications may represent high-grade DCIS, where an aggressive clinical approach is recommended.⁴⁴

A PRAGMATIC APPROACH TO INVESTIGATION OF MICROCALCIFICATIONS

Assessment of microcalcification is described in UK national guidance.⁴⁵ Calcifications that are not clearly benign at screening mammography are recalled for assessment, including further views, ultrasound and clinical examination. Biopsy is recommended in all cases where further imaging is not entirely normal or benign. A summary of assessment and microcalcification biopsy outcomes for Southwest London Breast Screening Service is shown in [Table 4](#).

If the microcalcification is confidently seen on ultrasound, biopsy may be performed under ultrasound guidance. Ultrasound guidance allows real-time visualization of the needle and is more comfortable for both the patient and the operator. Occasionally, more calcification is seen on ultrasound than on mammography and it is advisable to place a marker clip at the site of ultrasound-guided biopsy for calcification to ensure that the site of biopsy may be subsequently demonstrated on mammography.

If the microcalcification is not seen with confidence on ultrasound, then stereotactic biopsy with in-room specimen radiography is necessary. In our practice, 14-G biopsy is chosen as first-line approach for most microcalcifications. First-line vacuum biopsy is used if the cluster is small (<5 mm) or the calcification is scanty.

Occasionally, stereotactic biopsy is not possible because the individual is unable to tolerate the procedure or the calcification cannot be targeted on the small-field biopsy device. When stereotactic biopsy is not possible, it can help to draw a skin mark over the calcifications during attempted stereotactic localization to aid localization on ultrasound.

When a firm diagnosis of DCIS or invasive cancer is made, the radiologist aims to define the extent of disease such that the surgeon is able to remove all disease in a single operation. If the lesion is focal and amenable for local excision, only then the area

Table 4. Data for females assessed in Southwest London Breast Screening Service between April 2013 and March 2016 (from National Breast Screening System* assessment report)

Final non-operative diagnosis	Number of lesions sampled	% of total biopsies
B1 (no calcification)	45	2.5%
B2 (benign and concordant)	1212	66.5%
B3 (indeterminate pathology)	152	8.3%
B4 (suspicious for malignancy)	5	0.3%
B5a/c (<i>in situ</i> /microinvasive cancer)	360	19.7%
B5b (invasive cancer)	50	2.7%
No biopsy	332	

7443 females were recalled for assessment.

4338 biopsies were performed.

1824 (42%) of biopsies were performed for microcalcification.

69 (3.8%) of biopsies were repeated for non-concordance (B1).

12 (0.65%) biopsies were repeated after B4 diagnosis.

0 cancers were identified arising from an area previously assessed for calcification.

of most concern is biopsied. If the microcalcification is extensive and heterogeneous, or multifocal, such that mastectomy might be considered, two (or more) areas may need to be biopsied and marker clips deployed to determine disease extent.

Examination of the ipsilateral breast and axilla with ultrasound may demonstrate soft-tissue change associated with invasion and can give further information on axillary node changes. Nodes in the lower axilla with a thickened cortex are sampled by fine needle aspiration cytology or core biopsy.

DOCUMENTATION AND COMMUNICATION WITH THE PATIENT

There should be thorough documentation of the procedure, including identification of the clinician and radiographer, radiation dose, drugs administered and confirmation of the correct site check, in keeping with the National Safety Standards for Invasive Procedures.⁴⁶ Details of implanted marker clips should be recorded. As with all procedures, it is important to have formal training and update procedures in place and to evaluate the service continuously through audit and comparison with local and national standards and targets.

The cooperation of the patient is critical and is best gained by providing a calm environment and avoiding delay during the intervention. The patient should be fully informed regarding the nature of the procedure and the need to stay still. It helps if she can be supported by a healthcare assistant throughout. Written information should be given well before the procedure so that the patient has sufficient time to digest the information and ask questions if necessary. There is variation in approach to confirmation of consent depending on local protocols. As the patient is fully conscious, written consent is not essential.⁴⁷

The two main risks associated with biopsy are firstly, the harm of recall and intervention in a normal female who is not diagnosed with cancer and secondly, the treatment of females who have an abnormal diagnosis which would not cause harm during their

lifetime. This is explained in the screening invitation leaflet.⁴⁸ In addition, specific risks include haematoma, which can occasionally be extreme, and ongoing haemorrhage, which may need surgical intervention. Infection is rare. Post-biopsy pain is described but appears sporadic and unpredictable; it may be related to the extent of anxiety prior to the procedure.⁴⁹

Communication of biopsy results to females is important. When the biopsy is benign, females often ask whether they need more frequent follow-up, but they should be reassured that the area of the breast sampled is no more likely to develop malignant change than surrounding tissues. Identification and management of indeterminate lesions will be discussed separately. DCIS may be a difficult diagnosis to communicate and it is often helpful to use diagrams to demonstrate the difference between DCIS and invasive cancer. Clinicians vary in the phrases they use to describe non-invasive disease; some refer to it as “early cancer”, others as “pre-cancer”, and some feel strongly that it should not be referred to as cancer at all, because DCIS is not an obligate precursor of invasive disease. The BBC has an iWonder Interactive Guide that can be helpful.⁵⁰ Females may wish to know whether the biopsy can cause seeding along the biopsy tract. This may occur, but research has shown that the transplanted cells are not viable.⁵¹

SUMMARY

The identification and investigation of microcalcifications found on mammography have become more common with improving technology and there has been a parallel increase in the variety of associated lesions in pathology. This has resulted in an increase in the diagnosis of DCIS. In some cases, females may not benefit (overdiagnosis), but in others early treatment may pre-empt the development of invasive cancer. This is likely to have contributed to the reduction in mortality from breast cancer seen since the advent of screening. Clinicians responsible for the investigation of mammographic calcification should remain mindful of the need to balance harm and benefit.

REFERENCES

- Castellaro AM, Tonda A, Cejas HH, Ferreyra H, Caputto BL, Pucci OA, et al. Oxalate induces breast cancer. *BMC Cancer* 2015; **15**: 761. doi: <https://doi.org/10.1186/s12885-015-1747-2>
- Cox RF, Morgan MP. Microcalcifications in breast cancer: lessons from physiological mineralization. *Bone* 2013; **53**: 437–50. doi: <https://doi.org/10.1016/j.bone.2013.01.013>
- Morgan MP, Cooke MM, McCarthy GM. Microcalcifications associated with breast cancer: an epiphenomenon or biologically significant feature of selected tumors? *J Mammary Gland Biol Neoplasia* 2005; **10**: 181–7. doi: <https://doi.org/10.1007/s10911-005-5400-6>
- Scimeca M, Giannini E, Antonacci C, Pistolesi CA, Spagnoli LG, Bonanno E. Microcalcifications in breast cancer: an active phenomenon mediated by epithelial cells with mesenchymal characteristics. *BMC Cancer* 2014; **14**: 286. doi: <https://doi.org/10.1186/1471-2407-14-286>
- Choi S, Coonrod S, Estroff L, Fischbach C. Chemical and physical properties of carbonated hydroxyapatite affect breast cancer cell behavior. *Acta Biomater* 2015; **24**: 333–42. doi: <https://doi.org/10.1016/j.actbio.2015.06.001>
- Weerakkody Y, Kruger G; 2016. Available from: <http://radiopaedia.org/articles/dr-albert-salomon-1>
- Gold RH, Bassett LW, Widoff BE. Highlights from the history of mammography. *RadioGraphics* 1990; **10**: 1111–31. doi: <https://doi.org/10.1148/radiographics.10.6.2259767>
- Sickles EA. Breast calcifications: mammographic evaluation. *Radiology* 1986; **160**: 289–93. doi: <https://doi.org/10.1148/radiology.160.2.3726103>
- Cancer Research UK. Updated June 2016. Available from: <http://www.cancerresearchuk.org/health-professional/cancer-statistics/statistics-by-cancer-type/breast-cancer/incidence-in-situ#heading-Two>
- Weigel S, Decker T, Korsching E, Hungermann D, Böcker W, Heindel W. Calcifications in digital mammographic screening: improvement of early detection of invasive breast cancers? *Radiology* 2010; **255**: 738–45. doi: <https://doi.org/10.1148/radiol.10091173>
- Glynn CG, Farria DM, Monsees BS, Salcman JT, Wiele KN, Hildebolt CF. Effect of transition to digital mammography on clinical outcomes. *Radiology* 2011; **260**: 664–70. doi: <https://doi.org/10.1148/radiol.11110159>
- Bluekens AM, Holland R, Karssemeijer N, Broeders MJ, den Heeten GJ. Comparison of digital screening mammography and screen-film mammography in the early detection of clinically relevant cancers: a multicenter study. *Radiology* 2012; **265**: 707–14. doi: <https://doi.org/10.1148/radiol.12111461>
- Farshid G, Sullivan T, Jones S, Roder D. Performance indices of needle biopsy procedures for the assessment of screen detected abnormalities in services accredited by BreastScreen Australia. *Asian Pac J Cancer Prev* 2014; **15**: 10665–73. doi: <https://doi.org/10.7314/APJCP.2014.15.24.10665>
- Gilbert FJ, Astley SM, McGee MA, Gillan MG, Boggis CR, Griffiths PM, et al. Single reading with computer-aided detection and double reading of screening mammograms in the United Kingdom National Breast Screening Program. *Radiology* 2006; **241**: 47–53. doi: <https://doi.org/10.1148/radiol.2411051092>
- Spangler ML, Zuley ML, Sumkin JH, Abrams G, Ganott MA, Hakim C, et al. Detection and classification of calcifications on digital breast tomosynthesis and 2D digital mammography: a comparison. *AJR Am J Roentgenol* 2011; **196**: 320–4. doi: <https://doi.org/10.2214/AJR.10.4656>
- Bolmgren J, Jacobson B, Nordenström B. Stereotaxic instrument for needle biopsy of the mamma. *AJR Am J Roentgenol* 1977; **129**: 121–5. doi: <https://doi.org/10.2214/ajr.129.1.121>
- Updated June 2016. Available from: <https://www.spacefoundation.org/programs/space-technology-hall-fame/inducted-technologies/stereotactic-breast-biopsy-technology>
- Practical evaluation of Hologic Affirm digital breast tomosynthesis biopsy system NHS Breast Screening Programme Equipment Report 1501. Available from: https://www.gov.uk/government/uploads/system/uploads/attachment_data/file/488948/Practical_evaluation_of_Hologic_tomosynthesis_biopsy_system_FINAL_291215.pdf
- Non-operative Diagnosis Subgroup of the National Coordinating Group for Breast Screening Pathology. Guidelines for non-operative diagnostic procedures and reporting in breast cancer screening. NHSBSP publication no 50; 2001. Available from: <https://www.gov.uk/government/publications/nhs-breast-screening-non-operative-diagnostic-procedures>
- Parker SH, Burbank F, Jackman RJ, Aucreman CJ, Cardena G, Cink TM, et al. Percutaneous large-core breast biopsy: a multi-institutional study. *Radiology* 1994; **193**: 359–64. doi: <https://doi.org/10.1148/radiology.193.2.7972743>
- Park HL, Hong J. Vacuum-assisted breast biopsy for breast cancer. *Gland Surg* 2014; **3**: 120–7. doi: <https://doi.org/10.3978/j.issn.2227-684X.2014.02.03>
- Schrading S, Distelmaier M, Dirrichs T, Detering S, Brolund L, Strobel K, et al. Digital breast tomosynthesis-guided vacuum-assisted breast biopsy: initial experiences and comparison with prone stereotactic vacuum-assisted biopsy. *Radiology* 2015; **274**: 654–62. doi: <https://doi.org/10.1148/radiol.14141397>
- Sickles EA, D'Orsi CJ, Bassett LW. Acr BI-RADS® mammography. In: *ACR BI-RADS® Atlas, Breast imaging reporting and data system*. Reston, VA: American College of Radiology; 2013.
- Maxwell AJ, Ridley NT, Rubin G, Wallis MG, Gilbert FJ, Michell MJ; Royal College of Radiologists Breast Group. The Royal College of Radiologists Breast Group breast imaging classification. *Clin Radiol* 2009; **64**: 624–7. doi: <https://doi.org/10.1016/j.crad.2009.01.010>
- Evans A. The diagnosis and management of pre-invasive breast disease: radiological diagnosis. *Breast Cancer Res* 2003; **5**: 250–3. doi: <https://doi.org/10.1186/bcr621>
- Stehouwer BL, Merckel LG, Verkooijen HM, Peters NH, Mann RM, Duviolier KM, et al. 3-T breast magnetic resonance imaging in patients with suspicious microcalcifications on mammography. *Eur Radiol* 2014; **24**: 603–9. doi: <https://doi.org/10.1007/s00330-013-3029-1>
- Bae S, Yoon JH, Moon HJ, Kim MJ, Kim EK. Breast microcalcifications: diagnostic outcomes according to image-guided biopsy method. *Korean J Radiol* 2015; **16**: 996–1005. doi: <https://doi.org/10.3348/kjr.2015.16.5.996>
- Kim TE, Kim DB, Jung JH, Lee EK. Sonographic visibility and feasibility of biopsy under ultrasound guidance of suspicious microcalcification-only breast lesions: a single-centre study. *Hong Kong J Radiol* 2015; **18**: 125–33. doi: <https://doi.org/10.12809/hkjr1514264>
- Bagnall MJ, Evans AJ, Wilson AR, Burrell H, Pinder SE, Ellis IO. When have mammographic calcifications been adequately

- sampled at needle core biopsy? *Clin Radiol* 2000; **55**: 548–53. doi: <https://doi.org/10.1053/crad.1999.0483>
30. Houssami N, Ciatto S, Ellis I, Ambrogetti D. Underestimation of malignancy of breast core-needle biopsy: concepts and precise overall and category-specific estimates. *Cancer* 2007; **109**: 487–95.
 31. Soo AE, Shelby RA, Miller LS, Balmadrid MH, Johnson KS, Wren AA, et al. Predictors of pain experienced by women during percutaneous imaging-guided breast biopsies. *J Am Coll Radiol* 2014; **11**: 709–16. doi: <https://doi.org/10.1016/j.jacr.2014.01.013>
 32. Members of the National Coordinating Committee for Breast Pathology. Professor Ian Ellis, Nottingham City Hospital (Writing Group Lead). *Tissue pathways for breast pathology*: The Royal College of Pathologists; 2010.
 33. Pathology reporting of breast disease: a joint document incorporating the third edition of the NHS Breast Screening Programme's guidelines for pathology reporting in breast cancer screening and the second edition of The Royal College of Pathologists' minimum dataset for breast cancer histopathology. NHSBSP publication no 58; 2005. Available from: https://www.gov.uk/government/uploads/system/uploads/attachment_data/file/465530/nhsbsp58-high-resolution.pdf
 34. Marmot MG, Altman DG, Cameron DA, Dewar JA, Thompson SG, Wilcox M, et al; The Independent UK. Panel on Breast Cancer Screening. The benefits and harms of breast cancer screening: an independent review: a report jointly commissioned by Cancer Research UK and the Department of Health (England) October. *Br J Cancer* 2013; **108**: 2205–40. doi: <https://doi.org/10.1038/bjc.2013.177>
 35. Farshid G, Sullivan T, Downey P, Gill PG, Pieterse S. Independent predictors of breast malignancy in screen-detected microcalcifications: biopsy results in 2545 cases. *Br J Cancer* 2011; **105**: 1669–75. doi: <https://doi.org/10.1038/bjc.2011.466>
 36. NHS breast screening programme and Association of Breast Surgery. An audit of screen detected breast cancers for the year of screening April 2014 To March 2015. Public Health England. Published May 2016. Available from: http://www.associationofbreastsurgery.org.uk/media/63035/nhsbsp_abs_breast_screening_audit_201415_full_audit_v3.pdf
 37. Duffy SW, Dibden A, Michalopoulos D, Offman J, Parmar D, Jenkins J, et al. Screen detection of ductal carcinoma *in situ* and subsequent incidence of invasive interval breast cancers: a retrospective population-based study. *Lancet Oncol* 2016; **17**: 109–14. doi: [https://doi.org/10.1016/S1470-2045\(15\)00446-5](https://doi.org/10.1016/S1470-2045(15)00446-5)
 38. Hofvind S, Geller BM, Rosenberg RD, Skaane P. Screening-detected breast cancers: discordant independent double reading in a population-based screening program. *Radiology* 2009; **253**: 652–60. doi: <https://doi.org/10.1148/radiol.2533090210>
 39. Hoff SR, Abrahamsen AL, Samset JH, Vigeland E, Klepp O, Hofvind S. Breast cancer: missed interval and screening-detected cancer at full-field digital mammography and screen-film mammography—results from a retrospective review. *Radiology* 2012; **264**: 378–86. doi: <https://doi.org/10.1148/radiol.12112074>
 40. Warren R, Allgood P, Hunnam G, Godward S, Duffy S; East Anglian Breast Screening Programme. An audit of assessment procedures in women who develop breast cancer after a negative result. *J Med Screen* 2004; **11**: 180–6. doi: <https://doi.org/10.1258/0969141042467395>
 41. Evans AJ, Wilson AR, Burrell HC, Ellis IO, Pinder SE. Mammographic features of ductal carcinoma *in situ* (DCIS) present on previous mammography. *Clin Radiol* 1999; **54**: 644–9. doi: [https://doi.org/10.1016/S0009-9260\(99\)91083-8](https://doi.org/10.1016/S0009-9260(99)91083-8)
 42. LORIS: a Phase III trial of surgery versus active monitoring for low risk ductal carcinoma *in situ* (DCIS). Updated June 2016. Available from: <http://www.birmingham.ac.uk/research/activity/mds/trials/crctu/trials/loris/index.aspx>
 43. The Sloane Project. Updated June 2016. Available from: <http://www.sloaneproject.co.uk/>
 44. Evans A, Clements K, Maxwell A, Bishop H, Hanby A, Lawrence G, et al. Lesion size is a major determinant of the mammographic features of ductal carcinoma *in situ*: findings from the Sloane Project. *Clin Radiol* 2010; **65**: 181–4. doi: <https://doi.org/10.1016/j.crad.2009.05.017>
 45. Liston J, Wilson R. Clinical Guidelines for Breast Cancer Screening Assessment. 3rd edn. NHSBSP publication no 49; June 2010. Available from: https://www.gov.uk/government/uploads/system/uploads/attachment_data/file/465528/nhsbsp49_June2010.pdf
 46. National Safety Standards for Invasive Procedures (NatSSIPs). v. 1. First published: 7 September 2015. NHS England Patient Safety Domain and the National Safety Standards for Invasive Procedures Group. Available from: <https://www.england.nhs.uk/patientsafety/wp-content/uploads/sites/32/2015/09/natssips-safety-standards.pdf>
 47. The Royal College of Radiologists. Standards for patient consent particular to radiology. 2nd edn: The Royal College of Radiologists; 2012. Available from: <https://www.rcr.ac.uk/standards-patient-consent-particular-radiology-second-edition>
 48. NHS Breast Screening: Helping you decide: NHS Cancer Screening Programmes; 2013. Updated June 2016. Available from: https://www.gov.uk/government/uploads/system/uploads/attachment_data/file/440798/nhsbsp.pdf
 49. Miller SJ, Sohl SJ, Schnur JB, Margolies L, Bolno J, Szabo J, et al. Pre-biopsy psychological factors predict patient biopsy experience. *Int J Behav Med* 2014; **21**: 144–8. doi: <https://doi.org/10.1007/s12529-012-9274-x>
 50. BBC iWonder. Why isn't breast cancer screening totally reliable? Updated June 2016. Available from: <http://www.bbc.co.uk/guides/zcq7xnb>
 51. Loughran CF, Keeling CR. Seeding of tumour cells following breast biopsy: a literature review. *Br J Radiol* 2011; **84**: 869–74. doi: <https://doi.org/10.1259/bjr/77245199>

Received:
09 April 2019Revised:
15 August 2019Accepted:
19 August 2019<https://doi.org/10.1259/bjr.20190345>

Cite this article as:

Krammer J, Zolotarev S, Hillman I, Karalis K, Stsepankou D, Vengrinovich V, et al. Evaluation of a new image reconstruction method for digital breast tomosynthesis: effects on the visibility of breast lesions and breast density. *Br J Radiol* 2019; **92**: 20190345.

FULL PAPER

Evaluation of a new image reconstruction method for digital breast tomosynthesis: effects on the visibility of breast lesions and breast density

¹JULIA KRAMMER, ²SERGEI ZOLOTAREV, ³INGE HILLMAN, ³KONSTANTINOS KARALIS, ⁴DZMITRY STSEPANKOU, ²VALERIY VENGRINOVICH, ^{2,5,6}JÜRGEN HESSER and ^{7,8}TONY M. SVAHN¹Department of Clinical Radiology and Nuclear Medicine, University Medical Center Mannheim, Medical Faculty Heidelberg University Mannheim, Mannheim, Germany²National Academy of Science of Belarus, Institute of Applied Physics, Minsk, Belarus³Mammography Section, Gävle Hospital, Gävle, Sweden⁴Department of Experimental Radiooncology, Medical Faculty Mannheim, Heidelberg University, Germany⁵Central Institute for Computer Engineering (ZITI), Heidelberg University, Germany⁶Interdisciplinary Center for Scientific Computing (IWR), Heidelberg University, Germany⁷Centre for Research and Development, Uppsala University/Region Gävleborg, Gävle, Sweden⁸Department of Imaging and functional medicine, Division diagnostics, Gävle hospital, Gävle, Region Gävleborg, SwedenAddress correspondence to: Dr. Tony M. Svahn
E-mail: Tony.Svahn@regiongavleborg.se

Objective: To compare image quality and breast density of two reconstruction methods, the widely-used filtered-back projection (FBP) reconstruction and the iterative heuristic Bayesian inference reconstruction (Bayesian inference reconstruction plus the method of total variation applied, HBI).

Methods: Thirty-two clinical DBT data sets with malignant and benign findings, $n = 27$ and 17, respectively, were reconstructed using FBP and HBI. Three experienced radiologists evaluated the images independently using a 5-point visual grading scale and classified breast density according to the American College of Radiology Breast Imaging-Reporting And Data System Atlas, fifth edition. Image quality metrics included lesion conspicuity, clarity of lesion borders and spicules, noise level, artifacts surrounding the lesion, visibility of parenchyma and breast density.

Results: For masses, the image quality of HBI reconstructions was superior to that of FBP in terms of conspicuity, clarity of lesion borders and spicules ($p < 0.01$). HBI and FBP were not significantly different in calcification conspicuity. Overall, HBI reduced noise and suppressed

artifacts surrounding the lesions better ($p < 0.01$). The visibility of fibroglandular parenchyma increased using the HBI method ($p < 0.01$). On average, five cases per radiologist were downgraded from BI-RADS breast density category C/D to A/B.

Conclusion: HBI significantly improves lesion visibility compared to FBP. HBI-visibility of breast parenchyma increased, leading to a lower breast density rating. Applying the HBIR algorithm should improve the diagnostic performance of DBT and decrease the need for additional imaging in patients with dense breasts.

Advances in knowledge: Iterative heuristic Bayesian inference (HBI) image reconstruction substantially improves the image quality of breast tomosynthesis leading to a better visibility of breast carcinomas and reduction of the perceived breast density compared to the widely-used filtered-back projection (FBP) reconstruction. Applying HBI should improve the accuracy of breast tomosynthesis and reduce the number of unnecessary breast biopsies. It may also reduce the radiation dose for the patients, which is especially important in the screening context.

INTRODUCTION

Digital breast tomosynthesis (DBT) has been shown to overcome some limitations of standard two-dimensional full-field digital mammography (FFDM) that are caused by the overlap of normal and pathological tissues.¹⁻⁷ Several studies have demonstrated the advantages of DBT for breast cancer screening, such as increased cancer detection rates

and reduces callback rates.^{8,9} It has also been hypothesized that breast density, which is an image biomarker of tissue composition and an independent risk factor for breast cancer, can be more accurately determined by DBT.^{10,11} In DBT, volumetric reconstruction of the breast is typically obtained from a finite number of low-dose projections at different X-ray tube angles. Using a wider scan range

for DBT has shown to have a positive effect on image quality reducing artifacts and increasing depth resolution.¹² It should further improve the detection of breast masses by reducing superimposed breast anatomy.^{1,4} However, it may be associated with an elevated radiation dose to the breast.¹³ The acquired projection data are usually reconstructed as 1 mm slices using either filtered-back projection (FBP) or iterative reconstruction algorithms. At present, the diagnostic accuracy of DBT has almost exclusively been determined with systems incorporating FBP algorithms¹⁴, despite the fact that iterative reconstruction (IR) have played key roles in other fields of three-dimensional medical imaging, such as computed tomography. Studies using IR confirmed a better detectability of pathologies and reduction of the patient's radiation dose by suppressing image noise.^{15,16} IR improves image quality through cyclic image processing and has the advantage of allowing physical effects to be modelled, accounting for the probability distribution of the experimental measurements. Although all available IR solutions generally speaking reduce artifacts and radiation dose, the magnitude of these effects depends on the specific IR algorithm. IR techniques could potentially be particularly useful for mammography. Since various artifacts can mimic or obscure pathological changes and reduce the sensitivity or specificity of a modality,¹⁷ IR can identify subtle pathological changes through variations in tissue attenuation properties. To date, pure iterative algorithms are rarely used in a clinical DBT setting and are usually only applied in DBT systems employing sparse sampling, despite the fact that phantom-based studies have demonstrated promising results.^{12,18,19}

Recently, FBP in DBT was compared using two IR algorithms called maximum likelihood expectation (MLEM) and simultaneous iterative reconstruction technique (SIRT). MLEM has shown to provide a good balance between visibility of high-frequency components (like calcifications) and low-frequency components (like soft-tissue lesions).²⁰ Another study examined a variant of iterative total variation minimization (TVM) reconstruction, where it was shown that this technique preserved lesion contrast and high image quality while at the same time reducing the number of projections needed (and hence reducing radiation dose to the breast).²¹ In a third study, a Compton scattering suppression-based method for DBT based on Bayesian estimations was found to be superior to both SIRT and FBP in terms of object contrast.²²

In this study, we evaluate an IR method called heuristic Bayesian inference (HBI) reconstruction, which combines bayesian estimates and the TVM algorithm.^{21,22} We compare image reconstruction by HBI and FBP in a series of patient cases in terms of breast lesion characteristics and breast density assessment.

METHODS AND MATERIALS

Study population

This retrospective study was approved by the National Federal Radiation Commission and the Institutional Review Board, Germany. Data were analysed in accordance with the Health Insurance Portability and Accountability Act and the Declaration of Helsinki. Patient cases were retrospectively selected from the Institute of Clinical Radiology and Nuclear Medicine,

University Medical Center Mannheim, Heidelberg University, Germany. The study population included 14 females examined during a 17 month period from February 2016 to July 2017. All patients had suspicious findings on full-field digital mammography (BI-RADS category 4 and 5) and DBT was performed for further diagnostic workup. 3/14 (21.4%) patients underwent mammography for routine screening, 4/14 (28.6%) for aftercare following contralateral breast cancer and 10/14 (71.4%) patients presented with suspicious clinical symptoms and mammography was obtained for further diagnostic workup.

In 12 patients DBT was performed unilaterally. Two females had suspect findings in both breasts and DBT was obtained bilaterally. Subsequently, 16 breasts were scanned. Two projection views (medio-lateral oblique and craniocaudal) were acquired per breast. Finally, 32 consecutive data sets were included in the evaluation.

Histopathology served as reference standard for all primary lesions that led to the categorization BI-RADS 4 or 5. In case of additional lesions, that appear most likely benign on mammography a combination of breast MRI, ultrasound and mammography as well as follow-up imaging of at least 2 years were used to verify benign findings. Further, histopathology of benign findings was available for four breasts, since patients underwent total mastectomy for cancer cure.

Overall, 44 radiographic findings were registered and evaluated of which 27 were cancers and 17 were benign. Radiation dose data were extracted from the DICOM headers of the images.

Image acquisition

DBT projection data of 32 DBT scans of 16 breasts were extracted from the picture archiving and communication system at the Institute of Clinical Radiology and Nuclear Medicine, University Medical Center Mannheim (Heidelberg University, Germany). DBT images were acquired in mediolateral-oblique (MLO) and the craniocaudal (CC) projection views using the wide-angle DBT device Mammomat Inspiration by Siemens (Siemens Healthcare Sector, Erlangen, Germany). In each projection view, 25 projection images were acquired over an angular range of approximately 50° ($\pm 25^\circ$ around the MLO/CC position) using an anode/filter combination of W/Rh while the detector was stationary.

Reconstruction methods applied to patient data

The 25 unprocessed projection images were used for tomographic reconstructions. Graphics processing unit (GPU)-based reconstruction was performed using a NVIDIA GeForce GTX 470 (1280 MB) graphics card installed in an ACPI Multi-processor x64-based PC [Microsoft Windows XP Professional x64 Edition operating system, DualCore Intel Pentium D 945 processor, 3417 MHz, system Board: MSI 975X Platinum PowerUp Edition (MS-7246), system memory: 7296 MB].

Filtered-back projection reconstruction

For the FBP reconstructions, each projection image was filtered with a ramp filter (*i.e.*, von Hann filter, spectral filter) to

suppress high frequencies and a slice thickness filter to smooth the images. Images were then back-projected using cone beam geometry. This FBP method was an optimized variant integrated on commercially available Siemens Inspiration units.²³

Heuristic Bayesian Inference reconstruction

The statistical iterative method we tested, HBI reconstruction, is similar to a previously described method²⁴ but differs in its correction to minimise the residuals of the radial integrals while maintaining the intensities (*i.e.* by using the method of total variation minimization).²¹ The HBI reconstruction algorithm can be written as:

$$x_j^{(k+1)} = x_j^{(k)} \left[1 + \lambda^{(k)} \frac{\sum_{i=1}^I A_{ij} \left(p_i - \sum_{j=1}^J A_{ij} x_j^{(k)} \right)}{\sum_{j=1}^J A_{ij} x_j^{(k)}} \right],$$

where $x_j^{(k)}$ is the value of the j -th component of the vector of unknowns at the k -th iteration, A_{ij} is elements of the projection matrix, p_i is the value of the measured radial integral in the pixel number i , and $\lambda^{(k)}$ is sequence relaxation parameter values ($0 < \lambda^{(k)} < 1$). The parameter $\lambda^{(k)}$ for $k = 0$ was 0.3, while for $k = 1$ it was 0.15. In prior optimization work,²⁵ two iterations was found to yield the best anatomic reproduction and was therefore used in the current work.

Analysis of reconstruction methods

Three expert radiologists with 10, 2 and 6 years of experience in breast imaging interpretation independently evaluated the images on a clinical workstation using two five megapixel monitors that had been routinely calibrated yearly. The reviewing radiologists were blinded to any lesion-specific information, to the reconstruction method used and to the order the images were displayed. The radiologists were free to alter the window and level settings and use the zoom and pan function. No restriction was set on the interpretation time.

The analysis included the following steps:

Review of lesion-specific features

Each breast lesion was evaluated in a side-by-side-review using a 5-point scale (1 = much worse, 2 = slightly worse, 3 = equal, 4 = slightly better, 5 = much better) for the following attributes:

- clarity of lesion edge/spiculations
- noise level (distracting quantum-like noise surrounding the lesion)
- artifact suppression (how severe the artifacts around the lesion were)
- lesion conspicuity (how well the lesion contrasted with neighboring tissues)
- visibility of fibroglandular parenchyma (how much it stood out from fatty tissues)

Breast density assessment

Breast density was classified according to the American College of Radiology Breast Imaging-Reporting And Data System Atlas[®] fifth edition,²⁶ which has the following categories: *A* = The breasts are almost entirely fatty; *B* = There are scattered areas of fibroglandular density; *C* = The breasts are heterogeneously dense (which may obscure small masses); *D* = The breasts are extremely dense (which lowers the sensitivity of mammography). The breast density assessment was performed in a blinded setting at least 1 week after the side-by-side-review, and one single DBT case was interpreted at a time. The cases were displayed and interpreted in random order in two reading sessions. A minimum of one and a half week was allowed between the reading sessions to eliminate potential memory effects.²⁷

Statistical analysis

Statistical analyses of the radiologists' interpretations were done using the visual grading characteristics (VGC) analyzer software.²⁸ An area under the visual grading curve (AUC_{VGC}) was computed to measure image quality of the two image types being compared with 95% confidence intervals generated using bootstrapping.²⁹ AUC_{VGC} ranged from 0 to 1. An AUC_{VGC} value of 0.5 reflected similar image quality for the two image reconstruction types, while an $AUC_{VGC} > 0.5$ indicated the HBI-image quality to be higher than the conventional FBP method, and an $AUC_{VGC} < 0.5$ indicated the HBI image was lower quality. Image quality was considered significantly different from the reference settings when the 95% confidence intervals (within brackets) did not enclose the dashed line ($AUC_{VGC} = 0.5$), which is analogous to a p -value that is below an α of 0.05. Analyses was paired in terms of observations made on lesions, breast parenchyma, and breast density. Stratified analysis was performed by radiographic pattern and histopathology. Radiologists' inter-reader agreement of breast density assessments were analyzed using Fleiss' κ statistics.³⁰

RESULTS

Study population

The study population characteristics and radiographic pattern of each lesion type are presented in Table 1. All findings were visible on both reconstruction methods and were hence included in the side-by-side-analysis.²⁸ The mean pathological tumor size was 19.7 mm (4–75). Average glandular dose (AGD) was 0.72 mGy (0.4–1.22 mGy) per DBT view and 1.46 mGy (0.81–2.42) per breast. The median patient age was 62 (range 48–80 years).

Image quality of radiographic findings

Image quality (AUC_{VGC}) is presented for masses and calcifications (Table 2). For masses, HBI was rated significantly superior to FBP with an $AUC_{VGC} > 0.5$ for noise level, extent of artifacts, clarity of lesion edge and lesion conspicuity. For calcifications, HBI resulted in lower noise surrounding the lesion and a higher suppression of in-plane artifacts. Details of calcifications (conspicuity and border characteristics) were comparable for the two reconstruction methods ($AUC = 0.5$; $p > 0.05$). The visibility of fibroglandular parenchyma was significantly higher for the HBI method than the FBP method ($AUC_{VGC} = 0.82$, $p < 0.01$).

Table 1. Study population characteristics and radiographic presentation of histopathological lesion types.

Parameter		Radiographic presentation				
		Spiculated mass	Indistinct mass	Well-circumscribed mass	Architectural distortion	Calcifications
Lesion type	n (%)					
Carcinoma of no special type	19	11	7		1	
Invasive lobular carcinoma	4	1	3			
Invasive tubular carcinoma	1	1				
Ductal carcinoma <i>in situ</i>	3					3
Benign calcifications	8					8
Fibroadenoma	2			2		
Cysts	7			7		
Total	44	12	10	10	1	11

Subanalysis of lesion-specific image quality by radiographic pattern and histopathology

Figure 1 presents the image quality parameters (AUC_{VGC}) correlated to (a) the specific radiographic pattern of each lesion and (b) the histopathology of each lesion. HBI significantly improved the image quality of all masses regardless of their morphologic subtype. This was also the case for the lesions' borders, image noise level and severity of artifacts surrounding the lesion. The lesion's conspicuity was increased for HBI relative to FBP for all readers, but this increase was not statistically significant. For lesion histopathology, incremental effects of HBI reconstructions were found for malignant as well as benign lesions. Again, the lesions' borders, image noise level and artifact suppression improved for all histopathological subtypes except for ductal carcinomas *in situ*, where there was no difference in the lesions border visibility.

There was only one case of a carcinoma of no special type that presented as architectural distortion (the statistical power is low and the 95% confidence intervals wide). Nevertheless, even for

this case, HBI images provided improved characteristics of the lesions' borders, the image noise level and the severity of artifacts surrounding the lesion, but with no significant effect on conspicuity.

Figures 2–6 illustrate patients with breast lesions and the different types of DBT image reconstruction methods.

Breast density assessment

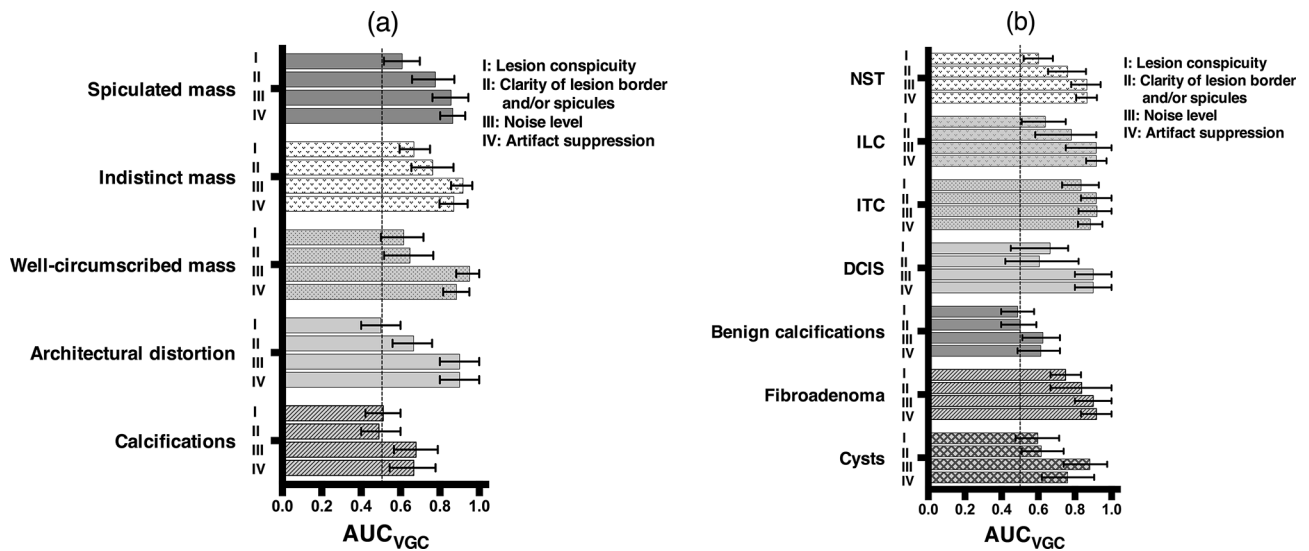
Assessed breast density categories were significantly lower using HBI compared to FBP ($p = 0.016$). On average, five cases per radiologist were downgraded when HBI was used, three of which changed from dense breasts (breast density category C or D) to fatty breasts (breast density category category A or B) (Figure 7). Figure 8 illustrates a case where the breast density category was downgraded using the HBI reconstruction. On average, two cases per radiologist were upgraded when HBI was used. Readers of FBP and HBI reconstructed images had a fair level of agreement ($K_{FBP} = 0.375$ and $K_{HBI} = 0.356$).

Table 2. Image quality assessment of the radiographic findings. Image quality metric is the AUC_{VGC} , which is presented with 95% CIs. When the CI values do not enclose 0.5, the difference is statistically significant.

Image quality Parameter	Radiographic findings							
	Masses ($n = 33$)				Calcifications ($n = 11$)			
	Reader #				Reader #			
	1	2	3	All	1	2	3	All
Lesion conspicuity	0.53 [0.42–0.64]	0.61 [0.52–0.68]	0.74 [0.63–0.83]	0.63 [0.57–0.68]	0.47 [0.27–0.67]	0.50 [0.40–0.60]	0.57 [0.50–0.67]	0.51 [0.42–0.60]
Clarity of lesion edges	0.83 [0.74–0.90]	0.66 [0.53–0.77]	0.73 [0.62–0.83]	0.74 [0.67–0.81]	0.46 [0.23–0.70]	0.43 [0.30–0.60]	0.57 [0.50–0.67]	0.49 [0.40–0.60]
Noise level	0.96 [0.91–0.99]	0.85 [0.75–0.93]	0.89 [0.80–0.97]	0.90 [0.85–0.95]	0.67 [0.43–0.87]	0.80 [0.60–0.93]	0.57 [0.50–0.67]	0.68 [0.57–0.79]
Artifact suppression	0.91 [0.86–0.97]	0.78 [0.68–0.87]	0.92 [0.87–0.97]	0.87 [0.83–0.91]	0.68 [0.38–0.94]	0.67 [0.54–0.81]	0.68 [0.54–0.81]	0.67 [0.54–0.78]

AUC_{VGC} , area under the visual grading curve; CI, confidence interval.

Figure 1. Subanalysis of the two reconstruction methods according to (a) radiographic pattern and (b) microscopic lesion type. A performance indicator (AUC_{VGC}) larger than 0.5 indicate a higher quality for the iterative Bayesian method when compared with the standard filtered-back projection method. Where the 95% confidence intervals do not enclose the line at 0.5, the difference is statistically significant. AUC_{VGC} , area under the visual grading curve; DCIS, ductal carcinomas *in situ*; ILC, invasive lobular carcinoma.



DISCUSSION

In this study, the HBI reconstruction and concurrent FBP reconstruction were compared for 32 DBT data sets acquired with a wide-angle DBT system. To the authors’ knowledge this study

is the first to evaluate these algorithms, which were applied on DBT data sets that were obtained in a clinical setting for the diagnostic workup of patients with unclear findings on conventional mammography.

Figure 2. A 50-year-old patient with two spiculated masses in the upper and lower quadrant of her left breast. Histology confirmed a bifocal carcinoma of no specific type (12mm and 25mm; indicated by white arrows). (a). Image reconstructed using FBP. (b). Image reconstructed using the iterative Bayesian-based method (HBI). Visibility of the fibroglandular tissue was rated higher on the HBI method by all three radiologists.

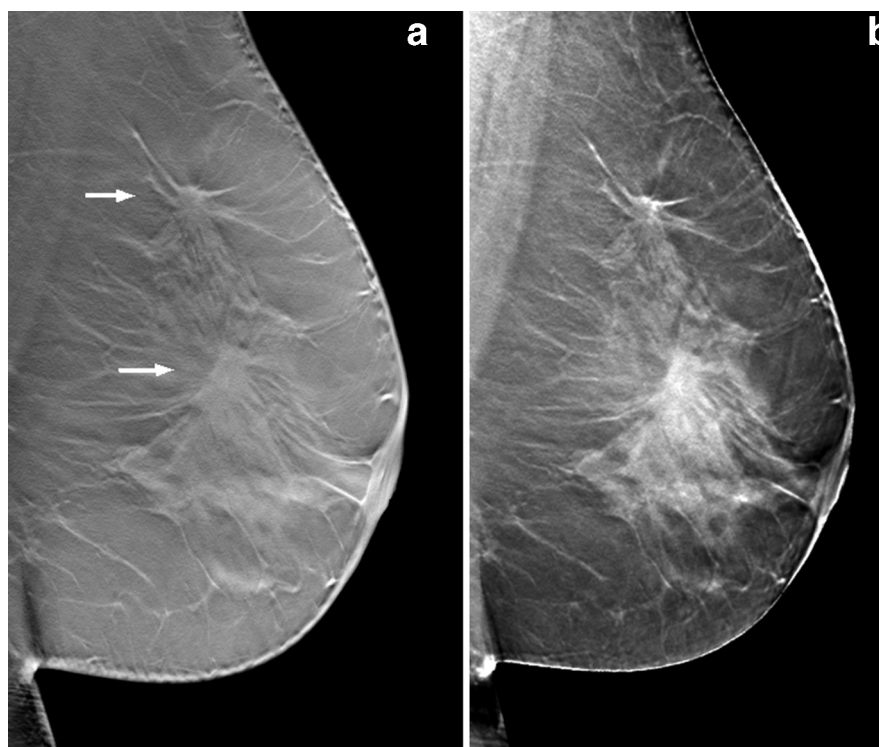
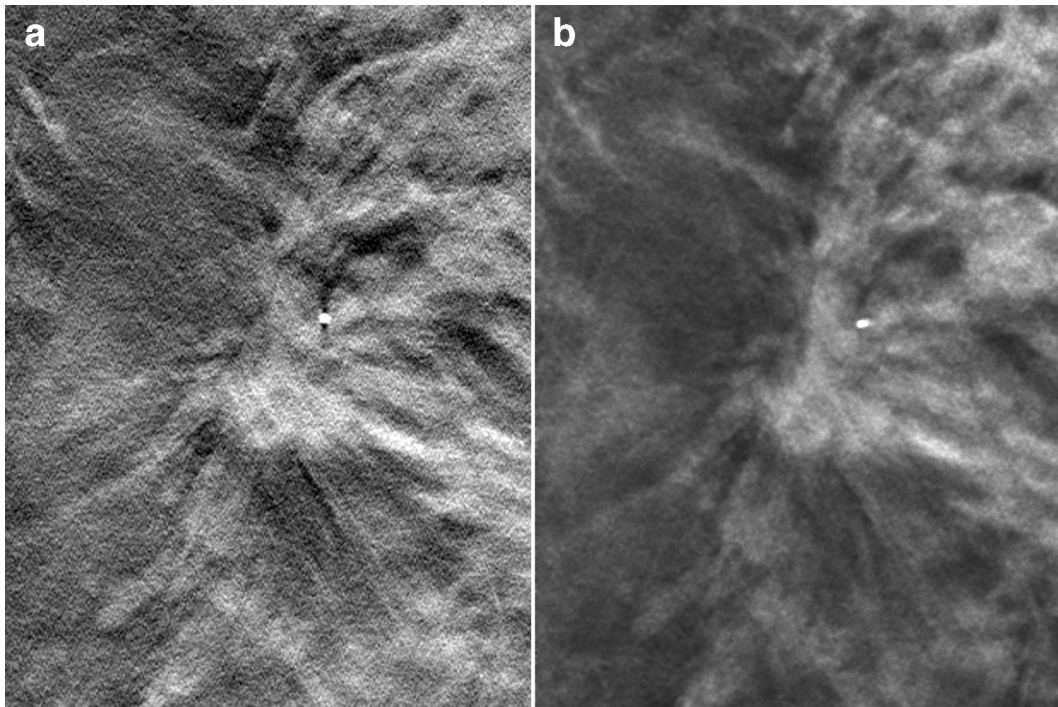


Figure 3. A unifocal 29mm invasive lobular carcinoma. (a) FBP reconstruction. (b) HBI reconstruction. The noise level and the artifacts surrounding the lesion and the image noise were significantly reduced using the HBI method.



We found that the HBI method significantly improved the image quality of breast lesions in DBT, which is important because increased image quality could in turn improve diagnostic accuracy. For all lesion types, two parameters in particular were significantly

improved, namely the image noise level and the artifacts surrounding the lesion. Interestingly, we found differences between masses and calcifications in lesion conspicuity and the clarity of lesion border. For masses ($n = 33$), conspicuity and border clarity significantly

Figure 4. Magnification view of the right breast containing a single macrocalcification typical for a calcified fat necrosis and a well-circumscribed oval mass (a cyst). (a) FBP reconstruction. (b) HBIR reconstruction. Artifacts (dark signals indicated with white arrows) surrounding the lesions in scan direction and skinline (brighter signals indicated with an arrow) are less pronounced with the HBIR method.

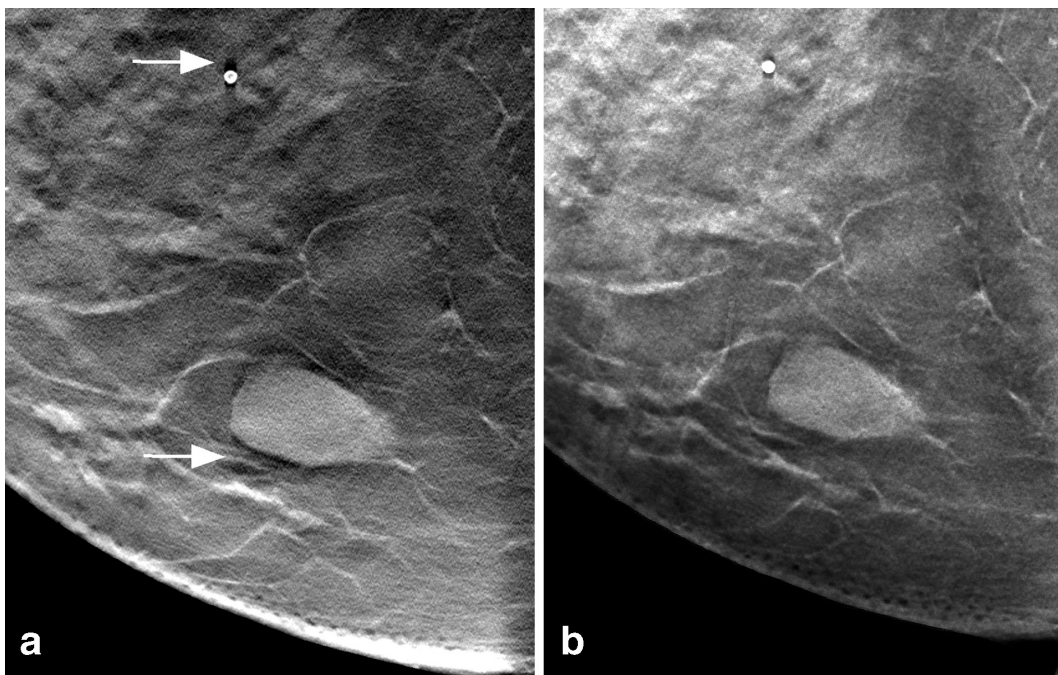
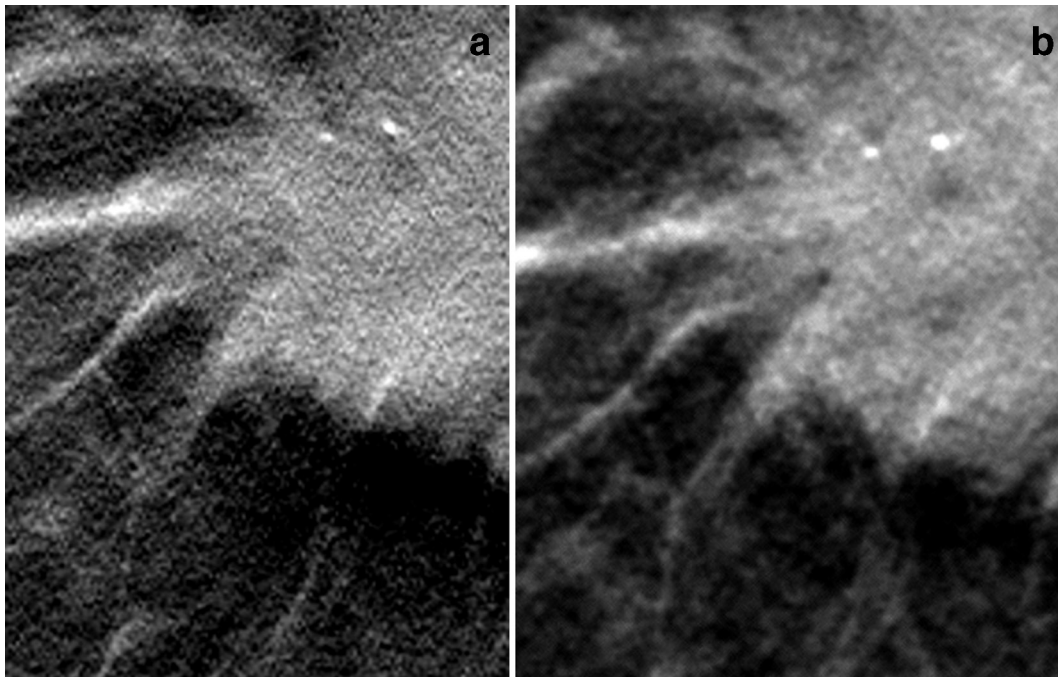
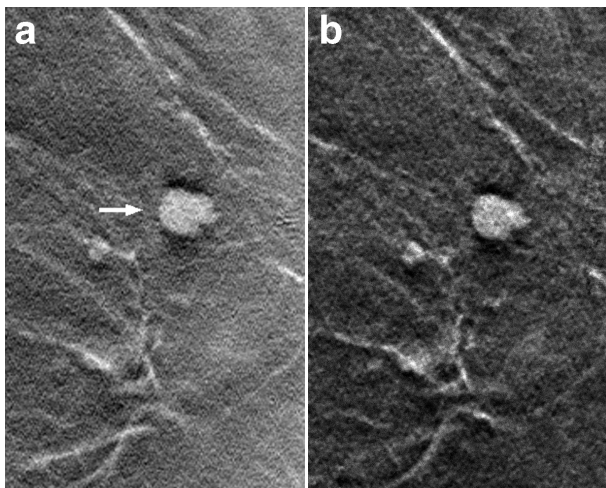


Figure 5. Magnification view of finer microcalcifications (from the left to the right; indicated with an arrow):-200 and 425 microns within a 22mm invasive ductal carcinoma using (a) FBP and (b) HBI.



improved using HBI method, while calcifications ($n = 11$) were found to be equally conspicuous with no difference in border visibility by the methods. This is mainly due to the high contrast that calcifications naturally exhibit compared to soft tissue lesions. In literature, the detection of calcifications was initially considered as one of the major limitations of DBT. Reducing the image noise level and the extent of artifacts surrounding the calcs might be advantageous here, especially for smaller and/or lower contrast lesions (Figure 5). Since there were only few patients with microcalcifications in this study, the majority of calcifications evaluated were

Figure 6. Well-circumscribed lobulated lesion. (a) FBP reconstruction. (b) HBI reconstruction. The overall noise level was significantly more pronounced when using the FBP method, which can affect the lesion edge (see also Table 2). Breast MRI confirmed a 5mm cyst.



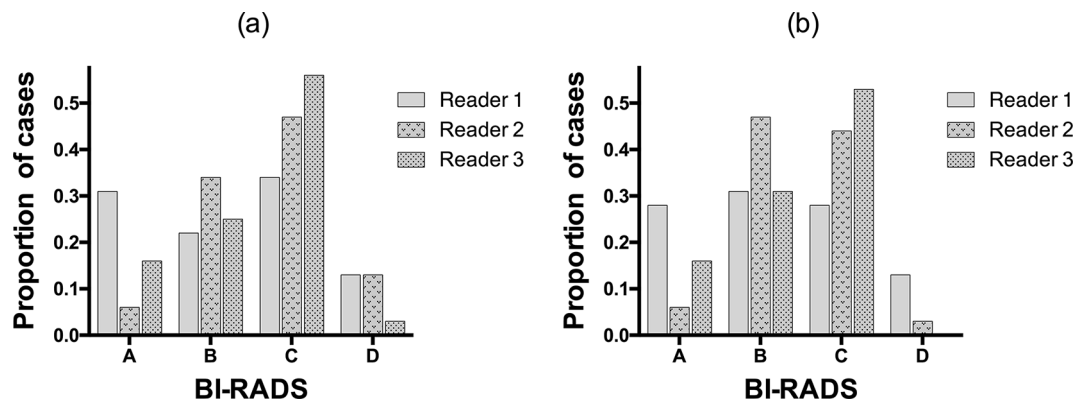
marcocalcifications (Table 1). Further studies are needed,^{6,31,32} that especially focus on the evaluation of micro- compared to macro-calcification, to proof our trend, that HBI reduces the artifacts surrounding the lesions but not impacts the border visibility.

We could not draw any conclusions about architectural distortions because the sample size was low with only one case. However, the image in that case followed the trend seen for masses, with improvement in image quality in the HBI reconstruction compared to that of FBP.

The potential reduction of artifacts using HBI reconstruction while at the same time reducing image noise level is a very important finding (Figures 2–6). In-plane artifacts typically surround a lesion and can appear as darker or brighter signals, depending on the attenuation of the surrounding tissue. These artifacts typically occur along the scan direction of the DBT system and are more pronounced for structures of higher contrasts such as large calcifications or metal clips. Artifacts surrounding the lesions may to a certain degree act as enhancers. Thus, it has been suggested they might be beneficial at the initial detection.³³ However, it is irrevocable, that these artifacts represent erroneous signals that mainly disturb the perception of the lesion's morphology and the visibility of surrounding structures^{33,34} and therefore obscure clinically relevant findings adjacent to the lesion.³⁵ Using HBI reconstruction should increase lesion detectability and improve lesion perception, which lead to higher cancer detection rates.

HBI reconstruction also significantly improved the clarity of borders and conspicuity of breast masses, which should allow easier differentiation between benign and malignant lesions. Improvement in this image parameter could lead to a reduction

Figure 7. Breast density BI-RADS categorized using either (a) FBP or (b) HBI reconstructed digital breast tomosynthesis images for the three readers.

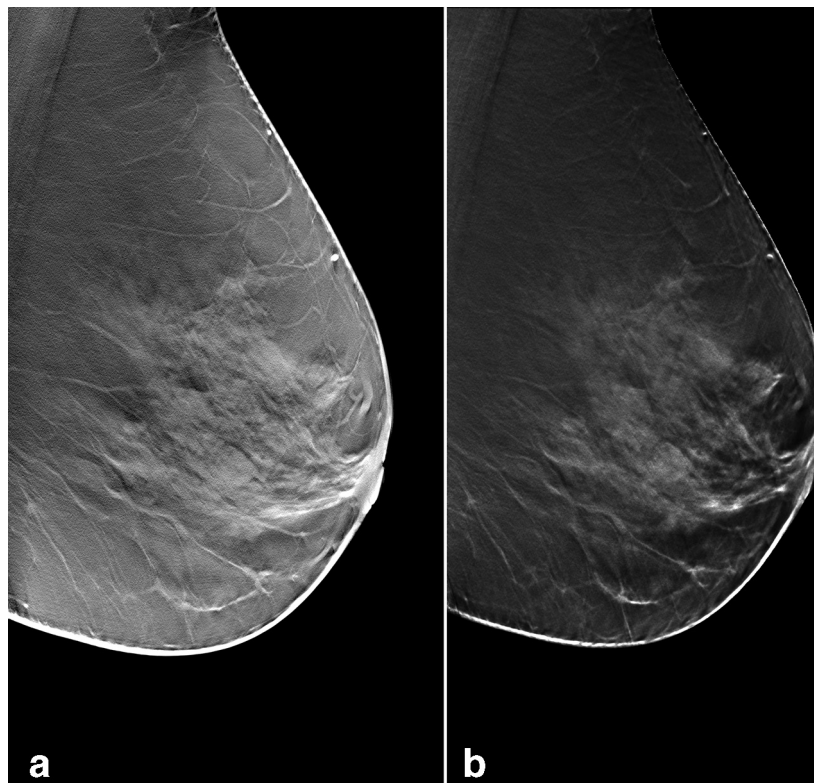


in the recall rate and a higher positive-predictive value for biopsy recommendation.

Invasive lobular carcinoma (ILC) is the second most common microscopic type of invasive breast carcinoma, and it is known to be difficult to detect with either standard full-field digital mammography (FFDM) or DBT.^{6,7} However, a number of studies have shown increased detectability of ILC on DBT compared to FFDM, and we also found improved image quality for ILCs (Figure 4), which should help to increase its' detection rate further.

Interestingly, visibility of fibroglandular breast tissue was significantly improved with HBI reconstructed images in the context of a significantly lower BI-RADS breast density score (Figures 7 and 8). Lower breast density increases image sensitivity and reduces the need for additional imaging (*e.g.* through breast MRI). Breast density is usually graded qualitatively on a visual basis during clinical routine, and this evaluation has high inter-reader variability. In this study, the readers had a fair level of agreement about breast density for both reconstruction types. It should be noted that this study included difficult diagnostic cases with a higher frequency

Figure 8. DBT MLO view of the left breast. (a) FBP reconstruction. (b) HBI reconstruction. Breast density was categorized as ACR BI-RADS C by all radiologists reviewing the FBP-reconstructions, which was downgraded to ACR BI-RADS B by two of the radiologists when reviewing the HBI-reconstructions, likely due to a clearer reproduction of fatty and fibroglandular tissues.



of dense breasts, which may have caused further inter-rating variability compared to the general screening population.

Most experts agree that the risks associated with the radiation dose of mammography are negligible in a curative clinical setting.^{36,37} However, the screening situation is different in that a very large population of healthy females are exposed to radiation. Therefore, any increase in risk, even if small, has to be taken seriously.^{36,37} By significantly increasing the image quality, our results indirectly suggest that the HBI method allow the use of lower radiation dosages while maintaining image quality.¹² It would be interesting to examine explicitly how much the radiation dose to the breast could be reduced by using the HBI method. Alternatively, it may allow more scan projections to be taken at a corresponding dose level yielding a more complete three-dimensional volume of the breast. However, acquiring more projections may be constrained by the stationary position of the detector.

A potential limitation of this study is the descriptive nature of the analysis. A side-by-side-analysis is a very direct type of evaluation but it is usually not blinded. Even if the radiologists were unaware of lesion-specific details such as histopathology and the type of reconstruction used, recognizing typical characteristics between reconstruction methods may cause a subjective preference among the readers. However, since the evaluation tasks were very specific and the readers agreed (Table 2) such an effect was probably negligible. In contrast, the breast density evaluation was performed in a blinded manner with a wash-out period of at least one and a half

week in between the reading sessions and the cases were displayed in random order.²⁷ Thus, we do not expect relevant memory effects.²⁷ Finally, the study material itself included a limited number of patients, although a relatively large number of pathologies were evaluated ($n = 44$).

The results of lower HBI-breast density classifications have implications in the subjective risk assessment of breast cancer in denser breast, and risk assessment may need to be revised with regards to the specific reconstruction method used. Future studies could compare reconstructed HBI-assessed breast density with breast density assessed on MRI, which is often regarded as the gold-standard for measuring breast density.

In conclusion, HBI significantly improves image quality and lesion visibility compared to FBP. HBI-visibility of fibroglandular breast tissue increased while breast densities were rated lower. Applying the HBI algorithm may improve the diagnostic performance of DBT and decrease the need for additional imaging in patients with dense breasts. This may lead to higher cancer detection rates and a reduced number of unnecessary biopsies. It may result in patient dose savings, which is of special relevance in the screening context.

ACKNOWLEDGEMENTS

The authors thank Dr. Jennifer C. Ast, Uppsala University, Sweden, for valuable and insightful discussions.

REFERENCES

1. Svahn T, Andersson I, Chakraborty D, Svensson S, Ikeda D, Förnvik D, et al. The diagnostic accuracy of dual-view digital mammography, single-view breast tomosynthesis and a dual-view combination of breast tomosynthesis and digital mammography in a free-response observer performance study. *Radiat Prot Dosimetry* 2010; **139**(1-3): 113–7. doi: <https://doi.org/10.1093/rpd/ncq044>
2. Svahn TM, Chakraborty DP, Ikeda D, Zackrisson S, Do Y, Mattsson S, et al. Breast tomosynthesis and digital mammography: a comparison of diagnostic accuracy. *Br J Radiol* 2012; **85**: e1074–82. doi: <https://doi.org/10.1259/bjr/53282892>
3. Rafferty EA, Park JM, Philpotts LE, Poplack SP, Sumkin JH, Halpern EF, et al. Assessing radiologist performance using combined digital mammography and breast tomosynthesis compared with digital mammography alone: results of a multicenter, multireader trial. *Radiology* 2013; **266**: 104–13. doi: <https://doi.org/10.1148/radiol.12120674>
4. Rafferty EA, Park JM, Philpotts LE, Poplack SP, Sumkin JH, Halpern EF, et al. Diagnostic accuracy and recall rates for digital mammography and digital mammography combined with one-view and two-view tomosynthesis: results of an enriched reader study. *AJR Am J Roentgenol* 2014; **202**: 273–81. doi: <https://doi.org/10.2214/AJR.13.11240>
5. Ciatto S, Houssami N, Bernardi D, Caumo F, Pellegrini M, Brunelli S, et al. Integration of 3D digital mammography with tomosynthesis for population breast-cancer screening (storm): a prospective comparison study. *Lancet Oncol* 2013; **14**: 583–9. doi: [https://doi.org/10.1016/S1470-2045\(13\)70134-7](https://doi.org/10.1016/S1470-2045(13)70134-7)
6. Krammer J, Stepniowski K, Kaiser CG, Brade J, Riffel P, Schoenberg SO, et al. Value of additional digital breast Tomosynthesis for preoperative staging of breast cancer in dense breasts. *Anticancer Res* 2017; **37**: 5255–61. doi: <https://doi.org/10.21873/anticancer.11950>
7. Mariscotti G, Durando M, Houssami N, Zuiani C, Martincich L, Londero V, et al. Digital breast tomosynthesis as an adjunct to digital mammography for detecting and characterising invasive lobular cancers: a multi-reader study. *Clin Radiol* 2016; **71**: 889–95. doi: <https://doi.org/10.1016/j.crad.2016.04.004>
8. Skaane P, Sebuødegård S, Bandos AI, Gur D, Østerås BH, Gullien R, et al. Performance of breast cancer screening using digital breast tomosynthesis: results from the prospective population-based Oslo Tomosynthesis screening trial. *Breast Cancer Res Treat* 2018; **169**: 489–96. doi: <https://doi.org/10.1007/s10549-018-4705-2>
9. Conant EF, Barlow WE, Herschorn SD, Weaver DL, Beaber EF, Tosteson ANA, et al. Association of digital breast Tomosynthesis vs digital mammography with cancer detection and recall rates by age and breast density. *JAMA Oncol* 2019; **5**: 635. doi: <https://doi.org/10.1001/jamaoncol.2018.7078>
10. Kontos D, Bakic PR, Carton A-K, Troxel AB, Conant EF, Maidment ADA. Parenchymal texture analysis in digital breast tomosynthesis for breast cancer risk estimation: a preliminary study. *Acad Radiol*

- 2009; **16**: 283–98. doi: <https://doi.org/10.1016/j.acra.2008.08.014>
11. Kontos D, Ikejimba LC, Bakic PR, Troxel AB, Conant EF, Maidment ADA. Analysis of parenchymal texture with digital breast tomosynthesis: comparison with digital mammography and implications for cancer risk assessment. *Radiology* 2011; **261**: 80–91. doi: <https://doi.org/10.1148/radiol.11100966>
 12. Maldera A, De Marco P, Colombo PE, Origgi D, Torresin A. Digital breast tomosynthesis: dose and image quality assessment. *Phys Med* 2017; **33**: 56–67. doi: <https://doi.org/10.1016/j.ejmp.2016.12.004>
 13. Svahn TM, Houssami N, Sechopoulos I, Mattsson S. Review of radiation dose estimates in digital breast tomosynthesis relative to those in two-view full-field digital mammography. *Breast* 2015; **24**: 93–9. doi: <https://doi.org/10.1016/j.breast.2014.12.002>
 14. Zackrisson S, Lång K, Rosso A, Johnson K, Dustler M, Förnvik D, et al. One-view breast tomosynthesis versus two-view mammography in the Malmö breast Tomosynthesis screening trial (MBTST): a prospective, population-based, diagnostic accuracy study. *Lancet Oncol* 2018; **19**: 1493–503. doi: [https://doi.org/10.1016/S1470-2045\(18\)30521-7](https://doi.org/10.1016/S1470-2045(18)30521-7)
 15. Svahn TM, Sjöberg T, Ast JC. Dose estimation of ultra-low-dose chest CT to different sized adult patients. *Eur Radiol* 2019; **29**: 4315–4323. doi: <https://doi.org/10.1007/s00330-018-5849-5>
 16. Goenka AH, Herts BR, Obuchowski NA, Primak AN, Dong F, Karim W, et al. Effect of reduced radiation exposure and iterative reconstruction on detection of low-contrast low-attenuation lesions in an anthropomorphic liver phantom: an 18-reader study. *Radiology* 2014; **272**: 154–63. doi: <https://doi.org/10.1148/radiol.14131928>
 17. Geiser WR, Einstein SA, Yang W-T. Artifacts in digital breast Tomosynthesis. *American Journal of Roentgenology* 2018; **211**: 926–32. doi: <https://doi.org/10.2214/AJR.17.19271>
 18. Rodríguez-Ruiz A, Castillo M, Garayoa J, Chevalier M. Evaluation of the technical performance of three different commercial digital breast tomosynthesis systems in the clinical environment. *Physica Medica* 2016; **32**: 767–77. doi: <https://doi.org/10.1016/j.ejmp.2016.05.001>
 19. Reiser I, Sechopoulos I. Review of digital breast tomosynthesis. *Med Phys Int J* 2014; **2**: 57–66.
 20. Wu T, Moore RH, Rafferty EA, Kopans DB. A comparison of reconstruction algorithms for breast tomosynthesis. *Med Phys* 2004; **31**: 2636–47. doi: <https://doi.org/10.1118/1.1786692>
 21. Gomi T, Koibuchi Y. Use of a total variation minimization iterative reconstruction algorithm to evaluate reduced projections during digital breast Tomosynthesis. *Biomed Res Int* 2018; **14**: 5239082: 5239082: 14. doi: <https://doi.org/10.1155/2018/5239082>
 22. Xu S. *Chen, Y. A Compton Scattering Suppression based Image Reconstruction method for Digital Breast Tomosynthesis*. San Antonio, Texas, USA.: IEEE International Workshop on Genomic Signal Processing and Statistics; 2011.
 23. Mertelmeier T, Orman J, Haerer W, Dudam MK. Optimizing filtered backprojection reconstruction for a breast tomosynthesis prototype device. *Proc SPIE* 2006;.
 24. Lange K, Fessler JA. Globally convergent algorithms for maximum a posteriori transmission tomography. *IEEE Trans. on Image Process.* 1995; **4**: 1430–8. doi: <https://doi.org/10.1109/83.465107>
 25. Zolotarev SA, Vengrinovich VL, Linev VN. Estimating the efficiency of the simultaneous algebraic reconstruction technique (SART), Bayesian inference reconstruction (BIR), and traditional shift-and-add (SAA) tomosynthesis using medical phantoms. *Pattern Recognit. Image Anal.* 2014; **24**: 324–32. doi: <https://doi.org/10.1134/S1054661814020187>
 26. Rao AA, Feneis J, Lalonde C, Ojeda-Fournier H. A pictorial review of changes in the BI-RADS fifth edition. *Radiographics* 2016; **36**: 623–39. doi: <https://doi.org/10.1148/rg.2016150178>
 27. Hardesty LA, Ganott MA, Hakim CM, Cohen CS, Clearfield RJ, Gur D. "Memory effect" in observer performance studies of mammograms. *Acad Radiol* 2005; **12**: 286–90. doi: <https://doi.org/10.1016/j.acra.2004.11.026>
 28. Båth M, Månsson LG. Visual grading characteristics (VGC) analysis: a non-parametric rank-invariant statistical method for image quality evaluation. *Br J Radiol* 2007; **80**: 169–76. doi: <https://doi.org/10.1259/bjr/35012658>
 29. Båth M, Hansson J. VGC analyzer: a software for statistical analysis of fully crossed MULTIPLE-READER multiple-case visual grading characteristics studies. *Radiat Prot Dosimetry* 2016; **169**(1-4): 46–53. doi: <https://doi.org/10.1093/rpd/ncv542>
 30. Landis JR, Koch GG. The measurement of observer agreement for categorical data. *Biometrics* 1977; **33**: 159–74. doi: <https://doi.org/10.2307/2529310>
 31. Zolotarev SA. Estimating the efficiency of the simultaneous algebraic recovery technique (SART), Bayesian inference reconstruction (BIR), and traditional shift-and-add (SAA) tomosynthesis using medical phantoms. pattern recognition and image analysis. 2014; **24**: 337–45.
 32. Alvare G, Gordon R. Foxels for high flux, high resolution computed tomography (foxelct) using broad X-ray focal spots. *Radiology and Diagnostic Imaging* 2017; **1**. doi: <https://doi.org/10.15761/RDI.1000103>
 33. Svahn TM, Houssami N. Evaluation of time-efficient reconstruction methods in digital breast tomosynthesis. *Radiat Prot Dosimetry* 2015; **165**(1-4): 331–6. doi: <https://doi.org/10.1093/rpd/ncv079>
 34. Tirada N, Li G, Dreizin D, Robinson L, Khorjekar G, Dromi S, et al. Digital breast Tomosynthesis: physics, artifacts, and quality control considerations. *Radiographics* 2019; **39**: 413–26. doi: <https://doi.org/10.1148/rg.2019180046>
 35. Hu Y-H, Zhao B, Zhao W. Image artifacts in digital breast tomosynthesis: investigation of the effects of system geometry and reconstruction parameters using a linear system approach. *Med Phys* 2008; **35**: 5242–52. doi: <https://doi.org/10.1118/1.2996110>
 36. International Commission on Radiological Protection 1990 recommendations of the International Commission on radiological protection. *Annals of ICRP* 1991; **21**: 1–3.
 37. The 2007 recommendations of the International Commission on radiological protection. ICRP publication 103. *Ann ICRP* 2007; **37**(2-4): 1–332.

Received:
26 September 2016

Revised:
17 December 2016

Accepted:
12 January 2017

<https://doi.org/10.1259/bjr.20160770>

Cite this article as:

Waade GG, Moshina N, Sebuødegård S, Hogg P, Hofvind S. Compression forces used in the Norwegian Breast Cancer Screening Program. *Br J Radiol* 2017; **90**: 20160770.

FULL PAPER

Compression forces used in the Norwegian Breast Cancer Screening Program

¹GUNVOR G WADE, MSc, ²NATALIIA MOSHINA, MD, MSc, ²SOFIE SEBUØDEGÅRD, MSc, ^{3,4}PETER HOGG, PhD and ^{1,2}SOLVEIG HOFVIND, PhD

¹Department of Life Sciences and Health, Faculty of Health Sciences, Oslo and Akershus University College of Applied Sciences, Oslo, Norway

²Cancer Registry of Norway, Oslo, Norway

³Directorate of Radiology, University of Salford, Manchester, UK

⁴Karolinska Institute, Stockholm, Sweden

Address correspondence to: Professor Solveig Hofvind

E-mail: solveig.hofvind@kreftregisteret.no

Objective: Compression is used in mammography to reduce breast thickness, which is claimed to improve image quality and reduce radiation dose. In the Norwegian Breast Cancer Screening Program (NBCSP), the recommended range of compression force for full-field digital mammography (FFDM) is 11–18 kg (108–177 N). This is the first study to investigate the compression force used in the programme.

Methods: The study included information from 17,951 randomly selected females screened with FFDM at 14 breast centres in the NBCSP, during January–March 2014. We investigated the applied compression force on the left breast in craniocaudal and mediolateral oblique views for breast centres, mammography machines within the breast centres and for the radiographers.

Results: The mean compression force for all mammograms in the study was 116 N and ranged from 91 N to

147 N between the breast centres. The variation in compression force was wider between the breast centres than that between mammography machines (range 137–155 N) and radiographers (95–143 N) within one breast centre. Approximately 59% of the mammograms in the study complied with the recommended range of compression force.

Conclusion: A wide variation in applied compression force was observed between the breast centres in the NBCSP. This variation indicates a need for evidence-based recommendations for compression force aimed at optimizing the image quality and individualizing breast compression.

Advances in knowledge: There was a wide variation in applied compression force between the breast centres in the NBCSP. The variation was wider between the breast centres than that between mammography machines and radiographers within one breast centre.

INTRODUCTION

Breast compression is used in mammography to reduce breast thickness with the intention of decreasing radiation dose and improving image quality.^{1–3} However, breast compression might lead to discomfort and pain for the females who undergo mammography⁴ and this might affect the female's experience, leading to reduced screening participation.^{5,6}

There are currently no evidence-based recommendations regarding optimal breast compression in mammography. The European guidelines for quality assurance in breast cancer screening and diagnosis state that “the breast should be properly compressed, but no more than is necessary to achieve a good image quality”.¹ The guidelines from the National Health Service Breast Screening Programme in

the UK state that “the force of the compression on the X-ray machine should not exceed 200 Newtons or 20 kg”.⁷ The lack of precise and objective recommendations for breast compression might lead to variations in applied compression between radiographers and breast centres. Studies by Mercer et al^{8–10} and Branderhorst et al¹¹ have reported large variations in compression force between radiographers^{8–10} and screening sites^{10,11} and that compression force is highly dependent on the radiographer rather than on the screened females. These findings have been reported for both screen film^{8–10} and full-field digital mammography (FFDM).¹¹

The quality assurance manual of the Norwegian Breast Cancer Screening Program (NBCSP) recommends that the compression force for FFDM be between 11 kg and 18 kg

(1 kg = 9.81 N; 11–18 kg = 108–177 N).¹² As the first step towards establishing evidence-based guidelines for compression force in mammography, we investigated the applied compression force for the breast centres, mammography machines within the breast centres and for the radiographers in the NBCSP.

METHODS AND MATERIALS

This study received ethical approval from the Data Protection Official of the Cancer Registry of Norway (Reference 2014/15279).

The NBCSP started in 1996 and expanded gradually to become nationwide in 2005.¹³ Females aged 50–69 years are invited biennially for two-view mammography, including craniocaudal (CC) and mediolateral oblique (MLO) views. About 300,000 females were invited in 2015. The programme includes 26 stationary and 4 mobile mammography machines administered by 16 breast centres. The breast centres cover different geographical areas corresponding to the counties. The Cancer Registry of Norway is responsible for administration and quality assurance of the programme.¹⁴ The National Radiation Protection Authority is responsible for regular technical quality control of the mammography equipment in the screening programme.¹⁵ This work is performed in collaboration with a dedicated quality assurance radiographer at each breast centre. The specification for compression force is that the compression force indicated on the machine be within ± 10 N of the measured value.¹⁵

Data collection

An e-mail with information about the study and a request for participation was sent from the head of the NBCSP to all the leaders at the 16 breast centres in the programme. Employees at the Cancer Registry performed the randomization for 1550 screening examinations for each breast centre performed in the period January–March 2014. The number of examinations was based on power analyses. A list was sent to each breast centre including a running number and the 11-digit personal identification number (PIN) given to all inhabitants in Norway. The PIN was used to identify the images.

The quality assurance radiographers at the breast centres used the PIN to identify the examinations in the Picture Archiving and Communication System (PACS). Information about compression force, compressed breast thickness and initials of the radiographers who performed the examinations was manually extracted and registered into Excel. 15 breast centres returned data to the Cancer Registry together with the running number. However, data from one breast centre were excluded, as digital breast tomosynthesis was used for screening during the study period.¹⁶ We received information from 19,114 examinations, varying from 297 to 1550 examinations per breast centre. Each breast centre had 1–3 stationary and mobile mammography machines, typically staffed by the same radiographers.

In this study, “breast centre” refers to one of the 14 breast centres, while “mammography machine” refers to the mammography machines used for screening within 1 breast centre (26 mammography machines in total). The breast centres were anonymized with letters (A–N) and the mammography

machines with a letter, indicating the centre, and a number indicating the different machines (*i.e.* A1).

We excluded screening examinations with less ($n = 143$) or more ($n = 670$) than four standard mammograms (left and right breast in CC and MLO views); examinations on females with breast implants ($n = 163$), pacemakers ($n = 7$), physical or psychological disorders ($n = 2$); or other reasons ($n = 27$). Further, examinations with single mammograms registered with an extreme value of compression force (outside range 20–200 N) or compressed breast thicknesses (outside range 10–110 mm) were considered as typographical errors and were therefore excluded ($n = 151$ examinations). This left 17,951 screening examinations for analysis.

There was no statistically significant difference in the compression force of left and right breasts. Therefore, information from the mammograms of only the left breast was used in the analyses to avoid double values from the same females. Information from 35,902 mammograms was available in total, 17,951 CC and 17,951 MLO. Descriptive results from the right breast are shown in Appendix A. The mammograms were acquired using FFDM systems from Siemens (Mammomat Inspiration; $n = 7282$ examinations), General Electric [GE; Senographe Essential; $n = 6215$ examinations (3336 on stationary mammography machines and 2879 on mobile mammography machines)], Philips (Microdose Mammography L50; $n = 1492$ examinations/Sectra Microdose Mammography L30; $n = 1502$ examinations) or Hologic (Hologic Selenia Dimensions; $n = 1460$ examinations) (Table 1).

Data analysis

All data regarding compression force were analyzed in Newtons. As data were normally distributed, means and 95% confidence intervals (CIs) were used for investigating compression force, by breast centre, mammography machines within breast centres and in total. The observed values of compression force were compared with the recommended level of compression force (108–177 N) indicated within the Quality Assurance Manual of the NBCSP;¹² the percentages of mammograms below, within and above the recommended values were calculated. This was performed by the breast centre.

A total of 200 radiographers were involved in the imaging, ranging from 8 to 28 radiographers within each breast centre. Information from mammograms without initials of the radiographer who performed the examination ($n = 39$ mammograms) or mammograms acquired by radiographers who had performed < 20 examinations ($n = 69$ mammograms) were excluded from analysis for radiographers. Analyses related to the individual radiographer who fulfilled the inclusion criteria were therefore based on 35,794 mammograms. Mean and median number of mammograms acquired by the radiographers were calculated. Mean and range of compression force were calculated for each radiographer.

Information about the radiographers such as age and years of experience within mammography was obtained by e-mail correspondence with the quality assurance radiographers at the breast centres. This information was available for 154 (77%)

Table 1. Number of screening examinations (*n*), radiographers (*n*), machine vendor, mean compression force (Newton, N) with 95% confidence interval (CI) for craniocaudal (CC) and mediolateral oblique (MLO) views, by breast centre and mammography machines within the breast centres.

Breast centre	Mammography machine	Study population (<i>n</i>)	Radiographers (<i>n</i>)	Machine vendor	Mean (95% CI) Compression force (N)		
					CC and MLO	CC	MLO
A		1506	16	Siemens	117.8 (117.0–118.6)	103.9 (103.2–104.6)	131.7 (130.6–132.8)
	A1	133		Siemens	113.2 (110.9–115.5)	99.0 (97.5–100.5)	127.4 (124.6–130.1)
	A2	462		Siemens	122.4 (120.9–123.9)	110.6 (109.1–112.1)	134.1 (132.0–136.3)
B	A3	911		Siemens	116.2 (115.1–117.2)	101.2 (100.5–102.0)	131.1 (129.8–132.4)
		1492	20	Philips	124.9 (123.7–126.1)	119.6 (118.1–121.0)	130.2 (128.5–132.0)
	B1	455		Philips	121.3 (119.3–123.3)	115.9 (113.6–118.3)	126.7 (123.6–129.8)
C	B2	1047		Philips	126.4 (125.0–127.8)	121.1 (119.3–122.9)	131.7 (129.6–133.9)
		931	9	Siemens/GE	107.3 (106.0–108.6)	94.5 (93.1–95.9)	120.1 (118.3–122.0)
	C1	737		Siemens	104.4 (102.9–105.8)	92.2 (90.8–93.7)	116.5 (114.4–118.6)
D	C2 ^{a,b}	194		GE	118.5 (115.6–121.3)	103.1 (99.7–106.4)	133.8 (130.4–137.3)
		1493	16	GE	118.5 (117.8–119.1)	111.0 (110.2–111.8)	125.9 (125.0–126.8)
	D1 ^d	1326		GE	118.7 (118.0–119.4)	110.8 (110.0–111.7)	126.6 (125.6–127.5)
E	D2	167		GE	116.7 (114.8–118.5)	112.5 (110.1–114.8)	120.9 (118.2–123.7)
		1529	16	Siemens	90.5 (89.7–91.3)	81.1 (80.5–81.7)	99.9 (98.7–101.2)
	E1	914		Siemens	90.3 (89.2–91.3)	78.6 (77.9–79.3)	102.0 (100.4–103.7)
F	E2	615		Siemens	91.8 (89.7–92.0)	84.8 (83.8–85.8)	96.9 (94.9–98.8)
		1466	8	GE	137.5 (136.5–138.5)	122.1 (120.9–123.2)	153.0 (151.7–154.2)
	F1	528		GE	142.8 (140.8–144.7)	125.2 (122.9–127.4)	160.3 (158.0–162.7)
G	F2 ^a	938		GE	134.5 (133.4–135.7)	120.3 (119.0–121.6)	148.8 (147.3–150.3)
		1523	9	Siemens	114.8 (113.9–115.7)	105.9 (105.0–106.9)	123.7 (122.4–125.1)
		1143	22	GE	124.8 (124.1–125.5)	121.1 (120.2–122.1)	128.4 (127.5–129.4)
H	H1	533		GE	129.9 (128.9–130.9)	126.2 (124.8–127.6)	133.6 (132.3–134.9)
		278		GE	118.0 (116.7–119.4)	115.9 (114.1–117.8)	120.1 (118.2–122.1)
	H3	332		GE	122.2 (121.0–123.4)	117.4 (115.7–119.0)	127.0 (125.4–128.6)
I		1502	8	Philips ^c	110.2 (109.0–111.4)	94.4 (93.2–95.6)	125.9 (124.2–127.6)

(Continued)

Table 1. (Continued)

Breast centre	Mammography machine	Study population (n)	Radiographers (n)	Machine vendor	Mean (95% CI) Compression force (N)		
					CC and MLO	CC	MLO
J	J1	622	28	Siemens/GE	114.6 (113.4–115.8)	111.2 (109.7–112.8)	118.0 (116.2–119.8)
	J2 ^a	231		Siemens	113.7 (112.0–115.5)	109.1 (107.1–111.0)	118.4 (115.7–121.1)
K		391		GE	115.1 (113.5–116.7)	112.5 (110.4–114.7)	117.4 (115.4–120.1)
		1498	9	GE	93.2 (92.6–93.8)	90.0 (89.1–90.8)	96.4 (95.6–97.3)
L		1460	13	Hologic	138.9 (138.3–139.6)	134.4 (133.6–135.2)	143.5 (142.5–144.4)
		278	18	Siemens/GE	146.8 (145.0–148.5)	143.9 (141.5–146.3)	149.6 (147.0–152.2)
M	M1	134		Siemens	155.3 (152.9–157.7)	152.1 (148.7–155.5)	158.5 (155.2–161.8)
	M2	114		Siemens	136.9 (134.5–139.4)	133.8 (130.7–136.9)	140.0 (136.2–143.8)
	M3 ^{a,b}	30		GE	146.0 (140.5–151.5)	145.7 (138.6–152.7)	146.3 (137.5–155.2)
N		1508	8	Siemens	112.6 (111.6–113.6)	109.8 (108.6–111.0)	115.4 (113.9–117.0)
Total		17,951	200		116.3 (116.0–116.6)	108.0 (107.6–108.4)	124.6 (124.2–125.0)

^aMobile unit.^bThe same mobile unit which the breast centres share.^cPhilips represents Sectra Microdose Mammography L30.

radiographers. Mean compression force was calculated by age groups (25–34, 35–44, 45–54 and 55–69 years) and years of experience in screening and/or clinical mammography (<5, 6–10, 11–15, 16–20 and >20 years) of the radiographers.

Linear regression was used to explore variation in compression force by breast centre, mammography machines within breast centres, radiographer, age and experience of the radiographer, machine vendor and female body mass index (BMI) (BMI: weight in kilograms/height in square metres). Information regarding weight and height was reported by the females in a questionnaire, which all females received at the same time as the invitation to attend breast screening. This information was available for 60.3% ($n = 10,830$) of the females. Backward elimination and Akaike information criterion were used for selection of the appropriate multivariate linear regression model.

Pearson correlation coefficient (r) was used to identify the correlation between compression force and compressed breast thickness. We also used Pearson correlation coefficient to estimate the accuracy of the manually reported data for two centres where Volpara software (VolparaDensity v. 4; Matakina, Wellington, New Zealand) is installed (Breast Centres D and H). The manually reported information on compression force and compressed breast thickness at the two breast centres ($n = 6226$ mammograms) was compared with information for the same examinations given by Volpara. We assessed correlation according to the following distribution: 0–0.3, negligible correlation; 0.3–0.5, low correlation; 0.5–0.7, moderate correlation; 0.7–0.9 high correlation; and 0.9–1, very high correlation.¹⁷

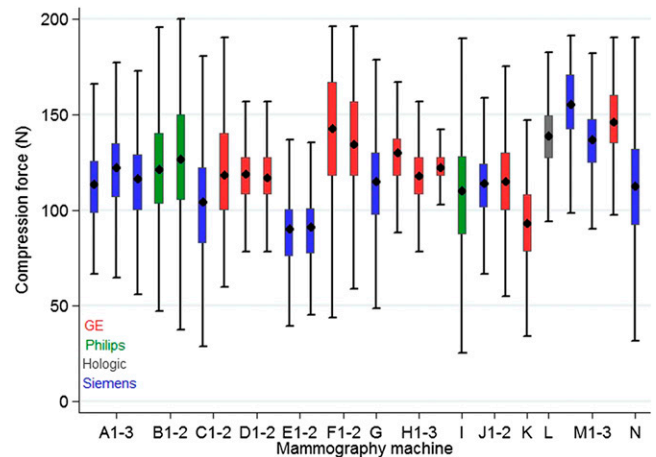
Analysis of variance and Tukey's honestly significant different pairwise comparisons were used to test statistical significance. All statistical analyses were conducted using Stata Statistical Software v. 14 (Stata Corp., College Station, TX).

RESULTS

Mean compression force for the mammograms performed in the NBCSP during the study period was 116 N (95% CI: 116.0–116.6) (Table 1). It was 108 N (95% CI: 107.6–108.4) for CC and 125 N (95% CI: 124.2–125.0) for MLO (Table 1). The range of mean compression force was wider between the breast centres than that between mammography machines within one breast centre (Figure 1). Mean compression force varied from 91 N (Breast Centre E) to 147 N (Breast Centre M) between the breast centres, while mean compression force between the mammography machines within one breast centre varied from 137 N to 155 N (Breast Centre M). Mean compression force differed statistically significantly for five breast centres when compared with each of the other breast centres ($p < 0.05$), while it differed statistically significantly between mammography machines in six breast centres ($p < 0.05$).

A total of 58.9% (21,161/35,902) mammograms performed in the NBCSP during the study period complied with the recommended compression force range (108–177 N) (Figure 2). We identified 38.2% (13,706/35,902) mammograms to be below and 2.9% (1035/35,902) mammograms to be above the recommended range. The lowest percentage of mammograms with

Figure 1. The mean compression force used (in Newton) (diamonds in the boxes), with 25% and 75% percentiles with adjacent values up to 1.5 intraquartile range (IQR) [excludes values >1.5 IQR (1.9%)], for craniocaudal and mediolateral oblique views combined, by mammography machines and breast centres in the Norwegian Breast Cancer Screening Program.



compression force within the recommended values was observed at Breast Centre E (16.5%, 505/3058), while the highest was observed at Breast Centre L (95.5%, 2788/2920).

Compression force by radiographers

Mean and median number of mammograms acquired by the radiographers who fulfilled the inclusion criteria were 304 and 284, respectively. Mean compression force ranged from 83 N to 164 N for the radiographers, while it ranged from 95 N to 143 N for radiographers working at the same breast centre (Breast Centre N) (Figure 3). Mean compression force decreased slightly as the radiographer age and experience increased ($p < 0.05$). The slight decrease was statistically significant for all groups of experience and between the two youngest age groups compared with the two oldest age groups ($p < 0.05$). The decrease in compression force was non-linear for radiographer experience.

Figure 2. The distribution of compression force (in Newton) within the recommended range of compression force from the Norwegian Breast Cancer Screening Program (108–177 N; medium grey) and outside the recommended range (below: <108 N, light grey; above: >177 N, black), by breast centre and in total.

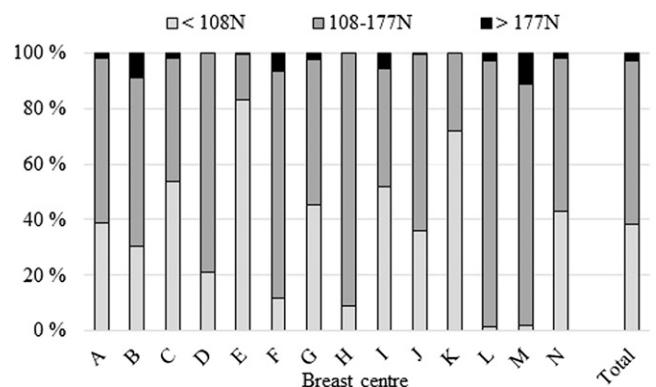
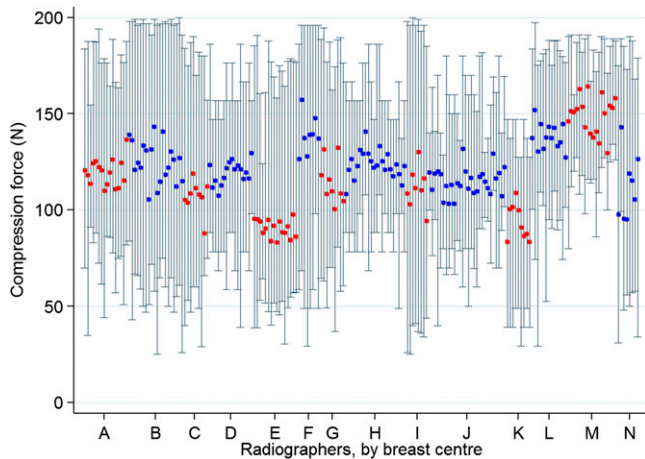


Figure 3. The mean (square) and range of compression force applied by the individual radiographers, by breast centre in the Norwegian Breast Cancer Screening Program. Each coloured square represents the mean compression force. Alternating coloured squares have been used to enable easier visual differentiation between contiguous breast centres on the x-axis.



Univariate linear regression showed that radiographer (r^2 : 0.358), mammography machines within breast centres (r^2 : 0.269), breast centre (r^2 : 0.261), machine vendor (r^2 : 0.073), BMI (r^2 : 0.042), years of age (r^2 : 0.001) and years of experience within mammography (r^2 : 0.002) for the radiographer were significant predictors of the compression force used in the NBCSP ($p < 0.001$). We could not include all the significant predictors of compression force in a multivariate linear regression model owing to collinearity. Backward elimination and Akaike information criterion identified radiographer, BMI and mammography machines within breast centres as the strongest predictors of compression force in a multivariate linear regression model. The overall fit of the model was 39.7%.

The correlation between compression force and compressed breast thickness was negligible ($r = 0.186$). The estimated accuracy of the manually reported data compared with the data given from Volpara was high for the two counties tested: $r = 0.93$ for compression force and $r = 0.99$ for compressed breast thickness.

DISCUSSION

A moderate percentage (58.9%) of mammograms in the NBCSP were performed with a compression force within the recommended range (108–177 N). Almost 40% of the mammograms were performed with a compression force below the recommended values. A substantial variation in compliance with the recommendations was observed between the breast centres.

There are several factors that might affect the applied compression force in mammography; the female,^{18–20} the equipment^{21,22} and the radiographer.^{8–11,22,23} Factors related to the screened female include differences in breast volume,¹⁸ breast stiffness and compressibility^{19,20} and acceptance of pain. Characteristics of the breast compression paddle,²⁴ positioning of the compression paddle,^{22,23} positioning of the detector

plate²¹ and use of automated compression force methods²² are factors related to the equipment. The positioning of the breast compression paddle and detector plate will affect how the pressure from breast compression is distributed across the breast.^{21–23} Studies have indicated that pressure is often concentrated to the firmer juxtathoracic structures of the breast, rather than on the breast itself.^{22,23} Whether the breast compression paddle is rigid or flexible might also affect the distribution of pressure in the breast. However, Broeders et al²⁴ reported no difference in mean compression forces when flexible and rigid breast compression paddles were compared. The presence and use of automated compression force methods (such as Siemens proprietary OPCOMP), where the machine holds further compression force application when the ratio between thickness reduction and applied force drops below a threshold, might also have an impact on the applied compression force. We did not have information about the paddles or the use of automated compression force methods in our study. However, we found that the machine vendor was not of great influence for the applied compression force.

Previous studies have suggested that radiographers or screening centres might have their own preferred compression force levels.^{10,11} The compression force might be influenced by the radiographer age, experience and attitude towards compression force for the radiographer and screening centre. The females' BMI, the radiographer who performed the examination and the mammography machines within the breast centres were the strongest predictors of compression force in our study. The females' BMI might be related to the breast volume and thereby affect the applied compression force.¹⁸ A subanalysis showed that the compression force decreased slightly by increasing age and years of experience in mammography of the radiographers. However, the correlation was not linear and further investigation is needed before any confident conclusion can be stated. The overall prediction of the multivariate model for compression force in our study was low (39.7%), as we were unable to include other factors to increase the prediction for the compression force. This suggests that application of compression force is an action influenced by several factors unavailable in this study, or is even random. Prediction of compression force is thus challenging.

The variation in applied compression force in the XBSCP might have consequences for the quality of the programme, such as image quality,^{25,26} radiation dose,^{27–29} the female's experience of the examination⁴ and reattendance.^{5,6} Contradictory results have been reported regarding the effect of compression force on visually assessed image quality. A study by O'Leary et al²⁵ concluded compression force to be having a significant effect on image quality, while Mercer et al²⁶ reported no difference in visually assessed image quality with different applied compression forces. Further studies investigating the effect of compression force on image quality including both visual and physical measurements of image quality are needed. Regarding radiation dose, studies have reported increased radiation dose with increased compressed breast thickness.^{27–29} Further, the compression force might influence reattendance.^{5,6} However, subsequent reattendance is complex and is affected by several

factors rather than simply the level of pain experienced during the screening examination.⁵ Studies exploring these factors are important for the quality of a screening programme.

While the UK guidelines⁷ for breast compression specify only the recommended maximum compression force (200 N or 20 kg), the Norwegian recommendations¹² specify a range of accepted compression force (11–18 kg). Both guidelines accept a large range of compression forces and this might be one of the reasons for the observed variation in compression forces in this study and Mercer et al's^{8–10} from the UK.

A more specified or narrow interval of accepted compression force might reduce the variation between radiographers and breast centres. As compression force has a different impact on different breast sizes and densities, there would still be differences in the level of breast thickness reduction for the individual female. This highlights the difficulties with the current compression force standardized guidelines. This explains why, in 2004, Poulos and McLean²⁰ required a new perspective on breast compression in mammography. However, today, 12 years later, compression force is still used in clinical practice. Several studies have asserted that compression force might not be the best measure for breast thickness reduction.^{11,20,22,30} The negligible correlation between compression force and compressed breast thickness ($r = 0.186$) observed in our study confirms this suggestion. Recently, compression pressure (force divided by contact area, Newton per square metre = Pascal) has been suggested as a better parameter for reducing breast thickness.^{31,32} This work is promising, as breast size might be a factor to take into account when moving towards individualized breast compression. There is a need for increased knowledge about optimal breast compression in mammography, which takes into account different breast characteristics. Such knowledge will allow us to

establish evidence-based and individualized recommendations for breast compression.

The strength of our study is the large number of mammograms included. There was a very high correlation between the information extracted from the radiographers and from the outcome of Volpara ($r = 0.93–0.99$), which indicates a strong validity of the data collected. Information about image quality or radiation dose was not available for this study, which would have provided a valuable insight into the effects of the variation in compression force in mammography.

CONCLUSION

This is the first study to investigate the compression force used in the Norwegian Breast Cancer Screening Program. Mean compression force varied substantially between the breast centres, mammography machines used at screening within the breast centres and between the radiographers. Six out of ten mammograms were performed with a compression force within the recommended range. The correlation between compression force and compressed breast thickness was negligible. The findings highlight the need for increased knowledge about optimal levels for breast compression in mammography. Future recommendations for breast compression should be evidence-based and aimed at individualizing the breast compression without compromising image quality.

ACKNOWLEDGMENTS

We want to thank all the radiographers who extracted and registered the data used in this study.

FUNDING

The project was partly funded by the Norwegian Society of Radiographers.

REFERENCES

- Perry N, Broeders M, de Wolf C, Törnberg S, Holland R, von Karsa L. *European guidelines for quality assurance in breast cancer screening and diagnosis*. 4th edn. Luxembourg: European Communities; 2006.
- Kopans D. *Breast imaging*. 3rd edn. London, UK: Lippincott Williams & Wilkins; 2007.
- Suleiman ME, Brennan PC, McEntee MF. Diagnostic reference levels in digital mammography: a systematic review. *Radiat Prot Dosimetry* 2015; **167**: 608–19. doi: <https://doi.org/10.1093/rpd/ncu365>
- Davey B. Pain during mammography: possible risk factors and ways to alleviate pain. *Radiography* 2007; **13**: 229–34. doi: <https://doi.org/10.1016/j.radi.2006.03.001>
- Whelehan P, Evans A, Wells M, MacGillivray S. The effect of mammography pain on repeat participation in breast cancer screening: a systematic review. *Breast* 2013; **22**: 389–94. doi: <https://doi.org/10.1016/j.breast.2013.03.003>
- Hofvind S, Wang H, Thoresen S. The Norwegian Breast Cancer Screening Program: re-attendance related to the women's experiences, intentions and previous screening result. *Cancer Causes Control* 2003; **14**: 391–8. doi: <https://doi.org/10.1023/A:1023918610664>
- Cush S, Johnson S, Jones S, Passmore D, Deogund K, Vegnuti Z. Quality assurance guidelines for mammography including radiographic quality control NHS Cancer Screening Programmes—National Quality Assurance Coordinating Group for radiography; 2006. p. 42. Available from: https://www.gov.uk/government/uploads/system/uploads/attachment_data/file/470807/nhsbsp63_uploaded_231015.pdf
- Mercer C, Hogg P, Lawson R, Diffey J, Denton ER. Practitioner compression force variability in mammography: a preliminary study. *Br J Radiol* 2013; **86**: 20110596. doi: <https://doi.org/10.1259/bjr.20110596>
- Mercer C, Hogg P, Szczepura K, Denton ERE. Practitioner compression force variation in mammography: a 6-year study. *Radiography* 2013; **19**: 200–6. doi: <https://doi.org/10.1016/j.radi.2013.06.001>
- Mercer C, Szczepura K, Kelly J, Milington SR, Denton ERE, Borgen R, et al. A 6-year study of mammographic compression force: practitioner variability within and between screening sites. *Radiography* 2015; **21**: 68–73. doi: <https://doi.org/10.1016/j.radi.2014.07.004>
- Branderhorst W, de Groot JE, Highnam R, Chan A, Böhm-Vélez M, Broeders MJ, et al. Mammographic compression—a need for mechanical standardization. *Eur J Radiol* 2015; **84**: 596–602. doi: <https://doi.org/10.1016/j.ejrad.2014.12.012>

12. Vee B, Gullien R, Handberg E, Hoftvedt IJ, Iden K, Ertzaas AK. Chapter 5: directions for radiographers in the quality assurance manual of the Norwegian Breast Cancer Screening Program (NBCSP), Oslo: The Cancer Registry of Norway, Institute of population-based cancer research, Oslo; 2011. p. 10. Available from: https://www.kreftregisteret.no/globalassets/mammografiprogrammet/arkiv/publikasjoner-og-brosjyrer/kval-man-radiograf_v1.0_innholdsfortegnelse.pdf
13. Hofvind S, Geller B, Vacek PM, Thoresen S, Skaane P. Using the European guidelines to evaluate the Norwegian breast cancer screening program. *Eur J Epidemiol* 2007; **22**: 447–55. doi: <https://doi.org/10.1007/s10654-007-9137-y>
14. Wang H, Pedersen K, Ertzaas AK. Chapter 2: NBCSP in the quality assurance manual of the Norwegian Breast Cancer Screening Program (NBCSP), Oslo: The Cancer Registry of Norway, Institute of population-based cancer research, Oslo; 2003. p. 4. Available from: https://www.kreftregisteret.no/globalassets/gammelt/kvalitetsmanualer/kvalitetsmanual_mammografiprogrammet.pdf
15. Pedersen K, Bredholt K, Landmark ID, Istad TS, Almen A, Hauge IH. Chapter 11: Technical quality control—routine controls for digital mammography systems in the quality assurance manual of the Norwegian Breast Cancer Screening Program (NBCSP), Oslo: The Cancer Registry of Norway, Institute of population-based cancer research, Oslo; 2010.
16. Skaane P, Bandos AI, Gullien R, Eben EB, Ekseth U, Haakenaasen U, et al. Comparison of digital mammography alone and digital mammography plus tomosynthesis in a population-based screening program. *Radiology* 2013; **267**: 47–56. doi: <https://doi.org/10.1148/radiol.12121373>
17. Hinkle DE, Wiersma W, Jurs SG. *Applied statistics for the behavioral sciences*. 5th edn. Boston, MA: Houghton Mifflin; 2003.
18. Khan-Perez J, Harkness E, Mercer C, Bydder M, Sergeant J, Morris J, et al. Volumetric breast density and radiographic parameters. In: Fujita H, Hara T, Muramatsu C, eds. *Breast imaging—12th International Workshop, IWDM 2014*. Gifu, Japan: Springer; 2014. pp. 265–72.
19. Boyd N, Li Q, Melnichouk O, Huszti E, Martin L, Gunasekara A, et al. Evidence that breast tissue stiffness is associated with risk of breast cancer. *PLoS One* 2014; **9**: e100937.
20. Poulos A, McLean D. The application of breast compression in mammography: a new perspective. *Radiography* 2004; **10**: 131–7. doi: <https://doi.org/10.1016/j.radi.2004.02.012>
21. Smith H, Szczepura K, Mercer C, Maxwell A, Hogg P. Does elevating image receptor increase breast receptor footprint and improve pressure balance? *Radiography* 2015; **21**: 359–63. doi: <https://doi.org/10.1016/j.radi.2015.02.001>
22. Dustler M, Andersson I, Brorson H, Fröjd P, Mattsson S, Tingberg A, et al. Breast compression in mammography: pressure distribution patterns. *Acta Radiol* 2012; **53**: 973–80. doi: <https://doi.org/10.1258/ar.2012.120238>
23. Dustler M, Andersson I, Förnvik D, Tingberg A. The effect of breast positioning on breast compression in mammography: a pressure distribution perspective. *SPIE Med Imaging* 2012; **8313**: 83134M. doi: <https://doi.org/10.1117/12.905746>
24. Broeders MJ, Voorde MT, Veldkamp WJ, von Engen RE, Landsveld-Verhoeven C, Jong-Gunneman MN, et al. Comparison of a flexible versus a rigid breast compression paddle: pain experience, projected breast area, radiation dose and technical image quality. *Eur J Radiol* 2015; **25**: 821–9. doi: <https://doi.org/10.1007/s00330-014-3422-4>
25. O’Leary D, Teape A, Hammond J, Rainford L, Grant T. Compression force recommendations in mammography must be linked to image quality. *Proc Eur Congress Radiol* 2011: 1–19.
26. Mercer C, Hogg P, Cassidy S, Denton ER. Does an increase in compression force really improve visual image quality in mammography? An initial investigation. *Radiography* 2013; **19**: 363–5. doi: <https://doi.org/10.1016/j.radi.2013.07.002>
27. McCullagh JB, Baldelli P, Phelan N. Measured dose versus organ dose performance in digital mammography systems. In: Martí J, Oliver A, Freixenet J, Martí R, eds. *Digital mammography—10th International Workshop, IWDM 2010*. Girona, Spain: Springer; 2010. pp. 86–91.
28. Young KC, Oduko JM. Radiation doses received in the United Kingdom breast screening programme in 2010 to 2012. *Br J Radiol* 2016; **89**: 20150831. doi: <https://doi.org/10.1259/bjr.20150831>
29. Korf A, Herbst C, Rae W. The relationship between compression force, image quality and radiation dose in mammography. *SA J Radiol* 2009; **13**: 86–92.
30. Förnvik D. *Measurement of tumor extent and effects of breast compression in digital mammography and breast tomosynthesis*. Lund, Sweden: Lund University; 2013.
31. de Groot JE, Broeders MJ, Branderhorst W, de Heeten GJ, Grimbergen CA. A novel approach to mammographic breast compression: improved standardization and reduced discomfort by controlling pressure instead of force. *Med Phys* 2013; **40**: 081901. doi: <https://doi.org/10.1118/1.4812418>
32. de Groot JE, Branderhorst W, Grimbergen CA, de Heeten GJ, Broeders MJ. Towards personalized compression in mammography: a comparison study between pressure- and force-standardization. *Eur J Radiol* 2015; **84**: 384–91.

APPENDIX A

Table A1. Mean compression force with 95% CI for CC and MLO views on right breast, by breast centre and mammography machines within the breast centres

Breast centre	Mammography machine	Mean (95% CI)		
		Compression force (N)		
		CC and MLO	CC	MLO
A		118.5 (117.7–119.4)	104.1 (103.5–104.8)	133.0 (131.8–134.1)
	A1	112.8 (110.4–115.1)	98.0 (96.5–99.5)	127.5 (124.9–130.2)
	A2	123.4 (121.8–125.0)	110.6 (109.1–112.1)	136.2 (133.9–138.5)
	A3	116.9 (115.9–117.9)	101.7 (101.1–102.4)	132.1 (130.7–133.5)
B		124.9 (123.7–126.0)	120.2 (118.7–121.6)	129.5 (127.7–131.3)
	B1	123.2 (121.2–125.2)	117.5 (115.1–119.9)	128.9 (125.8–132.0)
	B2	125.6 (124.2–127.0)	121.3 (119.6–123.1)	129.8 (127.6–132.0)
C		109.8 (108.4–111.1)	96.3 (94.9–97.8)	123.2 (121.4–125.1)
	C1	107.0 (105.5–108.5)	94.2 (92.7–95.7)	119.8 (117.7–122.0)
	C2 ^{a,b}	120.3 (117.4–123.3)	104.4 (100.7–108.0)	136.3 (132.9–139.6)
D		120.0 (119.3–120.6)	112.3 (111.5–113.1)	127.6 (126.8–128.5)
	D1 ^a	120.4 (119.7–121.1)	112.6 (111.7–113.5)	128.2 (127.2–129.1)
	D2	116.6 (114.8–118.4)	109.8 (107.5–112.0)	123.4 (121.0–125.8)
E		90.2 (89.4–91.0)	79.4 (78.8–80.0)	101.1 (99.8–102.3)
	E1	90.2 (89.1–91.3)	77.3 (76.7–78.0)	103.1 (101.4–104.8)
	E2	90.3 (89.2–91.4)	82.5 (81.5–83.5)	98.1 (96.3–99.9)
F		139.3 (138.3–140.3)	122.8 (121.7–123.8)	155.9 (154.7–157.0)
	F1	142.1 (140.3–143.9)	122.9 (121.0–124.9)	161.2 (159.3–163.1)
	F2 ^a	137.8 (136.6–139.0)	122.7 (121.3–124.0)	152.9 (151.4–154.3)
G		118.2 (117.2–119.1)	107.6 (106.6–108.6)	128.7 (127.2–130.1)
H		125.7 (125.0–126.4)	121.2 (120.3–122.1)	130.2 (129.3–131.2)
	H1	130.1 (129.1–131.0)	126.2 (124.8–127.6)	134.0 (132.7–135.3)
	H2	118.2 (116.9–119.5)	114.6 (113.2–116.0)	121.8 (119.6–124.0)
	H3	125.0 (123.8–126.3)	118.7 (117.1–120.4)	131.3 (129.7–132.9)
I		111.6 (110.3–112.8)	94.8 (93.5–96.1)	128.3 (126.6–130.1)
J		113.9 (112.7–115.1)	109.9 (108.3–111.4)	117.9 (116.2–119.7)
	J1	114.1 (112.4–115.8)	109.3 (107.3–111.3)	118.9 (116.2–121.6)
	J2 ^a	113.8 (112.2–115.4)	110.2 (108.0–112.4)	117.4 (115.1–119.6)
K		90.3 (89.7–90.9)	87.3 (86.5–88.1)	93.2 (92.4–94.1)
L		137.7 (137.1–138.3)	134.7 (133.9–135.4)	140.7 (139.8–141.6)
M		147.0 (145.2–148.8)	144.9 (142.4–147.3)	149.1 (146.4–151.8)
	M1	154.8 (152.5–157.1)	153.6 (150.4–156.7)	156.0 (152.6–159.5)
	M2	136.7 (133.9–139.5)	133.4 (130.0–136.9)	139.9 (135.5–144.3)
	M3 ^{a,b}	151.6 (146.7–156.5)	149.7 (142.6–156.8)	153.5 (146.4–160.7)
N		112.3 (111.2–113.3)	106.1 (104.8–107.4)	118.5 (116.9–120.1)
Total		116.8 (116.5–117.1)	107.8 (107.5–108.2)	125.8 (125.4–126.2)

^aMobile unit.^bThe same mobile unit which the breast centres share.

Received:
08 March 2018Revised:
07 March 2019Accepted:
21 March 2019<https://doi.org/10.1259/bjr.20180245>

Cite this article as:

Wessam R, Gomaa MMM, Fouad MA, Mokhtar SM, Tohamey YM. Added value of contrast-enhanced mammography in assessment of breast asymmetries. *Br J Radiol* 2019; **92**: 20180245.

FULL PAPER

Added value of contrast-enhanced mammography in assessment of breast asymmetries

¹RASHA WESSAM, PhD, ²MOHAMMED MOHAMMED MOHAMMED GOMAA, ¹MONA AHMED FOUAD, ³SHERIF MOHAMED MOKHTAR and ¹YASMIN MOUNIR TOHAMEY

¹Department of Radiology Faculty of Medicine, Kasr El Aini hospital, Cairo University, Egypt

²Department of Radiology Faculty of Medicine, National Cancer Institute Cairo University, Egypt

³Department of Surgery Faculty of Medicine, Kasr El Aini hospital Cairo University, Egypt

Address correspondence to: Dr Rasha Wessam
E-mail: rashakao@yahoo.com

Objective: To evaluate the clinical performance of contrast-enhanced spectral mammography (CESM) on asymmetries detected on a mammogram (MG).

Methods: This study was approved by the Scientific Research Review Board of the Radiology Department, and waiver of informed consent was applied for the uses of data of the included cases. The study included 125 female patients, 33 (26.4%) who presented for screening and 92 (73.6%) who presented for a diagnostic MG. All had breast asymmetries on MG. Ultrasound examination and CESM using dual-energy acquisitions were performed for all patients.

Results: In all, 88/125 (70.4%) females had focal asymmetry (seen in two views and occupying less than a quadrant), 26/125 (20.8%) had global asymmetry (occupying more than one quadrant), 10/125 (8%) had asymmetry (seen in a single view and occupying less than a quadrant), and 1/125 had developing asymmetry (0.8%) (not

present in the previous MG). Malignant lesions represented 91 cases, benign lesions represented 30 cases, and 4 cases were high-risk lesions. CESM sensitivity was 100% (vs 97.8% for sono-mammography), specificity was 55.88% (vs 81.8% for sono-mammography), and the positive- and negative-predictive values were 85.85 and 100% (vs 93.7 and 93% for sono-mammography respectively).

Conclusion: In our study, we conclude that focal and global asymmetries with other suspicious mammographic findings were statistically significant for malignancy and CESM played an important role in delineating tumor size and extension. Any non-enhancing asymmetrical density correlated with a benign pathology, if not associated with other suspicious imaging findings.

Advances in knowledge: Our study is the first to explore the added value of CESM to asymmetries detected in screening and diagnostic mammography.

INTRODUCTION

Screening and diagnostic mammography assessments encounter many presentations as masses, calcifications, distortion and asymmetries. Asymmetry commonly seen in healthy females, however in some cases it may be a presentation of underlying malignant disease. Thus, thoroughly reviewing mammograms is crucial when breast asymmetry is present.¹

The Breast Imaging Reporting and Data System has set definitions related to breast asymmetry; focal asymmetry is when the same features are observable on standard mammographic views, occupying less than a single quadrant, but lacking convex margins and containing interspersed fat. Asymmetry shares similarities with focal asymmetry, yet it is only visible on one of the standard mammography views. Conversely, developing asymmetry

is focal asymmetry not present on previous mammograms and is more conspicuous or displays increases in size.²

The American College of Radiology Breast Imaging Reporting and Data System (BI-RADS) lexicon has updated its guidelines regarding asymmetric breast findings. The nomenclature in the fourth edition replaced “asymmetric breast tissue” with “global asymmetry,” “density seen in only a single projection” with “asymmetry” and “focal asymmetric density” with “focal asymmetry.” The evaluation of a perceived asymmetry, whether it is a definite lesion or not, remains a diagnostic challenge.¹

The incidence of asymmetric findings on screening mammograms varies, where focal asymmetry was reported in 0.87%,² asymmetry was found in 3.3% and developing asymmetry was observed in 0.16% of screens, with the

latter comprising 0.11% of diagnostic mammogram findings.^{3,4} Still, these lesions comprise a minor percentage of screening-detected breast malignancy.

Digital mammography is considered the most consistent imaging modality utilized in the early detection of breast cancer. Dense breasts still represent a challenge, as they are associated with limited mammographic sensitivity and specificity when detecting and characterizing breast lesions.³ Contrast-enhanced spectral mammography (CESM) is an evolving technology budding from digital mammography; it includes information from tumor angiogenesis to improve the sensitivity of breast lesion characterization.⁴

Contrast-enhanced MRI (MRI) is currently considered a sensitive imaging tool for breast cancer detection, but it carries the burdens of limited availability and high costs. Conversely, CESM is a rapid scanning technique and is available in the mammography suite, thus saving time and there is no need for appointment reservation.⁵ In our study, we evaluated the clinical performance of CESM on asymmetry detected during mammography.

METHODS AND MATERIALS

Patients

This study is a retrospective analysis that included 125 females, 33 (26.4%) of whom presented for screening and 92 (73.6%) of whom were symptomatic and referred from the clinic for a diagnostic mammogram in the period spanning from March 2015 to March 2016. The patients' ages ranged from 25 to 81 years (mean: 48.87 years). None of the patients were treated with hormone replacement therapy. The study was approved by "Baheya Centre for Early Detection and Treatment of Breast Cancer" ethics committee and all enrolled patients provided their informed consent. During the mammogram, contrast injection was used to further evaluate any detected asymmetries. Patients with renal impairment, pregnant patients, and those with a history of allergy to contrast media were excluded from the study. The remaining patients were eligible to undergo CESM, the requirement to obtain informed consent was waived by our ethics committee. Compression magnification views were applied and revealed fibroglandular tissue in five cases presenting with focal asymmetries and these patients were scheduled for annual follow-up. Complementary ultrasound examination was performed for all cases. In our study, the reference standard was histopathology after ultrasound-guided true-cut biopsy and follow up for five cases.

Contrast-enhanced spectral mammography system Dual-energy (CESM) was performed using Senographe Essential, (Seno DS; GE, Buc, France) which obtained low-energy images that were comparable to the standard mammography image, and high-energy images were also acquired to show the contrast-enhanced areas for each mammography view.

Examination technique

The examination was performed with a digital mammography device developed by GE Healthcare; it allowed for dual-energy CESM image acquisition by means of an intravenous injection

of an iodinated contrast agent (iohexol, 300 mg I/mL) at a dose of 1.5 mL/kg before the application of breast compression. This was followed by a 2 min wait prior to a mammography exam and was performed using the two standard positions (cranio-caudal and mediolateral oblique views). Low- and high-energy images were consecutively acquired in each view. Low-energy images were acquired at peak kilovoltage values ranging from 26 to 31 kVp, which is below the K-edge of iodine. High-energy images were acquired at 45–49 kVp, which is above the K-edge of iodine. Enhanced images were calculated by weighted logarithmic subtraction of the two images through appropriate image processing, thus reducing the visibility of the parenchyma and generating contrast-enhanced images.

Image analysis

The analysis of sono-mammography and CESM images was performed using two different dedicated breast radiologists. The radiologists provided a BI-RADS classification for conventional mammography and ultrasound examination using the BI-RADS lexicon designed by the American College of Radiology.⁵ Subsequently, CESM images were viewed and the radiologists were allowed to up- or downgrade their BI-RADS classification. Images were analyzed with respect to:

- Localization and type of asymmetry.
- Associated distortion, microcalcifications, and skin and nipple changes.
- Assessment of ultrasound-detected masses regarding their number, shape, margins, and echogenicity. Any parenchymal heterogeneity and enlarged axillary lymph nodes were assessed. Any asymmetrical breast density associated with other suspicious mammographic or ultrasonographic findings was considered suspicious.
- Regarding CESM images, the presence or absence of contrast enhancement of asymmetrical density was assessed. In case of enhancement, its morphology—whether as a mass (margins, enhancement pattern) or non-mass (ductal, segmental, regional, or diffuse enhancement) was analyzed. The assessment also included the presence of other enhancing lesions in the same breast or on the other side. An ill-defined mass with heterogeneous enhancement or non-mass enhancement (ductal, segmental, regional, or unilateral diffuse) were considered suspicious and were categorized as BI-RADS four lesions. Well-defined homogeneously enhancing masses or non-enhancing asymmetries that were not associated with other suspicious mammographic findings were scored on a scale of 1–3 and were considered benign.

Statistical analysis

Data were coded and entered using the Statistical Package for the Social Sciences (SPSS) v. 24 (IBM Corporation, Armonk, NY). Data were summarized using the mean, standard deviation, median, minimum, and maximum for quantitative data, while frequency (count) and relative frequency (percentage) were used for categorical data. Standard diagnostic indices including sensitivity, specificity, positive-predictive value (PPV), and negative-predictive value (NPV) were calculated as described by Galen. To compare categorical data, a χ^2 test was performed. This

test was used when the expected frequency was less than 5 (Chan, 2003). A p -value < 0.05 was considered statistically significant.

RESULTS

Classification of asymmetries

Our study included 125 females; 88/125 (70.4%) females had focal asymmetry (seen in two views and occupying less than one quadrant), 26/125 (20.8%) had global asymmetry (occupying more than one quadrant), 10/125 (8%) had asymmetry (seen in a single view and occupying less than one quadrant), and 1/125 had developing asymmetry (0.8%); not present in the previous mammogram.

Malignant lesions represented 91 cases, including 53 cases of invasive duct carcinoma, 16 cases of invasive lobular carcinomas (ILC), 3 cases of invasive mixed carcinomas, 2 cases of ductal carcinomas *in situ*, 15 cases of invasive ductal carcinomas with ductal carcinomas *in situ*, 1 case of mucinous carcinoma and 1 case of tubular carcinoma. Four high-risk lesions were recorded, including three atypical ductal hyperplasias and one papilloma. Benign lesions represented 30 cases, including 5 granulomatous mastitis, 5 abscess cavities, 3 mastopathy, 3 fibroadenoma, 3 ductal hyperplasia, 2 fibrocystic changes 2 fat necrosis, 1 periductal mastitis and 1 fibroadenomatoid changes. Five cases of asymmetries were considered as condensed benign glandular tissue and were scheduled for annual follow-up (Table 1).

Further, 23 (26.1%) cases of focal asymmetry were benign and 65 cases (73.9%) were malignant. 7 (26.9%) out of 26 cases of global asymmetry were benign and 19 (73.1%) were malignant. Four cases of asymmetry (40%) were benign and six (60%) were malignant. The only case of developing asymmetry was malignant (100%) (Table 2).

Other mammographic findings

Other mammographic findings associated with asymmetrical densities and their correlation with the final diagnosis are listed in Table 3. Among the associated mammographic findings, there was a significant correlation between focal asymmetry associated with distortion, suspicious calcification, skin/nipple changes and malignancy. Focal asymmetries with no other associated mammographic findings were significantly correlated with a benign pathology ($p \leq 0.001$).

Asymmetry enhancement pattern

On CESM, enhancing asymmetrical densities represented 114 (91.2%) cases. Further, 59 out of 114 cases (52%) showed mass enhancement, 10 of which (17%) were benign and 49 (83%) of which were malignant. In addition, 55 cases (48.2%) showed non-mass enhancement, 13 (24%) of which were benign and 42 (76.4%) of which were malignant. Any enhancing asymmetry showing a mass or non-mass enhancement was significantly correlated with malignant pathology ($p \leq 0.001$), with 15 false positive cases, as listed in Table 4.

There was a significant correlation between non-enhancing asymmetrical findings and benign pathology with no other associated suspicious mammographic findings ($p \leq 0.001$); this was

Table 1. Histopathology of 125 cases of asymmetries

Histopathologic diagnosis	Number of lesions (n = 125)
Malignant lesions	91
Invasive duct carcinoma	53
Invasive lobular carcinoma	16
Invasive ductal with DCIS	15
Invasive mixed carcinoma	3
DCIS	2
Mucinous carcinoma	1
Tubular carcinoma	1
High-risk lesions	4
Atypical ductal hyperplasia	3
Papilloma	1
Benign lesions	30
Granulomatous mastitis	5
Abscess	5
Mastopathy	3
Fibroadenoma	3
Ductal hyperplasia	3
Fibrocystic changes	2
Fat necrosis	2
Fibroadenomatoid changes	1
Periductal mastitis	1
Benign tissue	5

DCIS, ductal carcinoma *in situ*.

observed in 11 cases (8.8%). The enhancement pattern of breast asymmetries and their correlation to the final diagnosis are listed in Table 5. Focal asymmetry showing mass enhancement was significantly correlated with malignancy, while non-enhancing focal asymmetry was correlated with benign pathology ($p \leq 0.001$).

Other detected breast lesions on CESM

26 cases of asymmetrical density had other enhancing malignant lesions. 22 cases had enhancing multifocal/multicentric carcinoma on the same side-of the breast asymmetry and 4

Table 2. Asymmetrical densities and their correlation to their final diagnosis

Asymmetry	Benign	Malignant	Total
Focal	23 (26.1%)	65 (73.9%)	88 (70.4%)
Global	7 (26.9%)	19 (73.1%)	26% (20.8%)
Asymmetry	4 (40%)	6 (60%)	10 (8%)
Developing	0 (0%)	1 (100%)	1 (0.8%)
Total	34 (27.2%)	91 (72.8%)	125 (100%)

Table 3. Mammographic findings of asymmetries and their correlation to the final diagnosis

Other associated mammographic findings	Asymmetries							
	Asymmetry		Focal		Global		Developing	
	Benign	Malignant	Benign	Malignant	Benign	Malignant	Benign	Malignant
Distortion	0	2	5	*34	1	6	0	0
	0%	-2.20%	-14.70%	-37.40%	-2.90%	-6.60%	0%	0%
Suspicious calcifications	0	1	0	*11	0	5	0	0
	0%	-1.10%	0%	-12.10%	0%	-5.50%	0%	0%
Skin/nipple changes	2	1	5	*31	3	16	0	0
	-5.90%	-1.10%	-14.70%	-34.10%	-8.80%	-17.60%	0%	0%
Axillary LN	1	1	0	13	1	4	0	0
	-2.90%	-1.10%	0%	-14.30%	-2.90%	-4.40%	0%	0%
No other findings	1	2	*14	7	4	0	0	1
	-2.90%	-2.20%	-41.20%	-7.70%	-11.80%	0%	0%	-1.10%

LN, lymph node.

34.4% of patients who had focal asymmetry and distortion had a malignancy.

12.1% of patients who had focal asymmetry and suspicious calcifications had a malignancy.

34.1% of patients who had focal asymmetry and skin/nipple changes had a malignancy.

41.2% of patients who had focal asymmetry with no other mammographic findings were considered benign cases.

^a $p \leq 0.001$

cases had bilateral enhancing lesions (3 were malignant lesions and 1 was a high-risk lesion). Sono-mammography diagnosed 17 out of 26 cases of multifocal/multicentric or bilateral malignant lesions.

Diagnostic performance of sono-mammography and CESM

Sono-mammography sensitivity, specificity, PPV and NPV were 97.8%, 81.8%, 93.7%, and 93%, respectively. CESM sensitivity, specificity, PPV and NPV were 100%, 55.88%, 85.85% and 100% respectively, with 15 false-positive and no false-negative findings.

Table 4. Histopathology of 15 CESM false-positive cases

Histopathologic diagnosis	Number of lesions (n = 15)
High -risk lesions	4
Atypical ductal hyperplasia	3
Papilloma	1
Inflammatory lesions	8
Granulomatous mastitis	4
Abscess	3
Periductal mastitis	1
Benign lesions	3
Fibrocystic mastopathy	1
Fatnecrosis	1

DISCUSSION

Breast asymmetries encountered during screening and diagnostic mammographic evaluation pose a challenge for radiologists in terms of proper assessment and management.

Our study is the first to evaluate the added value of using CESM in detected breast asymmetries in 125 females over the course of 1 year.

The increased sensitivity offered by CESM was demonstrated by Jochelson et al.⁶ In their study, the sensitivity of mammography increased from 81 to 96%, owing to CESM. Similar observations were published by Fallenberg et al, who showed that the sensitivity of mammography (82.5%) increased to 100% owing to CESM.⁷ The study of Lobbes et al also showed an increase in the sensitivity of CESM to 100%, specificity to 87.7%, PPV to 76.2% and NPV to 100%. The NPV of 100% found in this study population suggests that a negative CESM can rule out breast cancer.⁸ The study of Tardivel et al, also stated that the high CESM NPV was of great help when resolving cases with indeterminate lesions (*i.e.* BI-RADS 3 or 4a) by avoiding the additional need for biopsy;⁹ this matched the high sensitivity and high NPV of CESM. All non-enhancing asymmetries in our study were of benign histopathology ($p \leq 0.001$). Also, in our study, non-enhancing focal and global asymmetries on CESM with no associated suspicious mammographic findings were of benign pathology ($p \leq 0.001$). From this, we emphasize that any non-enhancing asymmetry on CESM that do not feature any other associated suspicious mammographic findings can be scheduled for follow up rather than biopsy.

Table 5. The enhancement pattern of breast asymmetries and their correlation to a final diagnosis

CESM	Asymmetries							
	Asymmetry		Focal		Global		Developing	
	Benign	Malignant	Benign	Malignant	Benign	Malignant	Benign	Malignant
Mass	2	5	7	a 43	1	0	0	1
	-5.90%	-5.50%	-20.60%	-47.30%	-2.90%	0%	0%	-1.10%
Non-mass	0	1	7	23	6	18	0	0
	0%	-1.10%	-20.60%	-25.50%	-17.60%	-19.80%	0%	0%
No enhancement	2	0	a8	0	1	0	0	0
	-5.90%	0%	-23.50%	0%	-2.90%	0%	0%	0%

CESM, contrast-enhanced spectral mammography.

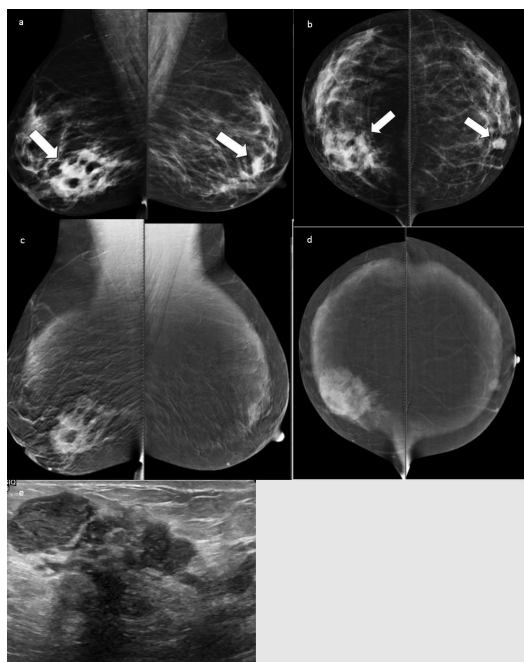
47.3% of patients with malignant focal asymmetry had mass enhancement on CESM.

23.5% of patients with benign focal asymmetry had no enhancement on CESM.

^a $p \leq 0.001$

Dromain et al were able to demonstrate the depiction of tumor angiogenesis of breast cancer independent of histologic type.¹⁰ Initial clinical trials,¹⁰⁻¹³ and the findings that emerged from the study of Tradivel et al, have described same false-positives⁹ that were encountered in the present study, including fibro-cystic changes, atypical ductal hyperplasia, adenosis, and steatonecrosis. Bhimani et al, reported that CESM has false-positive results that are similar to MRI.¹⁴ 15 false-positive findings were present in our study. 10 of which were categorized as benign

Figure 1. Low-energy images showing focal asymmetry at the right lower inner quadrant, a small well-circumscribed mass at the left para-areolar region is also noted (a, b). High-energy level images showing an ill-defined, heterogeneous enhancing lesion corresponding to asymmetry and homogenous enhancement of the left mass (c, d). Ultrasound showed multiple localized collections (e). The pathology was right granulomatous mastitis and left fibroadenoma.



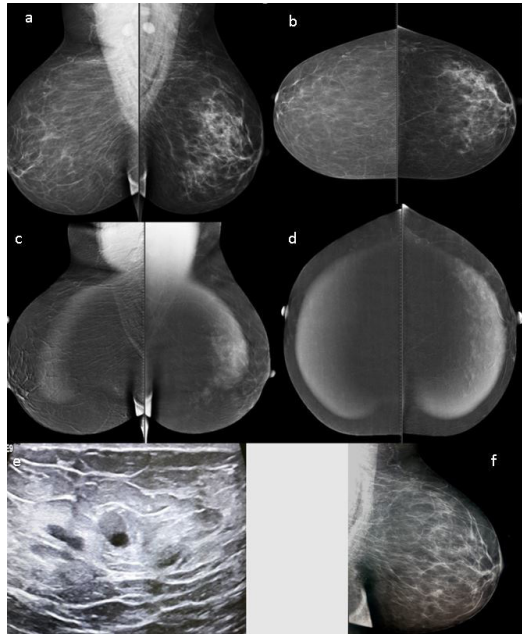
findings by ultrasound examination (Figure 1). Thus, target ultrasound examination can categorize asymmetrical mammographic density as benign findings, thus reducing the need for further imaging studies and reducing biopsy rates.

Focal asymmetry was the most frequently encountered asymmetrical density in the present study. Harvey et al considered focal asymmetry as being more suspicious than global asymmetry, especially if companion parenchymal distortion is present.¹⁵ In fact, most of our focal asymmetry cases were malignant, especially in instances when the focal asymmetry was associated with suspicious mammographic findings ($p \leq 0.001$). Conversely, focal asymmetry cases were more likely to be associated with a benign pathology if they did not present with other suspicious findings ($p \leq 0.001$). All non-enhancing focal asymmetries were benign ($p \leq 0.001$).

Most of the patients in our study with malignant focal asymmetry showed mass enhancement in our study (43 cases); these individuals were diagnosed using sono-mammography. 23 malignant cases of focal asymmetry showed non-mass enhancement, the extension and size of those depicted nonmass enhancement were better delineated by CESM when compared to sono-mammography.

Global asymmetry was the second most frequently represented asymmetrical density in our study; it was statistically correlated with benign findings if it was not associated with other suspicious findings on mammogram (Figure 2). On CESM, non-enhancing global asymmetry was associated with benign findings ($p \leq 0.001$). Further, 18 out of 26 cases of global asymmetry in our study were malignant. CESM was of value in the assessment of size and extension of enhancing global asymmetry due to malignant infiltration compared to sono-mammography examination (Figure 3). The studies⁶⁻⁸ confirmed the potential of CESM in being a reliable alternative to breast MRI in the assessment of the extent of the disease. In our study, 26 cases had other enhancing lesions detected by CESM compared to 17 out of 26 cases detected by sono-mammography. Asymmetric density seen only in one plane, as well as developing asymmetry, were

Figure 2. Low-energy level images (a, b) showing left global asymmetry. High-energy images (c, d) showing diffuse homogenous nonmass enhancement. On ultrasound examination no parenchymal changes are seen, and only a few small scattered cysts with partial turbid fluid contents are evident (e). At annual follow up, the left MLQ view showed almost complete resolution of the breast asymmetry (f). The pathology was fat necrosis. MLQ, mediolateral oblique.



the least represented asymmetries in our study, yet CESM was able to better delineate disease extension in two out of six cases of malignant asymmetry (Figure 4). Lee *et al* reported a series of 86 indeterminate breast lesions in the form of asymmetric breast

Figure 4. Asymmetry is seen in the lower region of the right breast with overlying skin retraction (MLQ view) (a, b). CESM showing regional clumped nonmass enhancement involving a larger area than the one seen on sono-mammography (c, d). The pathology was DCIS with microinvasion. CESM, contrast-enhanced spectral mammography; DCIS, ductal carcinomas *in situ*; MLQ, mediolateral oblique

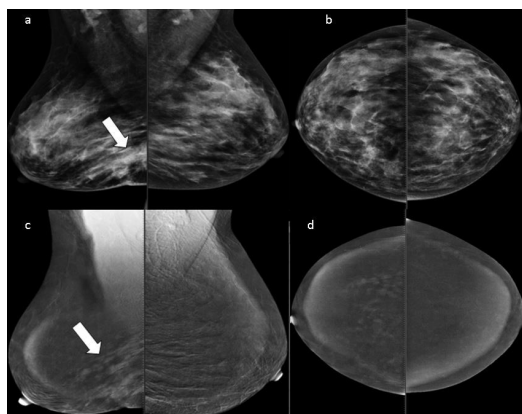
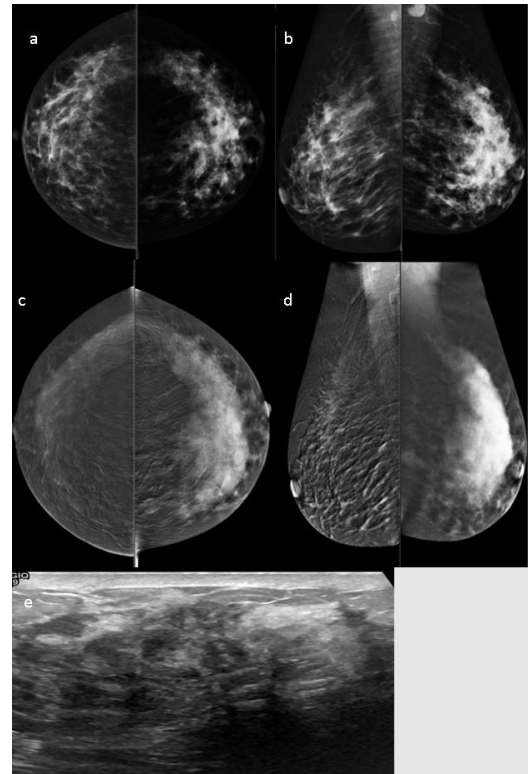


Figure 3. CESM showing left global asymmetry in low-energy images with minimal focal skin thickening and enlarged axillary LN (a, b). High-energy level images (c, d) showing diffuse heterogeneous nonmass enhancement with better delineations of tumor size and extension. Heterogeneous hypoechoic parenchyma with shadowing is noted on ultrasound examination (e). The pathology was IDC. CESM, contrast-enhanced spectral mammography; IDC, invasive duct carcinoma; LN, lymph node.



densities or architectural distortion, of which 39 cases (45%) were seen in one mammographic plane.¹⁷ The authors acknowledged the valuable additional role of breast MRI in solving some problematic cases identified by initial mammographic assessment. These cases warranted further histopathological diagnosis on positive MR results and follow up of mammographic surveillance on negative MR results.¹⁷

In our study, we conclude that focal and global asymmetries that present with other suspicious mammographic findings were statistically significant with malignancy and CESM played important roles in the delineation of tumor size and extension. Any non-enhancing asymmetrical densities that correlated with a benign pathology did not present with other suspicious imaging findings.

ACKNOWLEDGMENT

This research was carried out at Baheya Charity Females's Cancer Hospital which is fully equipped by modern machines for breast cancer diagnosis. We want to thank our colleagues who helped us to do such research work.

REFERENCES

1. Youk JH, Kim E-K, Ko KH, Kim MJ. Asymmetric mammographic findings based on the fourth edition of BI-RADS: types, evaluation, and management. *Radiographics* 2009; **29**: e33–47. doi: <https://doi.org/10.1148/rg.e33>
2. Sickles EA, D'Orsi CJ, Bassett LW et al. ACR BI-RADS Mammography. In: Reston, ed. *ACR BI-RADS Atlas, Breast Imaging Reporting and Data System. 5th*. VA: American College of Radiology; 2013. pp. 1–175.
3. Jong RA, Yaffe MJ, Skarpathiotakis M, Shumak RS, Danjoux NM, Guneseckara A, et al. Contrast-enhanced digital mammography: initial clinical experience. *Radiology* 2003; **228**: 842–50. doi: <https://doi.org/10.1148/radiol.2283020961>
4. Hill ML, Mainprize JG, Carton A-K, Muller S, Ebrahimi M, Jong RA, et al. Anatomical noise in contrast-enhanced digital mammography. Part I. Single-energy imaging. *Med Phys* 2013; **40**: 051910. doi: <https://doi.org/10.1118/1.4801905>
5. Dromain C, Thibault F, Muller S, Rimareix F, Delalogue S, Tardivon A, et al. Dual-energy contrast-enhanced digital mammography: initial clinical results. *Eur Radiol* 2011; **21**: 565–74. doi: <https://doi.org/10.1007/s00330-010-1944-y>
6. Jochelson MS, Dershaw DD, Sung JS, Heerdt AS, Thornton C, Moskowitz CS, et al. Bilateral contrast-enhanced dual-energy digital mammography: feasibility and comparison with conventional digital mammography and MR imaging in women with known breast carcinoma. *Radiology* 2013; **266**: 743–51. doi: <https://doi.org/10.1148/radiol.12121084>
7. Fallenberg EM, Dromain C, Diekmann F, Engelken F, Krohn M, Singh JM, et al. Contrast-enhanced spectral mammography versus MRI: initial results in the detection of breast cancer and assessment of tumour size. *Eur Radiol* 2014; **24**: 256–64. doi: <https://doi.org/10.1007/s00330-013-3007-7>
8. Lobbes MBI, Lalji U, Houwers J, Nijssen EC, Nelemans PJ, van Roozendaal L, et al. Contrast-enhanced spectral mammography in patients referred from the breast cancer screening programme. *Eur Radiol* 2014; **24**: 1668–76. doi: <https://doi.org/10.1007/s00330-014-3154-5>
9. Tardivel A-M, Balleyguier C, Dunant A, Delalogue S, Mazouni C, Mathieu M-C, et al. Added value of contrast-enhanced spectral mammography in Postscreening assessment. *Breast J* 2016; **22**: 520–8. doi: <https://doi.org/10.1111/tbj.12627>
10. Dromain C, Balleyguier C, Muller S, Mathieu M-C, Rochard F, Opolon P, et al. Evaluation of tumor angiogenesis of breast carcinoma using contrast-enhanced digital mammography. *AJR Am J Roentgenol* 2006; **187**: W528–W537. doi: <https://doi.org/10.2214/AJR.05.1944>
11. Dromain C, Thibault F, Muller S, Rimareix F, Delalogue S, Tardivon A, et al. Dual-energy contrast-enhanced digital mammography: initial clinical results. *Eur Radiol* 2011; **21**: 565–74. doi: <https://doi.org/10.1007/s00330-010-1944-y>
12. Lewin JM, Isaacs PK, Vance V, Larke FJ. Dual-energy contrast-enhanced digital subtraction mammography: feasibility. *Radiology* 2003; **229**: 261–8. doi: <https://doi.org/10.1148/radiol.2291021276>
13. Jong RA, Yaffe MJ, Skarpathiotakis M, Shumak RS, Danjoux NM, Guneseckara A, et al. Contrast-enhanced digital mammography: initial clinical experience. *Radiology* 2003; **228**: 842–50. doi: <https://doi.org/10.1148/radiol.2283020961>
14. Bhimani C, Matta D, Roth RG, Liao L, Tinney E, Brill K, et al. Contrast-enhanced spectral mammography: technique, indications, and clinical applications. *Acad Radiol* 2017; **24**: 84–8. doi: <https://doi.org/10.1016/j.acra.2016.08.019>
15. Harvey JA, Nicholson BT, Cohen MA. Finding early invasive breast cancers. *Radiology* 2008; **248**: 61–76.
16. Chesebro AL, Winkler NS, Birdwell RL, Giess CS. Developing asymmetries at mammography: a multimodality approach to assessment and management. *Radiographics* 2016; **36**: 322–34. doi: <https://doi.org/10.1148/rg.2016150123>
17. Lee CH, Smith RC, Levine JA, Troiano RN, Tocino I. Clinical usefulness of MR imaging of the breast in the evaluation of the problematic mammogram. *AJR Am J Roentgenol* 1999; **173**: 1323–9. doi: <https://doi.org/10.2214/ajr.173.5.10541112>

Received:
09 December 2018

Revised:
16 February 2019

Accepted:
20 February 2019

<https://doi.org/10.1259/bjr.20181034>

Cite this article as:

Aminololama-Shakeri S, Abbey CK, López JE, Hernandez AM, Gazi P, Boone JM, et al. Conspicuity of suspicious breast lesions on contrast enhanced breast CT compared to digital breast tomosynthesis and mammography. *Br J Radiol* 2019; **92**: 20181034.

FULL PAPER

Conspicuity of suspicious breast lesions on contrast enhanced breast CT compared to digital breast tomosynthesis and mammography

¹SHADI AMINOLOLAMA-SHAKERI, MD, ²CRAIG K. ABBEY, PhD, ³JAVIER E LÓPEZ, MD, ¹ANDREW M HERNANDEZ, ¹PEYMON GAZI, PhD, ¹JOHN M BOONE, PhD and ¹KAREN K LINDFORS, MD

¹Department of Radiology, University of California Davis Medical Center, California, USA

²Department of Psychological and Brain Sciences, University of California Santa Barbara, California, USA

³Internal Medicine Department, Cardiovascular Division, University of California Davis Medical Center, California, USA

Address correspondence to: Dr Shadi Aminololama-Shakeri
E-mail: sshakeri@ucdavis.edu

Objective: Compare conspicuity of suspicious breast lesions on contrast-enhanced dedicated breast CT (CEbCT), tomosynthesis (DBT) and digital mammography (DM).

Methods: 100 females with BI-RADS 4/5 lesions underwent CEbCT and/or DBT prior to biopsy in this IRB approved, HIPAA compliant study. Two breast radiologists adjudicated lesion conspicuity scores (CS) for each modality independently. Data are shown as mean CS \pm standard deviation. Two-sided *t*-test was used to determine significance between two modalities within each subgroup. Multiple comparisons were controlled by the false-discovery rate set to 5%.

Results: 50% of studied lesions were biopsy-confirmed malignancies. Malignant masses were more conspicuous on CEbCT than on DBT or DM (9.7 ± 0.5 , $n = 25$; 6.8 ± 3.1 , $n = 15$; 6.7 ± 3.0 , $n = 27$; $p < 0.05$). Malignant calcifications were equally conspicuous on all three modalities (CEbCT 8.7 ± 0.8 , $n = 18$; DBT 8.5 ± 0.6 , $n = 15$; DM 8.8 ± 0.7 , $n = 23$; $p = \text{NS}$). Benign masses were

equally conspicuous on CEbCT (6.6 ± 4.1 , $n = 22$); DBT (6.4 ± 3.8 , $n = 17$); DM (5.9 ± 3.6 , $n = 24$; $p = \text{NS}$). Benign calcifications CS were similar between DBT (8.5 ± 1.0 , $n = 17$) and DM (8.8 ± 0.8 , $n = 26$; $p = \text{NS}$) but less conspicuous on CEbCT (4.0 ± 2.9 , $n = 25$, $p < 0.001$). 55 females were imaged with all modalities. Results paralleled the entire cohort. 69% ($n = 62$) of females imaged by CEbCT had dense breasts. Benign/malignant lesion CSs in dense/non-dense categories were 4.8 ± 3.7 , $n = 33$, vs 6.0 ± 3.9 , $n = 14$, $p = 0.35$; 9.2 ± 0.9 , $n = 29$ vs. 9.4 ± 0.7 , $n = 14$; $p = 0.29$, respectively.

Conclusion: Malignant masses are more conspicuous on CEbCT than DM or DBT. Malignant microcalcifications are equally conspicuous on all three modalities. Benign calcifications remain better visualized by DM and DBT than with CEbCT. We observed no differences in benign masses on all modalities. CS of both benign and malignant lesions were independent of breast density.

Advances in knowledge: CEbCT is a promising diagnostic imaging modality for suspicious breast lesions.

INTRODUCTION

Unlike conventional two-dimensional (2D) digital mammography (DM) and digital breast tomosynthesis (DBT), dedicated breast CT (bCT), an emerging technology, provides fully three-dimensional isotropic image data sets without the need for breast compression. Unenhanced dedicated bCT has been shown in prior studies to be superior to mammography for the detection of masses but not microcalcifications.¹ More recently, contrast-enhanced dedicated bCT (CEbCT) was reported as a potential method for differentiating malignant from benign microcalcifications.² Differences in enhancement measured in Hounsfield units (HU), were shown to discriminate benign from malignant calcifications. These results suggest

that CEbCT is a potentially quantitative and qualitative modality for differentiating breast cancer from benign lesions including calcifications. As such, CEbCT may improve breast cancer detection as well as reduce the number of false-positive exams that frequently require an invasive procedure for making a definitive diagnosis.

DBT uses a modification of digital mammographic technique to reduce the effects of parenchymal superimposition. Large population studies^{3,4} have confirmed initial observations of reduced recall rates^{5,6} and improved radiologist performance^{7,8} as well as increased cancer detection with the addition of DBT to DM compared to DM alone. Several studies support the utility of tomosynthesis as a diagnostic

tool to potentially replace conventional 2D mammographic workups using additional projections and spot compression views⁹⁻¹¹ particularly for non-calcified lesions. DBT has been shown to characterize soft tissue lesions more accurately than 2D mammographic views.¹² In the diagnostic evaluation of calcifications, DM and DBT perform similarly.^{12,13}

Despite its advantages, tomosynthesis shares limitations with DM. DBT is a planar imaging modality where superimposition artifacts and masking of soft tissue lesions can occur in extremely dense tissues. More importantly, recall rates and cancer detection rates are not improved by the addition of tomosynthesis to DM in females with extremely dense breasts.¹⁴ In the diagnostic setting, multiple tomosynthesis projections, magnification views for calcified lesions and often ultrasound continue to be required for complete lesion characterization. It is yet unknown whether the use of DBT can decrease false-positive biopsies.

We report a cohort of patients with lesions recommended for biopsy after evaluation by conventional clinical diagnostic examination with mammography and targeted ultrasound. These patients were imaged with tomosynthesis and/or breast CT prior to biopsy. We hypothesize that CEbCT improves diagnostic evaluation of suspicious breast lesions when compared to tomosynthesis and 2D mammography. Our goal was to evaluate and compare the conspicuity of suspicious breast lesions on CEbCT, DBT and mammography.

METHODS AND MATERIALS

Females with BI-RADS category four or five lesions as determined by conventional clinical diagnostic work-up including full field digital 2D mammography (Selenia, Hologic®, Bedford, MA) or ultrasound were recruited and prospectively enrolled in our Institutional Review Board-approved and Health Insurance Portability and Accountability Act-compliant study. Written informed consent was obtained from all participants prior to the study. Patients with contraindications to the use of intravenous contrast material were excluded from the study. Alternating patients received craniocaudal (CC) and mediolateral oblique (MLO) tomosynthesis (Selenia Dimensions, Hologic®, Bedford, MA) or CEbCT. All tomosynthesis images were reviewed using SecureView workstations (Hologic®, Bedford, MA). All analyzed DM and DBT images were acquired directly without the use of synthetic 2D imaging. A subset of the participants had both tomosynthesis and CEbCT examinations. Consecutive patients in that subset cohort had alternating order of modalities. Patients whose lesions were matched on all three modalities were asked to complete a short questionnaire to rate their level of comfort on each of the modalities. The rating scale was from 1 to 10 with 1 defined as least comfortable and 10 as most comfortable. All subjects underwent core biopsy under ultrasound or stereotactic guidance for histopathological diagnosis of the clinically suspicious lesion. Only lesions with known histopathology were included in the study. Breast density was defined at mammography according to fourth (2003) edition of the BI-RADS manual.¹⁵

Image acquisition

The subjects of this study were imaged using a dedicated breast CT system previously reported.^{16,17} Briefly, images were acquired using a tube voltage of 80 kV. The tube current was adjusted according to breast size and mammographic breast density while keeping the mean glandular radiation dose approximately equivalent to that of two-view screening mammography. Images were acquired with patients in prone position after one breast at a time was placed through an opening in the scanner. The scan duration was 17 s during which the subject was instructed to hold her breath. Patients were instructed to remain still upon completion of the non-contrast scan of the affected breast, while 100 mL of intravenous iodixanol (Visipaque 320; GE Healthcare, Waukesha, WI) was administered at a rate of 4 mL/s using a power injector. The breast was rescanned approximately 90 s after the start of the injection.

Radiation dosimetry

A direct comparison of the mean glandular dose (MGD) from mammography and bCT was performed over 243 patients involved in breast CT studies. These patients received both two-view mammograms (CC & MLO) and a breast CT scan. Breast dosimetry for mammography and breast CT has been studied extensively in our laboratory^{18,19} and it is widely assumed that the dose in DBT is within 5% of the dose of mammography.²⁰ Thus, the comparison here is between two-view mammography, two-view tomosynthesis, and one breast CT examination.

Lesion analysis

To compare all three modalities (DM, DBT and CEbCT), a for each histologically proven lesion was assigned per modality by two independent observers. Lesion type and descriptors such as size, mass shape and margin were recorded. CC and MLO mammographic views, DBT and CEbCT were independently reviewed in sequential order by two breast imaging radiologists, each with at least 3 years of experience with dedicated breast CT. DBT or CEbCT images were reviewed first followed by review of the mammogram. All CEbCT images were reviewed on specialized software in coronal, axial and sagittal planes.²¹

The conspicuity of each lesion was scored on a continuous scale from 0 to 10, where 0 represented non-visualization and 10 indicated excellent conspicuity on each modality.

Statistical analysis

For a given lesion in an imaging modality, conspicuity scores from two radiologists were averaged into a single combined score. For the total of 255 lesion/modality combinations for which scores were available, a small number (6; 1.2%) were missing a score from one of the radiologists. In these cases, the single available conspicuity score served as the "combined" score. The cases were classified as mass or microcalcification lesions based on the dominant finding on the patient's clinical diagnostic presentation. Lesions were further subdivided based on histological outcomes of benign or malignant pathology.

The primary comparisons of this work consisted of differences in conspicuity of findings on CEbCT, DBT and DM. Comparisons

were made in each of the 4 subgroups of data (benign mass, malignant mass, benign microcalcifications, and malignant microcalcifications) for a total of 12 primary comparisons.

Univariate statistical summaries were performed with calculation of average conspicuity scores of each lesion for each modality. These data are shown as mean \pm standard deviation of conspicuity scores. Two-sided *t*-tests were used to compare conspicuity between two modalities within each subgroup. When significant unpaired data were available (five or more scores in each unpaired group) an optimal pooled *t*-test was used to assess significance.²² Otherwise unpaired data were ignored, and a standard paired *t*-test was used. Multiple comparisons were controlled using the method of Benjamini and Hochberg,²³ with the familywise false-discovery rate set to 5%.

RESULTS

102 patients with 103 BIRADS four or five lesions were prospectively enrolled. Two of the participants, one of whom had two lesions, were excluded due to incompleteness of the protocol. Of the remaining 100 patients, 90 had CEbCT and 65 were imaged with DBT. All had DM as part of their clinical diagnostic workup. A smaller cohort of these patients (55 out of 100) was imaged with all three modalities. All patients were females with an average age of 55 years (age range 36–77 years). One patient in the earlier phase of the recruitment process had a screen film mammogram. All others underwent DM. 54 patients had heterogeneously dense or dense fibroglandular tissues on their mammograms.

Histopathology distribution

Of 100 breast lesions, 50 (50%) were malignant and 50 (50%) were benign. The histopathological findings for these lesions are listed in Table 1. Out of the 50 malignant lesions, 27 (54%) were masses and 23 (46%) were calcifications. Of 50 benign lesions, 24 (48%) were masses and 26 (52%) were calcifications. 14 patients reported palpable findings, of which all but one were masses.

Lesion conspicuity

Malignant

Malignant masses were significantly more conspicuous on CEbCT than on DBT or DM (9.7 ± 0.5 $n = 25$, 6.8 ± 3.1 $n = 15$, 6.7 ± 3.0 $n = 27$ respectively $p < 0.05$) (Figure 1). Malignant mass sizes ranged from 6 to 22 mm with an average of 13 mm. Three cancers were occult on 2D mammography but highly conspicuous on CEbCT. One of these was also occult on tomosynthesis (Figure 2).

Malignant calcification lesions were equally conspicuous on all three modalities (CEbCT 8.7 ± 0.8 $n = 18$, DBT 8.5 ± 0.6 $n = 15$ DM 8.8 ± 0.7 $n = 23$; $p = \text{NS}$) (Figure 3). The average size of the malignant calcification lesions was 9 mm with lesion sizes ranging from 2 to 26 mm (Figure 4).

Benign

Benign masses were equally conspicuous on CEbCT (6.6 ± 4.1 $n = 22$), DBT (6.4 ± 3.8 $n = 17$) and DM (5.9 ± 3.6 $n = 24$) ($p = \text{NS}$) (Figure 1). Conspicuity scores of benign calcifications were

Table 1. Histopathology of lesions

	Lesions ($N = 100$)	
	N	%
Malignant Lesions	50	
Invasive ductal carcinoma	23	46%
Grade 1	8	
Grade 2	12	
Grade 3	3	
Invasive lobular carcinoma	3	6%
Grade 1	2	
Grade 2	1	
Grade 3	0	
DCIS	24	48%
Grade 1	3	
Grade 2	9	
Grade 3	12	
Benign lesions	50	
Adenosis	3	
Atypical ductal hyperplasia	6	
Apocrine metaplasia	2	
Benign, NOS	7	
Columnar cell change	4	
Cyst	1	
Fat necrosis	1	
Fibroadenoma	11	
FibroadiPOSE tissue	1	
Fibrocystic changes	10	
Flat epithelial atypia	1	
Papilloma	2	
Stromal fibrosis	1	

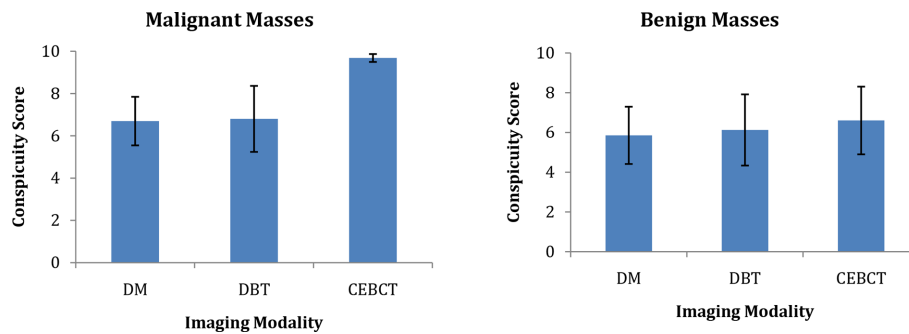
DCIS, ductal carcinoma *in situ*.

equal on DBT (8.5 ± 1.0 $n = 17$), and DM (8.8 ± 0.8 $n = 26$) ($p = \text{NS}$) but significantly less on CEbCT (4.0 ± 2.9 $n = 25$ $p < 0.001$) (Figure 3). The benign calcifications ranged in size from 4 to 18 mm with an average of 8 mm.

Matched subset analysis

55 out of 100 were imaged with all three modalities prior to biopsy. In this subset, 13 patients had malignant masses, 10 had malignant calcifications, 16 had benign masses and another 16 had benign calcifications. Results from this smaller group of patients followed the above analysis of the larger cohort closely. In this matched group, malignant masses were also significantly more conspicuous on CEbCT than on DBT or DM (9.5 ± 0.6 , 6.9 ± 3.2 , 5.6 ± 3.8 $n = 13$ respectively $p < 0.05$). Malignant calcification

Figure 1. Mass conspicuity on DM, DBT and CEbCT. CEbCT, contrast-enhanced breast CT; DBT, dedicated breast tomosynthesis; DM, digital mammography.



lesions were equally conspicuous on all three modalities (CEbCT 8.4 ± 0.8 , DBT 8.6 ± 0.6 , DM 8.8 ± 0.6 $n = 10$; $p = NS$).

Benign masses were equally conspicuous on CEbCT (6.5 ± 4.2), DBT (6.3 ± 3.9) and DM (6.0 ± 3.7 , $p = NS$). Conspicuity scores of benign calcifications were equal on DBT (8.5 ± 1.0), and DM (8.8 ± 0.7 , $p = NS$) but significantly less on CEbCT (4.8 ± 2.9 , $p < 0.001$).

Radiation dosimetry

For the database of patients used exclusively for dose comparisons ($N = 243$), the breast CT dose was on average 50.1% higher than two-view mammography, and thus was also about 50% higher than DBT as well. For the 55 patients in this study who underwent both two-view mammography and two-view DBT, the dose from breast CT was on average about 33% lower than the combination of mammography and DBT.

Comfort survey

50 out of 55 (91%) patients who were imaged by all three modalities completed a short survey regarding their comfort level on CEbCT. Responses are shown in Table 2. The score scales were

from 1 to 10 where 1 was very uncomfortable and 10 was designated as very comfortable. The respondents rated the comfort of the breath hold and contrast injection as 7.28 ± 2.76 and 8.36 ± 1.51 respectively and the overall exam as 6.50 ± 2.42 . The patients rated CEbCT as being more comfortable than both DM and DBT.

CEbCT CS correlation with breast density

62 of the 90 patients imaged by CEbCT had dense breast tissue (heterogeneously dense and extremely dense combined) and 28/90 had non-dense tissue (fatty and scattered fibroglandular tissue combined). The mean conspicuity scores \pm standard deviation of benign lesions were 4.8 ± 3.7 $n = 33$, vs 6.0 ± 3.9 $n = 14$, $p = 0.35$ in the dense vs non-dense categories respectively. The malignant lesion conspicuity scores (Figure 5, $n = 14$) were also not significantly different in the dense vs non-dense breasts (9.2 ± 0.9 $n = 29$ vs. 9.4 ± 0.7 , $p = 0.29$).

DISCUSSION

This study demonstrates that malignant masses are more conspicuous on dedicated CEbCT than both mammography and tomosynthesis. Malignant microcalcifications are equally conspicuous on all three modalities even for lesions as small as a

Figure 2. Invasive ductal carcinoma is occult on DM (a) and DBT (b) in extremely dense breast and enlarged axillary lymph node as the sole finding (white arrow). Abnormally enhancing irregular mass with extension to skin (yellow arrow) as well as metastatic lymph node (white arrow) visualized on coronal (c), sagittal (d) and axial (e) CEbCT. CEbCT, contrast-enhanced breast CT; DBT, dedicated breast tomosynthesis; DM, digital mammography.

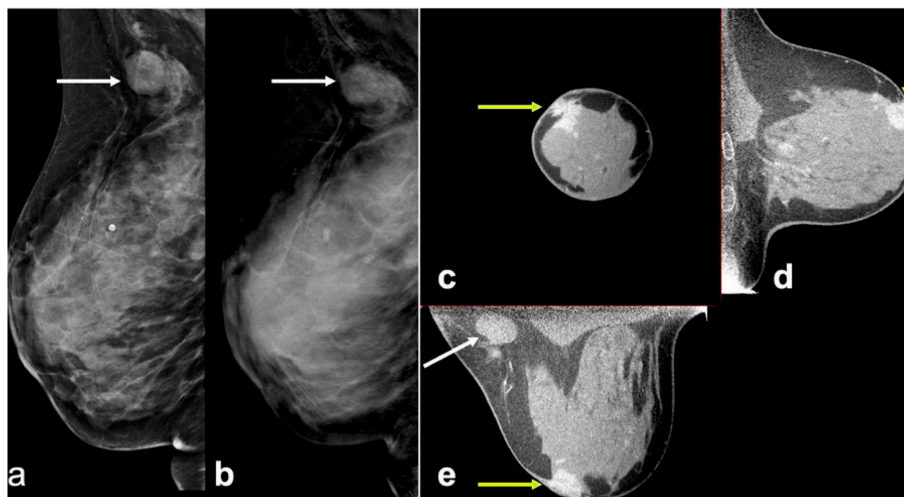
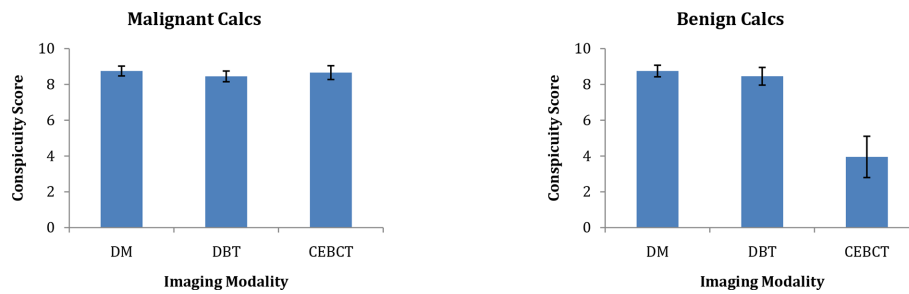


Figure 3. Comparison of microcalcification conspicuity on DM, DBT and CEbCT. CEbCT, contrast-enhanced breast CT; DBT, dedicated breast tomosynthesis; DM, digital mammography.



few millimeters. Benign calcifications on the other hand, remain better visualized by mammography and tomosynthesis when compared to CEbCT. There is no significant difference for visualization of benign masses on the three modalities.

Malignant microcalcifications are visualized equally on CEbCT and mammography—the gold-standard for calcification evaluation as well as with tomosynthesis. In contrast to both mammography and tomosynthesis, where benign and malignant microcalcifications are equally visualized, on CEbCT benign microcalcifications are not as conspicuous as malignant microcalcifications. This differential conspicuity between benign and malignant calcifications on CEbCT is advantageous over both DM and DBT, where all calcifications—benign and

malignant—may be equally visible and require tissue sampling to discriminate the two categories.

Overlap of mammographic features of benign and malignant lesions, both indolent and aggressive, necessitates core biopsy for definitive diagnosis. This decreases biopsy positive-predictive values (PPV) in standard clinical work-up of detected lesions. The enhancement differential between benign and malignant masses on CEbCT as reported previously¹ may be used as a quantitative tool for the assessment of these lesions. Recently, enhancement values for benign microcalcifications have been shown to be lower than that of malignant ones.² Used as a diagnostic tool, CEbCT may avert unnecessary biopsies for findings without enhancement that may be more appropriate for surveillance. As

Figure 4. Malignant microcalcification lesion on DM, DBT and CEbCT. Optical enlargement of mammographic magnification view (a) and tomosynthesis (b) show a group of pleomorphic microcalcifications. Coronal (c), sagittal (d) and axial (e) views on CEbCT show a 5 mm enhancing mass corresponding to the microcalcifications. Histopathology showed DCIS and invasive ductal carcinoma. CEbCT, contrast-enhanced breast CT; DBT, dedicated breast tomosynthesis; DCIS, ductal carcinoma in situ; DM, digital mammography.

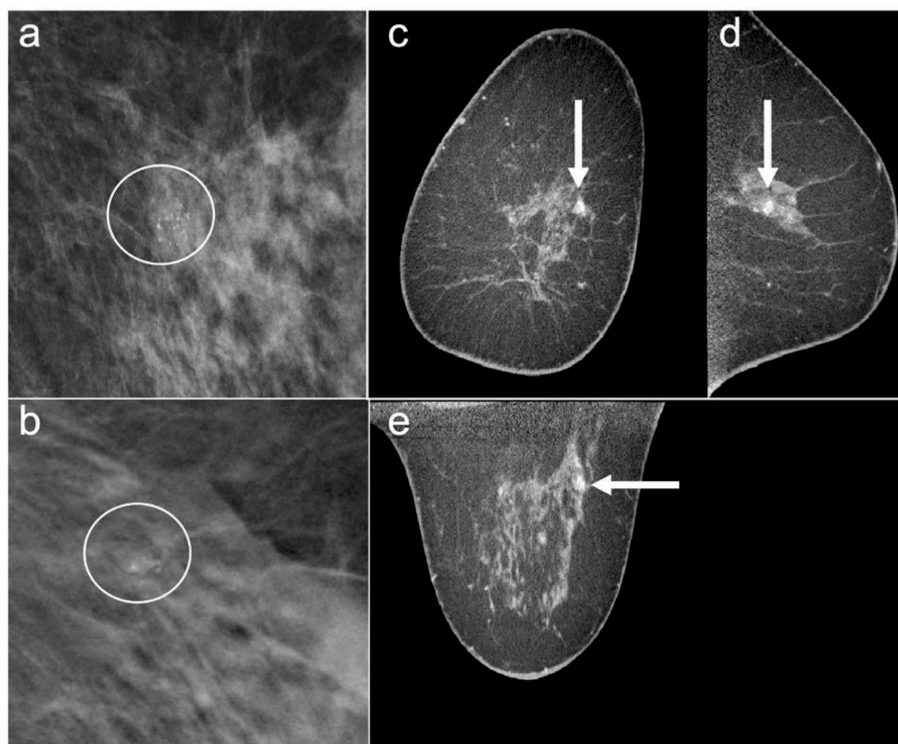


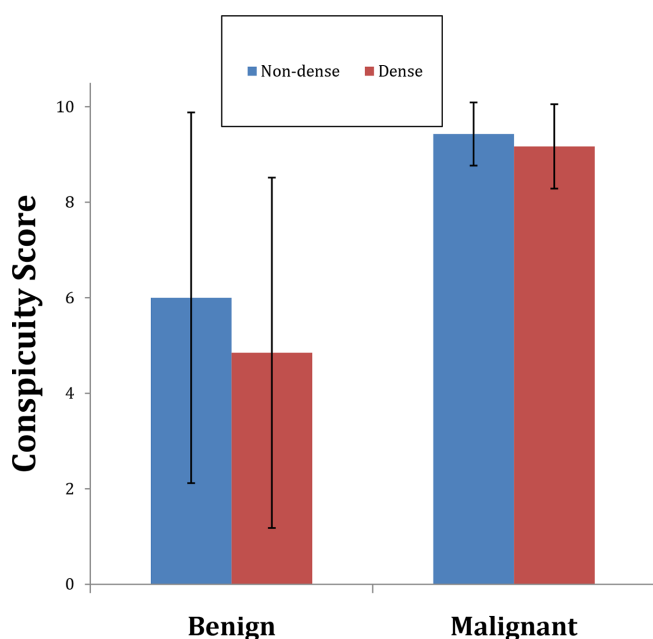
Table 2. Summary of responses to questionnaire completed by 50/55 females who were imaged with DM, DBT and CEbCT regarding the comfort level on CEbCT

	Mean (Std dev)	Median
How difficult was it for you to hold your breath during the breast CT exam? 1 = Very 10 = Not at all	7.28 (2.76)	8
How uncomfortable was the contrast (dye) injection? 1 = Very uncomfortable 10 = Very comfortable	8.36 (1.51)	9
Please rate your overall comfort level during the entire breast CT exam. 1 = Very uncomfortable 10 = Very comfortable	6.50 (2.42)	6.5
Please rate the overall comfort of the entire contrast breast CT exam compared to mammography. 1 = Much worse 10 = Much better	6.90 (2.41)	7.5
Please rate the overall comfort of the entire contrast breast CT exam compared to tomosynthesis. 1 = Much worse 10 = Much better	6.44 (2.14)	6

such, reducing biopsies of those lesions that do not enhance on CEbCT would increase biopsy PPV as well as potentially reduce the cost burden and the anxiety related to having an interventional procedure.

Biological characteristics of breast lesions may be obtained from any imaging technique that utilizes contrast material such as

Figure 5. Conspicuity scores of both benign and malignant lesions are not significantly different in dense and non-dense breasts on CEbCT. CEbCT, contrast-enhanced breast CT.



dynamic contrast-enhanced breast MRI (DCE-MRI), contrast enhanced spectral mammography (CESM) or contrast-enhanced tomosynthesis (CET). Tumor enhancement may correlate with the biological activity of tumor cells and provide a biomarker for disease progression. With DCE-MRI, the lack of enhancement of low grade ductal carcinoma *in situ* lesions has been described as advantageous for discriminating those indolent lesions which may not require the same treatment attention as more biologically aggressive ones.²⁴ There is developing evidence that CESM may have improved sensitivity over DM.²⁵ Comparisons of CESM, CET and DCE-MRI have also shown similar diagnostic accuracy and improved performance in comparison to DM and DBT.²⁶ As a fully three-dimensional modality, breast CT provides superior anatomical information in comparison to mammography and its derivative technologies, DBT, CESM and CET. CEbCT does not require compression like DM and DBT and has potential to quantify enhancement like MRI, which has potential for informing biopsy decision thresholds as opposed to CESM and CET where evaluation of enhancement is not quantitative. Additionally, each breast is imaged in less than 20 s in comparison to the time required to reposition the breast to obtain the standard mammographic CC and MLO views as well as MRI. One of the shortcomings of using CEbCT like any technique requiring contrast enhancement is the necessity of an intravenous injection as well as the potential for contrast reactions. In this study, patients did not find the contrast injection and breath hold for CEbCT to pose a barrier to performing the exam. Similar to the use of CT for imaging of other body parts, screening for contrast allergy history and renal disease would be prudent in clinical implementation.

Clinical trials comparing the performance of CEbCT to DCE-MRI are currently underway. Prospective studies directly comparing CEbCT to contrast-enhanced mammography and CET would be useful to define its role in clinical practice. These studies should not only focus on measuring diagnostic accuracy, but also, cost analysis and patient preferences.

CEbCT depicts breast tissue without compression and at the same radiation dose but without being affected by breast tissue density in contrast to mammograms. In this study we have shown that conspicuity of lesions, particularly, visualization of cancers on CEbCT is unaffected by breast density. This feature overcomes the most significant limitation of mammography and tomosynthesis performance in extremely dense breasts¹⁴ thereby decreasing false negative exams. In addition, tomosynthesis continues to require compression for adequate image production.

Our study has limitations. It is based on a small number of subjects in each category of lesions. Larger blinded studies evaluating receiver operating curves are needed to allow the evaluation of enhancement values in the spectrum of breast lesions. Another limitation of our study is the subjective scoring of lesion conspicuity on the three modalities by the two readers. The readers were involved in patient recruitment, therefore there is potential for recall bias.

In summary, we have shown that CEbCT is superior in the visualization of malignant masses and has potential for discriminating benign from enhancing malignant calcification lesions when compared to DM and DBT. The differences in appearance of lesions on CEbCT in comparison to tomosynthesis and mammography may be related to the biology of the findings characterized by degree of contrast enhancement and are independent of breast density. As a diagnostic tool, CEbCT may potentially decrease false-negative exams in extremely dense breasts where malignant lesions may be difficult to discern on mammography and tomosynthesis due to masking. CEbCT also holds promise in increasing biopsy PPV and thus avoiding costly interventions for lesions that are indistinguishable from malignancies on mammographic derivative studies. The potential for quantitation

of enhancement of breast lesions with CEbCT is advantageous when compared to contrast-enhanced mammographic techniques. Although randomized, blinded, multicentered trials with a larger number of participants are needed, our results demonstrate a promising role in the diagnostic setting for CEbCT in the detection of breast cancer.

ACKNOWLEDGMENT

This communication was funded in part by NIH grants P30 CA093373 and R01 CA181081. Comments made are solely the responsibility of the authors and do not necessarily represent the official views of the National Cancer Institute or the National Institutes of Health.

REFERENCES

- Prionas ND, Lindfors KK, Ray S, Huang S-Y, Beckett LA, Monsky WL, et al. Contrast-enhanced dedicated breast CT: initial clinical experience. *Radiology* 2010; **256**: 714–23. doi: <https://doi.org/10.1148/radiol.10092311>
- Aminololama-Shakeri S, Abbey CK, Gazi P, Prionas ND, Nosratieh A, Li C-S, et al. Differentiation of ductal carcinoma in-situ from benign micro-calcifications by dedicated breast computed tomography. *Eur J Radiol* 2016; **85**: 297–303. doi: <https://doi.org/10.1016/j.ejrad.2015.09.020>
- Skaane P, Bandos AI, Gullien R, Eben EB, Ekseth U, Haakenaasen U, et al. Comparison of digital mammography alone and digital mammography plus tomosynthesis in a population-based screening program. *Radiology* 2013; **267**: 47–56. doi: <https://doi.org/10.1148/radiol.12121373>
- Friedewald SM, Rafferty EA, Rose SL, Durand MA, Plecha DM, Greenberg JS, et al. Breast cancer screening using tomosynthesis in combination with digital mammography. *JAMA* 2014; **311**: 2499–507. doi: <https://doi.org/10.1001/jama.2014.6095>
- Gur D, Abrams GS, Chough DM, Ganott MA, Hakim CM, Perrin RL, et al. Digital breast tomosynthesis: Observer performance study. *AJR Am J Roentgenol* 2009; **193**: 586–91. doi: <https://doi.org/10.2214/AJR.08.2031>
- Gennaro G, Toledano A, di Maggio C, Baldan E, Bezzon E, La Grassa M, et al. Digital breast tomosynthesis versus digital mammography: a clinical performance study. *Eur Radiol* 2010; **20**: 1545–53. doi: <https://doi.org/10.1007/s00330-009-1699-5>
- Rafferty EA, Park JM, Philpotts LE, Poplack SP, Sumkin JH, Halpern EF, et al. Assessing radiologist performance using combined digital mammography and breast tomosynthesis compared with digital mammography alone: results of a multicenter, multireader trial. *Radiology* 2013; **266**: 104–13. doi: <https://doi.org/10.1148/radiol.12120674>
- Svahn TM, Chakraborty DP, Ikeda D, Zackrisson S, Do Y, Mattsson S, et al. Breast tomosynthesis and digital mammography: a comparison of diagnostic accuracy. *Br J Radiol* 2012; **85**: e1074–82. doi: <https://doi.org/10.1259/bjr/53282892>
- Brandt KR, Craig DA, Hoskins TL, Henrichsen TL, Bendel EC, Brandt SR, et al. Can digital breast tomosynthesis replace conventional diagnostic mammography views for screening recalls without calcifications? A comparison study in a simulated clinical setting. *AJR Am J Roentgenol* 2013; **200**: 291–8. doi: <https://doi.org/10.2214/AJR.12.8881>
- Noroozian M, Hadjiiski L, Rahnema-Moghadam S, Klein KA, Jeffries DO, Pinsky RW, et al. Digital breast tomosynthesis is comparable to mammographic spot views for mass characterization. *Radiology* 2012; **262**: 61–8. doi: <https://doi.org/10.1148/radiol.11101763>
- Zuley ML, Bandos AI, Ganott MA, Sumkin JH, Kelly AE, Catullo VJ, et al. Digital breast tomosynthesis versus supplemental diagnostic mammographic views for evaluation of noncalcified breast lesions. *Radiology* 2013; **266**: 89–95. doi: <https://doi.org/10.1148/radiol.12120552>
- Morel JC, Iqbal A, Wasan RK, Peacock C, Evans DR, Rahim R, et al. The accuracy of digital breast tomosynthesis compared with coned compression magnification mammography in the assessment of abnormalities found on mammography. *Clin Radiol* 2014; **69**: 1112–6. doi: <https://doi.org/10.1016/j.crad.2014.06.005>
- Spangler ML, Zuley ML, Sumkin JH, Abrams G, Ganott MA, Hakim C, et al. Detection and classification of calcifications on digital breast tomosynthesis and 2D digital mammography: a comparison. *AJR Am J Roentgenol* 2011; **196**: 320–4. doi: <https://doi.org/10.2214/AJR.10.4656>
- Rafferty EA, Durand MA, Conant EF, Copit DS, Friedewald SM, Plecha DM, et al. Breast cancer screening using Tomosynthesis and digital mammography in dense and Nondense breasts. *JAMA* 2016; **315**: 1784–6. doi: <https://doi.org/10.1001/jama.2016.1708>
- D'Orsi, C. J, Mendelson, E. B, Ikeda, D. M, al, e. eds. *Breast Imaging Reporting and Data System: ACR BI-RADS-Breast Imaging Atlas*. Reston, VA: American College of Radiology; 2003.
- Kwan ALC, Boone JM, Yang K, Huang S-Y. Evaluation of the spatial resolution characteristics of a cone-beam breast CT scanner. *Med Phys* 2007; **34**: 275–81. doi: <https://doi.org/10.1118/1.2400830>
- Boone JM, Yang K, Burkett GW, Packard NJ, Huang S-ying, Bowen S, et al. An X-ray computed tomography/positron emission tomography system designed specifically for breast imaging. *Technol Cancer Res Treat* 2010; **9**: 29–43. doi: <https://doi.org/10.1177/153303461000900104>
- Boone JM, dose Nglandular. Normalized glandular dose (DgN) coefficients for arbitrary x-ray spectra in mammography: computer-fit values of Monte Carlo derived data. *Med Phys* 2002; **29**: 869–75. doi: <https://doi.org/10.1118/1.1472499>
- Boone JM, Kwan ALC, Seibert JA, Shah N, Lindfors KK, Nelson TR, et al. Technique factors and their relationship to radiation

- dose in pendant geometry breast CT. *Med Phys* 2005; **32**: 3767–76. doi: <https://doi.org/10.1118/1.2128126>
20. Sechopoulos I, Sabol JM, Berglund J, Bolch WE, Brateman L, Christodoulou E, et al. Radiation dosimetry in digital breast tomosynthesis: report of AAPM Tomosynthesis Subcommittee task group 223. *Med Phys* 2014; **41**: 091501. doi: <https://doi.org/10.1118/1.4892600>
21. Aminololama-Shakeri S, Hargreaves JB, Boone JM, Lindfors KK. Dedicated breast CT: screening technique of the future. *Curr Breast Cancer Rep* 2016; **8**: 242–7. doi: <https://doi.org/10.1007/s12609-016-0227-2>
22. Guo B, Yuan Y. A comparative review of methods for comparing means using partially paired data. *Stat Methods Med Res* 2017; **26**: 1323–40. doi: <https://doi.org/10.1177/0962280215577111>
23. Benjamini Y, Hochberg Y. Controlling the false discovery rate: a practical and powerful approach to multiple testing. *Journal of the Royal Statistical Society. Series B* 1995;: 289–300.
24. Kuhl CK, Schrading S, Bieling HB, Wardelmann E, Leutner CC, Koenig R, et al. MRI for diagnosis of pure ductal carcinoma in situ: a prospective observational study. *Lancet* 2007; **370**: 485–92. doi: [https://doi.org/10.1016/S0140-6736\(07\)61232-X](https://doi.org/10.1016/S0140-6736(07)61232-X)
25. Dromain C, Thibault F, Muller S, Rimareix F, Delalogue S, Tardivon A, et al. Dual-energy contrast-enhanced digital mammography: initial clinical results. *Eur Radiol* 2011; **21**: 565–74. doi: <https://doi.org/10.1007/s00330-010-1944-y>
26. Chou C-P, Lewin JM, Chiang C-L, Hung B-H, Yang T-L, Huang J-S, et al. Clinical evaluation of contrast-enhanced digital mammography and contrast enhanced tomosynthesis--Comparison to contrast-enhanced breast MRI. *Eur J Radiol* 2015; **84**: 2501–8. doi: <https://doi.org/10.1016/j.ejrad.2015.09.019>

Received:
23 January 2018

Revised:
15 August 2018

Accepted:
15 September 2018

<https://doi.org/10.1259/bjr.20180101>

Cite this article as:

Yi A, Chang JM, Shin SU, Chu AJ, Cho N, Noh D-Y, et al. Detection of noncalcified breast cancer in patients with extremely dense breasts using digital breast tomosynthesis compared with full-field digital mammography. *Br J Radiol* 2019; **92**: 20180101.

FULL PAPER

Detection of noncalcified breast cancer in patients with extremely dense breasts using digital breast tomosynthesis compared with full-field digital mammography

^{1,2}ANN YI, MD, ¹JUNG MIN CHANG, MD, ^{1,2}SUNG UI SHIN, MD, ¹A JUNG CHU, MD, ¹NARIYA CHO, MD, ³DONG-YOUNG NOH, MD and ¹WOO KYUNG MOON, MD

¹Department of Radiology, Seoul National University Hospital, Seoul, Republic of Korea

²Department of Radiology, Seoul National University Hospital Healthcare System Gangnam Center, Seoul, Republic of Korea

³Department of Surgery, Seoul National University Hospital, Seoul, Republic of Korea

Address correspondence to: Prof Jung Min Chang
E-mail: imchangjm@gmail.com

Objective: To evaluate the tumour visibility and diagnostic performance of digital breast tomosynthesis (DBT) in patients with noncalcified T_1 breast cancer.

Methods: Medical records of 106 females with noncalcified T_1 invasive breast cancer who underwent DBT and full-field digital mammography (FFDM) between January 2012 and December 2014 were retrospectively reviewed. To assess tumour visibility (score 1-3), all DBT and FFDM images were reviewed by two radiologists blinded to clinicopathological information. A reference standard was established by an unblinded consensus review of all images. Clinicopathological and imaging variables were analysed based on tumour visibility. After adding 159 negative controls, the diagnostic performance of DBT + FFDM was compared with that of FFDM.

Results: The tumour visibility was significantly higher through DBT + FFDM (2.5 vs 1.8; $p = 0.002$) than FFDM

alone. Breast composition was the independent variable for tumour visibility through DBT + FFDM (extremely dense; odds ratio, 0.02; $p < 0.001$). Sensitivity ($p = 0.642$), specificity ($p = 0.463$), positive-predictive value ($p = 0.078$), and negative-predictive value ($p = 0.072$) of DBT + FFDM were not significantly superior to those of FFDM in 55 females with extremely dense breast composition, whereas specificity ($p = 0.002$) and positive-predictive value ($p < 0.001$) were significantly higher in 210 females with other breast compositions.

Conclusion: Addition of DBT to FFDM showed no significant increase in the tumour visibility and diagnostic performance in patients with noncalcified T_1 cancer in extremely dense breasts.

Advances in knowledge: Addition of DBT to FFDM did not further improve the detection of noncalcified early breast cancers in females with extremely dense breasts.

INTRODUCTION

Breast density-tailored screening for breast cancer in females is of great interest.¹ Breast density is a predictor of breast cancer; it reduces the sensitivity of mammography, leading to an increased risk of interval cancer in the screening population.^{2,3} Several breast imaging modalities have been used as adjuncts to screening mammography in females with dense breasts, including ultrasound (US; handheld or automated), MRI, and the more recently applied digital breast tomosynthesis (DBT). DBT is an emerging technique that allows the breast to be viewed quasi-three-dimensionally, which reduces superimposition of the breast tissue.^{4,5} Previous studies showed that DBT improved the accuracy of full-field digital mammography (FFDM) in screening across all breast densities by reducing

the recall rates and increasing the cancer detection rates.⁶⁻¹⁰ In addition, a recent study including females with dense breasts reported that the addition of DBT increased the sensitivity of FFDM.¹¹⁻¹³

To date, the effect of breast density on the diagnostic performance of DBT was evaluated based on percentage-based classification. Breast density assessed using mammography, reflects the breast composition. High breast density can comprise various breast compositions. The tumour located in the dense breast with small amount of interposed fat tissue that overlaps individual sections may result in mammographically occult cancer and even with the use of DBT.¹⁴ Moreover, in case of the occurrence of small tumour without noticeable calcification,

the dense breast tissue might more easily obscure the tumour visibility.

We hypothesized that the visibility of small noncalcified breast cancers on DBT is affected by the breast composition. Therefore, the purpose of our study was to evaluate the tumour visibility and diagnostic performance of DBT in patients with noncalcified T_1 breast cancers according to the breast composition.

METHODS AND MATERIALS

Study population

Our Institutional Review Board approved the retrospective study and waived the requirement for patients' informed consent. Of 2673 females who had undergone DBT and FFDM between January 2012 and December 2014, 106 females (median age, 51.2 years; age range, 22–77 years) who had undergone subsequent curative surgery for single noncalcified T_1 -stage invasive breast cancer (median size, 8 mm; size range, 4–20 mm on surgical histopathology) were included. Among these patients, 68 females were referred from other hospitals with nonspecific clinical manifestation (64.2%), 31 females had a palpable lump (29.2%), and seven had nipple discharge (6.6%). The tumours were detected using DBT + FFDM ($n = 91$), ultrasound ($n = 103$), or both ($n = 88$) at the time of diagnosis.

Imaging data acquisition

All imaging data were acquired as part of our hospitals' routine clinical practice using an FFDM unit with integrated DBT acquisition (Selenia Dimensions mammography system, Hologic, Inc., Bedford, MA). Patients underwent bilateral two-view FFDM and DBT [craniocaudal (CC) and mediolateral oblique (MLO)] in the Combo mode, and FFDM and DBT images were obtained with single breast compression for each projection. In patients with the breast of 5.0 cm compressed thickness and 50 glandular fraction, DBT acquisition resulted in 8% higher mean glandular dose per view than that of digital mammography acquisition (1.30 and 1.20 mGy, respectively).

Imaging data analysis

Four board-certified radiologists participated in the two retrospective review sessions. Each radiologist had more than 12 years' clinical experience in FFDM and more than 4 years' experience in DBT at the respective academic institution.

Table 1. Tumour visibility score: DBT + FFDM vs FFDM

Tumour visibility score	DBT + FFDM	FFDM	P-value ^a
1	22 (20.8)	56 (52.8)	0.011
2	11 (10.3)	13 (12.3)	
3	73 (68.9)	37 (34.9)	
Mean \pm SD	2.5 \pm 0.1	1.8 \pm 0.2	0.002

DBT, digital breast tomosynthesis; FFDM, full-field digital mammography; SD, standard deviation.

Data are numbers of cases, and data in parentheses are percentages.

^aP-values were obtained by the Pearson's Chi-square test for categorical variables and Mann-Whitney test for continuous variables.

Tumour visibility

Two radiologists (JMC and AY) performed unblinded consensus review of the 106 tumour cases. First, the tumour site was determined on both the FFDM and DBT images and correlated with clinical, surgical, and pathologic findings. In case of uncertain tumour on the FFDM or DBT image, the estimated tumour locations were determined on the basis of the other imaging (ultrasound and MRI) findings. Subsequently, the visibility score (1–3) for the determined tumour location was assessed on both the DBT and FFDM images. The tumour that was obvious and conspicuous in both the CC and MLO views was assigned a score of 3; the tumour that was conspicuous in only one view or faintly visible was assigned a score of 2; and the tumour that was uncertain and not visible in both views was assigned a score of 1. The breast composition (a,b,c,d), and imaging characteristics of the mass (shape, margin, density) were determined per the Breast Imaging Reporting and Database System, fifth Edition.¹⁴ In addition, the breast thickness (mm) at the time of mammographic image acquisition was recorded.

Diagnostic performance

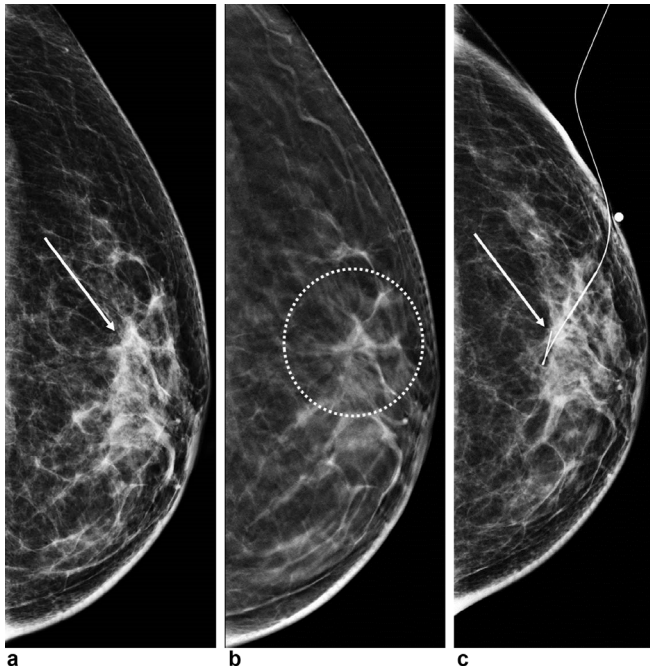
To assess the diagnostic performance, the other two radiologists (SUS and AJC) performed blinded consensus review of total 265 cases including 106 tumour cases, and 159 negative control cases. In addition, 159 negative control cases were identified from among the screening mammographies conducted between January 2012 and December 2014 with the results of final assessment Category 1, and absence of tumour occurrence after clinical or imaging follow-up for 1 year in our hospitals' medical report. The number of tumour cases and negative control cases were matched with a statistical ratio of 1:1.5 per breast composition.

Two separate review sessions were performed on the FFDM alone and DBT + FFDM images, respectively at 4 weeks' interval. In each reading session, all cases were randomized and presented in alternating order in a blinded manner with respect to the clinical, surgical, pathologic, and other imaging findings. With regard to the presence of suspected tumour on mammographic images, the presumptive tumour site was marked; and in case of the absence of suspected tumour, the images were left unmarked. Subsequently, the results of the blinded review were correlated with the reference data by two radiologists (JMC and AY) as follows: The case of tumour correctly marked on either CC and MLO views was assigned as true positive; the case of tumour wrongly marked or negative control case with marking was assigned as false positive; the negative control case with no marks was assigned as true negative; and the tumour case with no marks in any view was assigned as false-negative.

Histopathological analysis

All 106 patients with tumours underwent curative surgery, including breast conserving surgery ($n = 78$) and mastectomy ($n = 28$). The tumour histology, histologic grade, and size (greatest dimension of the invasive tumour) were determined based on results obtained from the surgically excised specimens.^{15,16} In addition, expression of the estrogen receptor (ER), progesterone receptor (PR), and human epidermal growth factor receptor Type 2 (HER2) was evaluated.^{17,18} A cut-off value of 1% was used

Figure 1. Images of a 53-year-old female diagnosed with an invasive ductal carcinoma (0.9 cm in size) in the left breast (breast composition b). The left craniocaudal view on FFDM (a) showed an irregular hyperdense mass in the subareolar area of the left breast (visibility score 2). The left craniocaudal view on DBT (b) showed an irregular mass with more conspicuous spicules in the left breast (visibility score 3). Mammography-guided wire localization was performed (c). DBT, digital breast tomosynthesis; FFDM, full-field digital mammography.



to define ER and PR positivity.¹⁷ HER2 expression was initially scored as 0, 1+, 2+, or 3+ based on results from the immunohistochemistry (IHC) staining; tumours with a score of 3+ were classified as HER2-positive, and tumours with a score of 0 or 1+ were classified as negative. In case of the tumour with score of 2+, gene amplification using fluorescence *in-situ* hybridization was used to determine the HER2 status. HER2 expression was considered as positive if the ratio of HER2 gene copies to chromosome 17 signals was >2.2. Moreover, the IHC subtypes were classified as ER positive (ER positive; and HER2 and PR positive or negative), HER2 enriched (HER2 positive; and ER and PR positive or negative), or triple negative (all ER, PR, and HER2 negative) subtypes.¹⁹ A cutoff value of 14% was used to define Ki-67 positivity.²⁰

Statistical analysis

Tumour visibility scores were compared between the DBT + FFDM and FFDM images. The tumour visibility score on the DBT + FFDM images was correlated with the clinicopathological and imaging variables using Pearson's chi-square test or Fisher's exact test for categorical variables, and the Mann-Whitney test for continuous variables. Multivariate logistic regression analysis was performed to identify independent variables for the tumour visibility on the DBT + FFDM images. After stratification by independent variables, the diagnostic performance of DBT + FFDM was compared with that of FFDM according to the pathologic results or 12 months' clinical follow-up as reference standard.^{21,22}

All statistical analyses were performed using Statistical Package for the Social Sciences for Windows, v. 19.0 (IBM Corp., Armonk, NY), and MedCalc for Windows, v. ersion 9.3.1, (MedCalc

Figure 2. Images of a 40-year-old female diagnosed with invasive ductal carcinoma (0.9 cm in size) combined with a ductal carcinoma *in situ* (2.1 cm in size) in the right breast (breast composition d). The right mediolateral oblique views of FFDM (a) and DBT (b) showed a uncertainly visible tumour (visibility score 1). A breast ultrasound (c) showed a discrete mass (1.3 cm in size) in the far upper outer area of the right breast. An isodense mass was demarcated on FFDM (d) after ultrasound-guided wire localization. DBT, digital breast tomosynthesis; FFDM, full-field digital mammography.

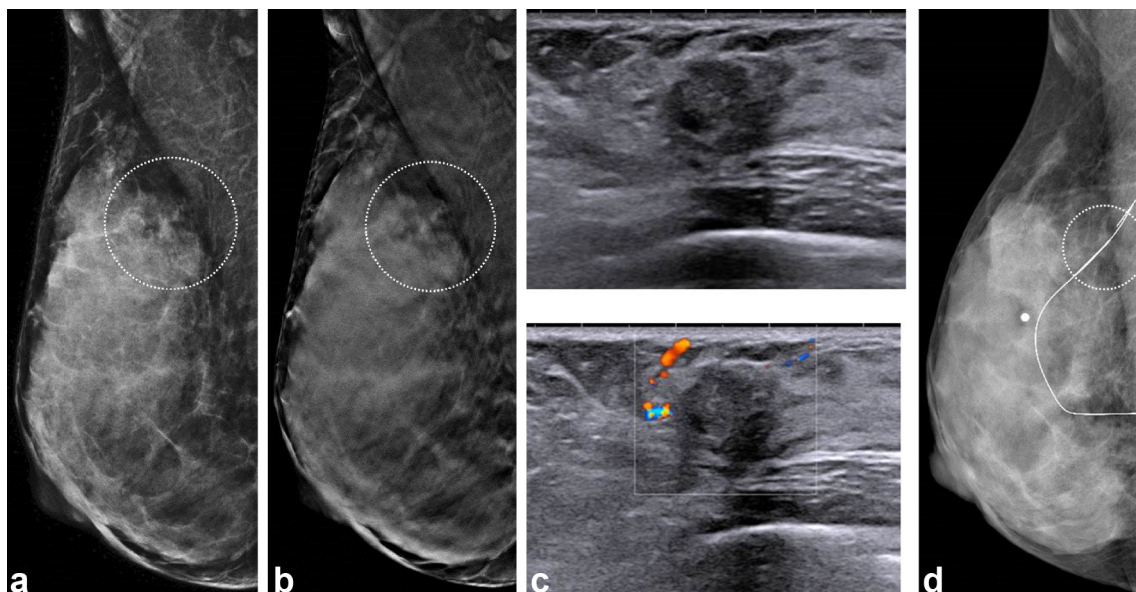


Table 2. Tumour visibility on DBT + FFDM and Clinicopathologic variables: Univariate analysis

Clinicopathologic variables	Total (n = 106)	Tumour visibility on DBT + FFDM			
		1 (n = 22)	2 (n = 11)	3 (n = 73)	P-value ^a
Age (years)					
Mean ± SD	52.2 ± 11.4 (range 22–77)	47.6 ± 7.9	50.6 ± 8.2	53.9 ± 12.3	0.078
Tumour size(mm) ^b					
Mean ± SD	14.6 ± 4.6 (range 4–20)	12.7 ± 5.1	12.7 ± 3.4	14.1 ± 4.6	0.728
Tumour histology					
Ductal	97 (91.5)	18 (81.8)	11 (100.0)	68 (93.2)	0.396
Lobular	5 (4.7)	2 (9.1)	0 (0)	3 (4.1)	
Others ^c	4 (3.8)	2 (9.1)	0 (0)	2 (2.7)	
Histologic grade					
1 or 2	55 (51.9)	13 (59.1)	7 (63.6)	35 (47.9)	0.468
3	51 (48.1)	9 (40.9)	4 (36.4)	38 (52.1)	
KI-67 (%)					
≤14	95 (89.6)	20 (90.9)	11 (100)	64 (87.7)	0.222
>14	11 (10.4)	2 (9.1)	0 (0)	9 (12.3)	
IHC subtype					
ER-positive	86 (81.1)	20 (90.9)	9 (81.8)	57 (78.1)	0.318
HER2-enriched	10 (9.4)	2 (9.1)	0 (0)	8 (11.0)	
Triple negative	10 (9.4)	0 (0)	2 (18.2)	8 (11.0)	

DBT, digital breast tomosynthesis; FFDM, full-field digital mammography; SD, standard deviation; ER, estrogen receptor; HER2, human epidermal growth factor receptor 2; IHC, immuno histo chemistry.

Data are numbers of cases, and data in parentheses are percentages.

^aP-values were obtained by the Pearson's Chi-square test or Fisher's exact test for categorical variables and Mann-Whitney test for continuous variables. P-value < 0.050 was considered to indicate a statistically significant difference.

^bDetermined by the greatest dimension of the invasive tumour on the basis of the surgically excised specimens.

^cPapillary (n = 2, 1.9%), mucinous (n = 1, 0.9%), and tubular (n = 1, 0.9%) cancers.

Software, Mariakerke, Belgium). P-value of less than 0.05 was considered as significant.

RESULTS

Tumour visibility

The surgical histopathology revealed that of 106 tumours, 97 (91.5%) were ductal, 5 (4.7%) were lobular, 2 (1.9%) were papillary, 1 (0.9%) was mucinous, and 1 (0.9%) was tubular carcinoma. Molecular subtypes included the ER positive (n = 86, 81.1%), HER2 enriched (n = 10, 9.4%), and triple negative (n = 10, 9.4%) subtypes.

Tumour visibility scores are listed in Table 1. The tumour visibility score was significantly higher in the DBT + FFDM images (mean, 2.5 vs 1.8; p = 0.002) than that in the FFDM images (Figures 1 and 2). Univariate analysis revealed that the breast composition (p < 0.001) and mass density (p = 0.006) were associated with the tumour visibility through DBT + FFDM (Tables 2 and 3). Multivariate logistic regression analysis revealed that composition d (odds ratio, 0.02; p < 0.001) was independently associated with poor tumour visibility through DBT + FFDM (Table 4).

Diagnostic performance

The diagnostic performance of FFDM vs DBT + FFDM in 265 cases is described in Table 5. The diagnostic performance of DBT + FFDM including sensitivity (63.6% vs 59.1%; p = 0.642), specificity (84.8% vs 75.8%; p = 0.463), positive-predictive value (79.2% vs 61.9%; p = 0.078), and negative-predictive value (90.3% vs 73.5%; p = 0.072) was not significantly superior to those of FFDM in 55 females with composition d breast, whereas specificity (98.4% vs 81.7%; p = 0.002) and positive-predictive value (97.6% vs 76.8%; p < 0.001) were significantly higher in 210 females with the other breast compositions.

DISCUSSION

The results of our study indicated that the addition of DBT did not significantly increase the tumour visibility and diagnostic performance of FFDM for noncalcified T₁ cancers in patients with breast composition d. Recent studies demonstrated that the use of DBT + FFDM is likely to show a decrease in the rate of false-positive results, and an increase in the cancer-detection rate compared with the use of FFDM alone, despite presence of the dense breasts.^{6–13} In these studies, the breast density was assessed as an approximate percentage value of

Table 3. Tumour visibility on DBT + FFDM and Imaging variables: Univariate analysis

Imaging variables	Total (n = 106)	Tumour visibility on DBT + FFDM			
		1 (n = 22)	2 (n = 11)	3 (n = 73)	P-value ^a
Breast composition					
a	22 (20.8)	0 (0)	1 (9.1)	21 (28.8)	<0.001
b	18 (17.0)	0 (0)	1 (9.1)	17 (23.3)	
c	44 (41.5)	5 (22.7)	9 (81.8)	30 (41.1)	
d	22 (20.8)	17 (77.3)	0 (0)	5 (6.8)	
Breast thickness (mm) ^b					
Mean ± SD	45.8 ± 11.0 (range 11.0–67.8)	41.2 ± 11.6	51.2 ± 9.2	46.4 ± 10.7	0.211
Mass shape					
Oval or round	24 (22.6)	2 (9.1)	3 (27.3)	19 (26.0)	0.232
Irregular	82 (77.4)	20 (90.9)	8 (72.7)	54 (74.0)	
Mass margin					
Circumscribed	5 (4.7)	0 (0)	2 (18.2)	3 (4.1)	0.061
Not-circumscribed	101 (95.3)	22 (100)	9 (81.9)	70 (95.9)	
Mass density					
Iso	37 (34.9)	14 (63.6)	3 (27.3)	20 (27.4)	0.006
Hyper	69 (65.1)	8 (36.4)	8 (72.7)	53 (72.6)	

DBT, digital breast tomosynthesis; FFDM, full-field digital mammography; SD, standard deviation.

Data are numbers of cases, and data in parentheses are percentages.

^aP-values were obtained by the Pearson's Chi-square test or Fisher's exact test for categorical variables and Mann-Whitney test for continuous variables. P-value < 0.050 was considered to indicate a statistically significant difference.

^bAutomatically measured at the time of mammographic image acquisition.

the fibroglandular tissue in relation to the whole breast area on mammography scans. Rafferty et al reported that addition of DBT to FFDM for screening purpose was associated with improved diagnostic performance in both females with the dense and non-dense breast tissue; however, the combined gain was largest in those with composition *c*, but not significant in those with composition *d*.²³ In case of the lesion located in the extremely dense breast without interposed radiolucent fat densities that overlaps individual sections on the DBT image, a false-negative result may be obtained. Accordingly, our results showed that added DBT to FFDM was not equally effective in all females with the dense breast. In addition, in case of the lesion comprising noncalcified isodense small cancer obscured in dense fibroglandular tissue, there is high probability of failed detection on both the DBT and FFDM images. Therefore, requirement of interfacing between the radiodense

fibroglandular tissue and radiolucent fat tissue might be a necessary precondition for effective application of DBT in patients with the dense breast.²⁴

The tumour visibility through DBT might be affected by the morphologic features of the tumour despite the low statistical significance of our results. Reports have indicated that breast cancers showed different imaging features according to their molecular subtype.²⁵ In our study, since we only included *T*₁ stage cancers, the total number of cancers was small; hence, there is limitation to generalizing our data. However, Lee et al reported that in patients undergoing DBT, despite the finding of characteristic imaging features of breast cancer per molecular subtype, cancer detectability on the DBT image was unaffected by molecular subtype of the breast cancer.²⁶

Table 4. Tumour visibility on DBT + FFDM: Multivariate analysis

Variables	Multivariate analysis		
	Odds ratio	95% Confidence interval	P-value ^a
Breast composition: grade <i>d</i>	0.02	0.04–0.09	<0.001
Mass density: isodense	0.29	0.07–1.15	0.203

DBT, digital breast tomosynthesis; FFDM, full-field digital mammography.

^aP-values were obtained by the multivariate logistic regression model after controlling for significant variables (p-value < 0.05 on univariate analysis in Table 2).

Table 5. Diagnostic performance according to breast composition: DBT + FFDM vs FFDM

		Composition a,b,c (n = 210) ^a			Composition d (n = 55) ^b		
		DBT + FFDM	FFDM	P-value	DBT + FFDM	FFDM	P-value
Diagnostic performance (%)	Sensitivity	95.2 (80/84)	90.5 (76/84)	0.451	63.6 (14/22)	59.1 (13/22)	0.642
	Specificity	98.4 (124/126)	81.7 (103/126)	0.002	84.8 (28/33)	75.8 (25/33)	0.463
	Positive predictive value	97.6 (80/82)	76.8 (76/99)	<.001	79.2 (19/24)	61.9 (13/21)	0.078
	Negative predictive value	96.9 (124/128)	92.8 (103/111)	0.589	90.3 (28/31)	73.5 (25/34)	0.072

DBT, digital breast tomosynthesis; FFDM, full-field digital mammography.

Note.—Data in parentheses are the raw figures from which the percentages were calculated.

^a84 tumour cases and 126 negative controls.

^b22 tumour cases and 33 negative controls.

^cP-values were obtained by the McNemar test. P-value <0.050 was considered to indicate a statistically significant difference.

A study comparing DBT and ultrasound reported limited diagnostic values of DBT in patients with breasts with composition *d*.²⁷ Moreover, despite equivalent overall performances, the diagnostic performance of ultrasound tended to be high in participants with breast composition *d*, with higher sensitivity than that of DBT.¹³ In our study, among the 22 tumours located in breasts with composition *d*, 8 (36.4%) tumours were not detected on both the DBT and FFDM images, but all tumours were visible through prospective ultrasound performed at the time of initial diagnosis. MRI or contrast-enhanced mammography were indicated as supplemental imaging modalities in females with dense breasts according to the individuals' risk level.^{28–30} Therefore, studies aimed to optimize the imaging modalities, screening intervals, and assessment of patients' individual and familial risk are required to develop optimal strategy for breast cancer screening in females with breast composition *d*.

Our study had several limitations. First, this was a retrospective study including a relatively small sample size. Of the cohort of 106 females, only 22 females had breasts with composition *d*. Further investigation including a larger study population is necessary. Second, we performed consensus review sessions but did not assess the inter- or intraobserver variance; however, through discussion of results between the two radiologists, the best concordant results were determined. In addition, assessment of the tumour visibility was performed in an unblinded manner with regard to the tumour location. Although the unblinded review may have

bias, assessment of the tumour visibility is required to determine the exact tumour site on the mammographic images. Fourth, our study population was limited to noncalcified *T*₁ breast cancer in Asian females; future studies are required to reassess the diagnostic performance of DBT compared with FFDM for all stages of tumours across characteristic of all breast densities and races. Finally, this was a single-institution study focused on FFDM and DBT by a single manufacturer. Further study including a larger population is necessary to determine optimum imaging strategy in such patients.

In conclusion, breast composition was significantly associated with the tumour visibility and diagnostic performance of DBT + FFDM in the evaluation of females with noncalcified *T*₁ invasive breast cancer. Addition of DBT to FFDM showed no further improvement in the rate of diagnostic accuracy of noncalcified *T*₁ breast cancer in females with breast composition *d*. Therefore, for screening of females with breast composition *d*, the use of supplemental imaging other than DBT may be considered even though large prospective studies are warranted.

ACKNOWLEDGMENT

This research was supported by a grant of the Korea Health Technology R&D Project through the Korea Health Industry Development Institute (KHIDI), funded by the Ministry of Health & Welfare, Republic of Korea (grant number : HI15C1532). Kyung Sook Yang kindly provided statistical advice for this manuscript.

REFERENCES

- Melnikow J, Fenton JJ, Whitlock EP, Miglioretti DL, Weyrich MS, Thompson JH, et al. Supplemental screening for breast cancer in women with dense breasts: a systematic review for the U.S. Preventive Services Task Force. *Ann Intern Med* 2016; **164**: 268–78. doi: <https://doi.org/10.7326/M15-1789>
- McCormack VA, dos Santos Silva I, Silva DS I. Breast density and parenchymal patterns as markers of breast cancer risk: a meta-analysis. *Cancer Epidemiol Biomarkers Prev* 2006; **15**: 1159–69. doi: <https://doi.org/10.1158/1055-9965.EPI-06-0034>
- Kerlikowske K, Zhu W, Tosteson AN, Sprague BL, Tice JA, Lehman CD, et al. Identifying women with dense breasts at high risk for interval cancer: a cohort study. *Ann Intern Med* 2015; **162**: 673–81. doi: <https://doi.org/10.7326/M14-1465>
- Helvie MA. Digital mammography imaging: breast tomosynthesis and advanced applications. *Radiol Clin North Am* 2010; **48**: 917–29. doi: <https://doi.org/10.1016/j.rcl.2010.06.009>
- Houssami N, Skaane P. Overview of the evidence on digital breast tomosynthesis in breast cancer detection. *Breast* 2013; **22**: 101–8. doi: <https://doi.org/10.1016/j.breast.2013.01.017>
- McDonald ES, Oustimov A, Weinstein SP, Synnestvedt MB, Schnall M, Conant EF. Effectiveness of digital breast tomosynthesis

- compared with digital mammography: outcomes analysis from 3 years of breast cancer screening. *JAMA Oncol* 2016; **2**: 737–43. doi: <https://doi.org/10.1001/jamaoncol.2015.5536>
7. Ciatto S, Houssami N, Bernardi D, Caumo F, Pellegrini M, Brunelli S, et al. Integration of 3D digital mammography with tomosynthesis for population breast-cancer screening (STORM): a prospective comparison study. *Lancet Oncol* 2013 Jun; **14**: 583–9. doi: [https://doi.org/10.1016/S1470-2045\(13\)70134-7](https://doi.org/10.1016/S1470-2045(13)70134-7)
 8. Skaane P, Bandos AI, Gullien R, Eben EB, Ekseth U, Haakenaasen U, et al. Comparison of digital mammography alone and digital mammography plus tomosynthesis in a population-based screening program. *Radiology* 2013; **267**: 47–56. doi: <https://doi.org/10.1148/radiol.12121373>
 9. Skaane P, Bandos AI, Gullien R, Eben EB, Ekseth U, Haakenaasen U, et al. Prospective trial comparing full-field digital mammography (FFDM) versus combined FFDM and tomosynthesis in a population-based screening programme using independent double reading with arbitration. *Eur Radiol* 2013; **23**: 2061–71. doi: <https://doi.org/10.1007/s00330-013-2820-3>
 10. Friedewald SM, Rafferty EA, Rose SL, Durand MA, Plecha DM, Greenberg JS, et al. Breast cancer screening using tomosynthesis in combination with digital mammography. *JAMA* 2014; **311**: 2499–507. doi: <https://doi.org/10.1001/jama.2014.6095>
 11. Gilbert FJ, Tucker L, Gillan MG, Willsher P, Cooke J, Duncan KA, et al. Accuracy of digital breast tomosynthesis for depicting breast cancer subgroups in a UK retrospective reading study (TOMMY Trial). *Radiology* 2015; **277**: 697–706. doi: <https://doi.org/10.1148/radiol.2015142566>
 12. Houssami N, Turner RM. Rapid review: Estimates of incremental breast cancer detection from tomosynthesis (3D-mammography) screening in women with dense breasts. *Breast* 2016; **30**: 141–5. doi: <https://doi.org/10.1016/j.breast.2016.09.008>
 13. Tagliafico AS, Calabrese M, Mariscotti G, Durando M, Tosto S, Monetti F. Adjunct screening with tomosynthesis or ultrasound in women with mammography-negative dense breasts: interim report of a prospective comparative trial. *J Clin Oncol* 2016; **9**: JCO634147.
 14. Sickles EA, D'Orsi CJ, Bassett LW, Appleton CM, Berg WA, Burnside ES. ACR BI-RADS Mammography. In: Reston, ed. *ACR BI-RADS Atlas, Breast Imaging Reporting and Data System*. 5th; 2013.
 15. Elston CW, Ellis IO. Pathological prognostic factors in breast cancer. I. The value of histological grade in breast cancer: experience from a large study with long-term follow-up. *Histopathology* 2002; **41**(3A): 154–61.
 16. Edge SB, Compton CC. The American Joint Committee on Cancer: the 7th edition of the AJCC cancer staging manual and the future of TNM. *Ann Surg Oncol* 2010; **17**: 1471–4.
 17. Hammond ME, Hayes DF, Dowsett M, Allred DC, Haggerty KL, Badve S, et al. American Society of Clinical Oncology/College Of American Pathologists guideline recommendations for immunohistochemical testing of estrogen and progesterone receptors in breast cancer. *J Clin Oncol* 2010; **28**: 2784–95. doi: <https://doi.org/10.1200/JCO.2009.25.6529>
 18. Wolff AC, Hammond ME, Schwartz JN, Haggerty KL, Allred DC, Cote RJ, et al. American Society of Clinical Oncology/College of American Pathologists guideline recommendations for human epidermal growth factor receptor 2 testing in breast cancer. *J Clin Oncol* 2007; **25**: 118–45. doi: <https://doi.org/10.1200/JCO.2006.09.2775>
 19. Goldhirsch A, Wood WC, Coates AS, Gelber RD, Thürlimann B, Senn HJ, et al. Strategies for subtypes--dealing with the diversity of breast cancer: highlights of the St. Gallen International Expert Consensus on the Primary Therapy of Early Breast Cancer 2011. *Ann Oncol* 2011; **22**: 1736–47. doi: <https://doi.org/10.1093/annonc/mdr304>
 20. Cheang MC, Chia SK, Voduc D, Gao D, Leung S, Snider J, et al. Ki67 index, HER2 status, and prognosis of patients with luminal B breast cancer. *J Natl Cancer Inst* 2009; **101**: 736–50. doi: <https://doi.org/10.1093/jnci/djp082>
 21. McNEMAR Q. Note on the sampling error of the difference between correlated proportions or percentages. *Psychometrika* 1947; **12**: 153–7. doi: <https://doi.org/10.1007/BF02295996>
 22. Breslow NE, Day NE. *Statistical methods in cancer research: vol 1—the analysis of case-control studies*. Lyon, France: IARC; 1981.
 23. Rafferty EA, Durand MA, Conant EF, Copit DS, Friedewald SM, Plecha DM, et al. Breast cancer screening using tomosynthesis and digital mammography in dense and nondense breasts. *JAMA* 2016; **315**: 1784–6. doi: <https://doi.org/10.1001/jama.2016.1708>
 24. Peppard HR, Nicholson BE, Rochman CM, Merchant JK, Mayo RC, Harvey JA. Digital breast tomosynthesis in the diagnostic setting: indications and clinical applications. *Radiographics* 2015; **35**: 975–90. doi: <https://doi.org/10.1148/rg.2015140204>
 25. Tamaki K, Ishida T, Miyashita M, Amari M, Ohuchi N, Tamaki N, et al. Correlation between mammographic findings and corresponding histopathology: potential predictors for biological characteristics of breast diseases. *Cancer Sci* 2011; **102**: 2179–85. doi: <https://doi.org/10.1111/j.1349-7006.2011.02088.x>
 26. Lee SH, Chang JM, Shin SU, Chu AJ, Yi A, Cho N, et al. Imaging features of breast cancers on digital breast tomosynthesis according to molecular subtype: association with breast cancer detection. *Br J Radiol* 2017; **90**: 20170470. doi: <https://doi.org/10.1259/bjr.20170470>
 27. Kim WH, Chang JM, Lee J, Chu AJ, Seo M, Gweon HM, et al. Diagnostic performance of tomosynthesis and breast ultrasonography in women with dense breasts: a prospective comparison study. *Breast Cancer Res Treat* 2017; **162**: 85–94. doi: <https://doi.org/10.1007/s10549-017-4105-z>
 28. Berg WA, Zhang Z, Lehrer D, Jong RA, Pisano ED, Barr RG, et al. Detection of breast cancer with addition of annual screening ultrasound or a single screening MRI to mammography in women with elevated breast cancer risk. *JAMA* 2012; **307**: 1394–404. doi: <https://doi.org/10.1001/jama.2012.388>
 29. Lewin J. Comparison of contrast-enhanced mammography and contrast-enhanced breast MR imaging. *Magn Reson Imaging Clin N Am* 2018; **26**: 259–63. doi: <https://doi.org/10.1016/j.mric.2017.12.005>
 30. Emaus MJ, Bakker MF, Peeters PH, Loo CE, Mann RM, de Jong MD, et al. MR imaging as an additional screening modality for the detection of breast cancer in women aged 50–75 years with extremely dense breasts: the DENSE trial study design. *Radiology* 2015; **277**: 527–37. doi: <https://doi.org/10.1148/radiol.2015141827>

Received:
16 May 2018

Revised:
19 July 2018

Accepted:
25 July 2018

<https://doi.org/10.1259/bjr.20180444>

Cite this article as:

Sánchez-Camacho González-Carrato MP, Romero Castellano C, Aguilar Angulo PM, Cruz Hernández LM, Sánchez Casado M, Ruiz Martín J, et al. Diagnostic value of halo sign in young women (aged 45 to 49 years) in a breast screening programme with synthesized 2D mammography. *Br J Radiol* 2018; **91**: 20180444.

FULL PAPER

Diagnostic value of halo sign in young women (aged 45 to 49 years) in a breast screening programme with synthesized 2D mammography

¹MARÍA PILAR SÁNCHEZ-CAMACHO GONZÁLEZ-CARRATO, MD, ¹CRISTINA ROMERO CASTELLANO, MD, PhD, MSc, PAUL MARTÍN AGUILAR ANGULO, MD, ¹LINA MARCELA CRUZ HERNÁNDEZ, MD, ²MARCELINO SÁNCHEZ CASADO, MD, PhD, ³JUAN RUIZ MARTÍN, MD, PhD, ⁴IÑAKI FRAILE ALONSO, MD, ¹JOSÉ MARÍA PINTO VARELA, MD and ⁵VICENTE MARTÍNEZ-VIZCAÍNO, MD, PhD, MSc

¹Department of Radiology, Breast Imaging Section, Virgen de la Salud hospital, Toledo, Spain

²Department of Intensive Care Unit, Virgen de la Salud hospital, Toledo, Spain

³Department of Pathological Anatomy, Virgen de la Salud hospital, Toledo, Spain

⁴Department of Breast Surgery, Virgen de la Salud hospital, Toledo, Spain

⁵Department of Intensive Care Unit, University of Castilla-La Mancha, Health and Social Research Center, Cuenca, Spain

Address correspondence to: Mrs María Pilar Sánchez-Camacho González-Carrato
E-mail: pilar.scgc@hotmail.com

Objective: To assess the clinical performance of the halo sign in tomosynthesis and synthesized 2D mammography, and to identify age groups where its diagnostic value may be greater.

Methods: 183 patients with nodules were recalled from the breast screening programme (with tomosynthesis and 2D synthesized mammograms). The patients were separated into two groups, 45–49 years and 50–69 years, and depending on the presence or not of halo sign. We calculated the predictive values for the different age groups.

Results: In 45–49 years group, 86 nodular lesions were recalled, 66 (76.7%) with positive halo sign and 20 (23.3%) with negative halo sign. In positive halo sign group, biopsy was considered in 23 (34.8%), with histological features of benignity. In 50–69 years group, 98

nodular lesions from 97 patients were recalled, 51 (52%) with positive halo sign and 47 (48%) with negative halo sign. In positive halo sign group, biopsy was considered in 13 (25.5%); four (30.8%) were malignant and nine (69.2%) were benign.

Conclusion: Halo sign could be considered as a marker of benign lesion in females < 50 years. In females ≥ 50 years, other breast imaging techniques should be considered, with or without histological studies, to rule out malignancy.

Advances in knowledge: The trend of a positive halo sign to act as a marker of benign lesion could be improve the recall rate and positive predictive values in the breast screening programme with tomosynthesis and synthesized 2D mammography, especially in young females.

INTRODUCTION

In 2011, the United States Food and Drug Administration (FDA) approved digital breast tomosynthesis used in combination with digital mammography for breast cancer screening; the effectiveness of this technology has been since then documented in multiple large-scale studies.^{1,2} In 2013, the FDA approved a version of 2D synthesized mammography software, which together with tomosynthesis for breast cancer detection, was not inferior to digital mammography alone, suggesting that it could be more effective for breast cancer screening with the additional benefit of limiting exposure to radiation.³

The results in some studies show that breast cancer screening with 2D synthesized mammograms and tomosynthesis improve the recall rate and positive predictive values without affecting cancer detection rates, in comparison to tomosynthesis and digital mammography or digital mammography alone.⁴ Most improvements in the detection results with 2D mammograms and tomosynthesis are associated to a better distinction between overlapping glandular tissue and the margins of the nodules, particularly in dense breasts.⁵ This would imply a decrease of recall or false positive in females aged 45 to 49 years. A well-circumscribed nodule is usually indicative of benign lesion. Sickles⁶ reported low probability of malignancy in circumscribed, non-palpable, non-calcified nodules, from which 1.4% were malignant.

Halo signs are frequently present in tomosynthesis images; thus, the margins of the circumscribed nodules appear lighter when this technique is used. On the other hand, it is unclear if 2D mammograms and tomosynthesis can help differentiate between benign and malignant circumscribed nodules.⁷ There is an emerging problem associated to the management of circumscribed nodules detected through this type of mammographic technique in the screened population.

We aim to assess the accuracy of the presence of a halo sign as a prognostic marker in recalled females from breast cancer screening programme. Furthermore, we intend to evaluate the possibility of differentiation by age group and to evaluate if we can identify specific age groups where its diagnostic value may be greater.

PATIENTS AND METHODS

The breast cancer early detection program in the province of Toledo (Spain) covers a health area of around 74,350 females between 45 and 69 years of age. We conducted a retrospective, descriptive study between October 2015 and May 2016. During this period, 18,511 females attended the screening program, from which 334 were recalled (1.8%). We detected 184 nodules with or without other associated disorders (such as microcalcifications and skin retraction) in 183 females recalled after the screening. Written informed consent was obtained from all subjects in this study.

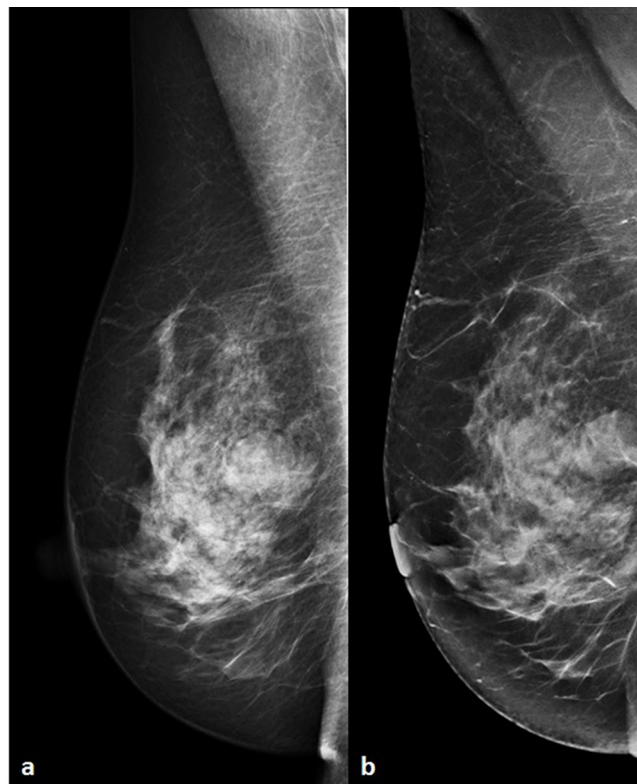
Mammographic technique

For the study, we used 2D synthesized mammograms and tomosynthesis using the Selenia Dimensions mammography system (Hologic, Bedford, MA). Two views per breast were performed (craniocaudal and mediolateral oblique) that were interpreted by two breast imaging experts during the screening (2 to 20 years of professional experience), including the support of a computer-aided detection system.

Once nodules detected, additional examinations for recalled patients were performed with a 12 MHz Ultrasound Linear Probe (Aplio MX, Toshiba Medical Systems, Tokyo, Japan). Depending on the findings, ultrasound-guided 14G core-needle biopsy was also performed. Breast MRI (1.5 T Avanto, Siemens, Erlangen, Germany; using T_1 - and T_2 weighted imaging sequences, diffusion, and dynamic study post-gadolinium administration) was used in cancer staging. Nodule follow-up was done for 23 to 30 months, until April 2018.

The analysis of data was conducted in a comprehensive manner; the patients were separated into two age groups, 45–49 years and 50–69 years (pre- and postmenopausal females) and depending on the presence or not of a halo sign. The halo sign was defined as a thin hyperlucent ring that surrounds >50% of the contour of the nodule, detected in at least one mammographic view,⁷ as shown in the example of the [Figure 1](#) and [Supplementary Video 1](#), where positive halo sign is better visualized in 3D images of tomosynthesis followed by synthesized 2D mammogram and conventional 2D mammogram.

Figure 1. (a) Medium lateral oblique views of conventional 2D mammogram and (b) synthesized 2D mammogram, in woman from screening with a fibroadenoma in heterogeneously dense breast, whose edge with positive halo sign (thin radiolucent-line) is defined in more 75% in synthesized 2D mammogram compared to conventional 2D mammogram. Go to [Supplementary Video 1](#) to see the complete delimitation of halo sign in 3D image soft tomosynthesis.



Breast density was analyzed in each study subgroup (per age and presence of a halo sign) using the BI-RADS lexicon (predominantly fat -a-, scattered fibroglandular density -b-, heterogeneously dense -c-, and extremely dense -d-).⁸ In this work, the number of patients in the predominantly fat and extremely dense categories was small. Because of this, we grouped the four breast density categories in two: predominantly fatty or dispersed (low-density group) and heterogeneously or extremely dense (high-density group).

The following findings were also analyzed: type of lesion (nodule, nodule with microcalcifications, or nodule with skin retraction), existence or not of previous mammography, density of the nodule compared to the density of the surrounding breast tissue (same or higher), evolution of nodule size, initial BI-RADS classification, presence or not of interventionism, and histological results.

Statistical analysis

Categorical variables were expressed as counts (percentages). We calculated the predictive values (sensitivity, specificity, positive and negative predictive value) for the general population and for the different age groups, aiming to evaluate the halo sign as predictor of benign breast disease.

Table 1. Main features of mammographic breast density, radiological findings, and histological results of nodular lesions in patients aged 45–49 and 50–69 years>

	45–49 years		50–69 years	
	Halo (+) (n = 66)	Halo (-) (n = 20)	Halo (+) (n = 51)	Halo (-) (n = 47)
Breast density				
Low density	31 (47%)	8 (40%)	35 (68.6%)	35 (74.5%)
High density	35 (53%)	12 (60%)	16 (31.4%)	12 (25.5%)
Radiological findings				
Nodule	66 (100%)	17 (85%)	49 (96.1%)	43 (91.5%)
Nodule with microcalcifications	–	2 (10%)	2 (3.9%)	4 (8.5%)
Nodule with skin retraction	–	1 (5%)	–	–
Histological results ^a				
No biopsy	43 (65.2%)	5 (25%)	38 (74.7%)	9 (19.1%)
Benign	23/23 (100%)	6/15 (40%)	9/13 (69.2%)	2/38 (5.3%)
Risk lesion	–	–	–	1/38 (2.6%)
Malignant	–	9/15 (60%)	4/13 (30.8%)	35/38 (92.1%)

^aIn each age group there is a statistically significant difference ($p < 0.001$) between the groups with or without halo sign in relation to the histological results of benignity and malignancy (including risk lesions as malignant).

RESULTS

183 (54.8%) patients out of 334 were recalled because of nodular lesions with or without other associated disorders; 174 (52.1%) were nodules, 8 (2.4%) nodules with microcalcifications, and one (0.3%) nodule with skin retraction. One patient over 50 years old was recalled because of two nodules, one in each breast, with ultrasound diagnosis of simple cysts. There were 130 (70.7%) previous mammography in the total population, where the evolution of the size of the nodule was 12 (9.2%) equal, 52 (40%) greater and 66 (50.8%) new. Regarding density of the nodule compared to the density of the surrounding breast tissue, there were 83 (45.1%) with same density and 101 (54.9%) with higher density in the total population. In terms of initial BI-RADS classification, there were 143 (77.7%) BI-RADS 0 and 41 (22.3%) BI-RADS 4/5. In all this, no significant differences were found between the two age groups. Nodule follow-up was performed between 23 and 30 months, until April 2018, without changes in diagnostic behaviour.

The main features of mammographic breast density, radiological findings, and histological results of nodular lesions in study patients are described in Table 1. 86 patients between 45 and 49 years with 86 nodular lesions were recalled, 66 (76.7%) with positive halo sign and 20 (23.3%) with negative halo sign. The 66 (100%) patients with positive halo sign had nodules without other associated findings. Biopsy was considered in 23 nodules (34.8%), for which histological analyses revealed to be benign. Within the group of patients with negative halo sign (20 patients), 17 (85%) nodules, two (10%) nodules with microcalcifications, and one (5%) nodule with skin retraction were analyzed. Biopsy was considered in 15 cases (75%), from which nine (60%) showed histological features of malignancy and six (40%) were benign. From the nine nodules with malignant histology, eight (88.9%) were invasive ductal carcinoma and one (11.1%) carcinoma *in*

situ. The two nodules with microcalcifications, as well as the nodule with skin retraction were invasive ductal carcinomas as per the histological results.

98 nodular lesions from 97 patients older than 50 years were recalled, 51 of which (52%) had positive halo sign and 47 (48%) negative halo sign. Regarding the type of lesions with positive halo sign, 49 (96.1%) nodules and two (3.9%) nodules with microcalcifications were found. One of the two nodules with microcalcifications was stable with respect to tests performed in another center and provided by the patient; a biopsy was performed in the other nodule with a benign result. Biopsy was considered in 13 nodules (25.5%), for which the histology showed malignancy in four (30.8%) cases and nine (69.2%) appeared to be benign. The radiological evaluation of the four nodules with positive halo sign and malignant on histology, revealed lobulated/microlobulated contours. The anatomopathological characterization is shown in Table 2. Cases 1 and 2 (Figures 2 and 3, and Supplementary Videos 2 and 3), under 2 cm, underwent immediate surgery. The anatomopathological analysis of all borders for these two lesions showed a fibrous band with haemorrhagic foci. Case 3, being larger than 2 cm, underwent neoadjuvant chemotherapy; pathological complete remission was achieved following surgery. Case 4 was a diffuse large B-cell lymphoma; percutaneous biopsy and chemotherapy was performed. Within the groups of patients with negative halo sign (47 patients), 43 (91.5%) nodules and four (8.5%) nodules with microcalcifications were analyzed. The four nodules with microcalcifications were invasive ductal carcinomas. Biopsy was considered in 38 (80.9%) cases; in 35 (92.1%), the histology was malignant, one (2.6%) was determined to be a risk lesion (papilloma and radial scar), and two (5.3%) histologically benign. From the 35 histologically malignant nodules, 25 (71.4%) were determined to be invasive ductal

Table 2. Anatomopathological features of the four nodules with positive halo sign with malignant histology

	Case 1	Case 2	Case 3	Case 4
Type	Invasive carcinoma	Invasive carcinoma	Invasive carcinoma	Lymphoma
Subtype	Medullary signs	Medullary signs	Medullary signs	–
Tumour grade	3	3	3	–
Hormone receptors	Negative	Negative	Negative	–
HER2	Negative	Negative	Negative	–
Ki-67	60%	90%	45%	80%
p53	Positive	Positive	Negative	Negative

carcinomas, seven (20%) invasive lobular carcinomas, and three (8.6%) were classified as other (invasive tubular-lobular, colloid, and tubular).

In the total population, including risk lesions as malignant, there was negative halo sign in 8 (15.1%) benign lesions and 45 (84.9%) malignant lesions, and positive halo sign in 32 (88.9%) benign lesions and 4 (11.1%) malignant lesions, with statistical significance ($p < 0.001$) between the two groups with or without halo sign, in relation to the distribution of the lesions.

In both age groups, there were statistically significant differences ($p < 0.001$) between the groups with or without halo sign in the distribution of benign and malignant histological results. We found four malignant lesions with positive halo sign in only within the 50–69 years group.

Table 3 describes the sensitivity, specificity and predictive values for the general population and the various age groups, establishing the halo sign as a predictor of benign lesion.

DISCUSSION

Nodular lesions are frequently found in recalled patients that participate in a screening program (54.8% in our series). The evaluation of the contours of these nodular lesions is possible with the aid of slices obtained by tomosynthesis and 2D mammograms that minimize tissue overlapping. This is of great relevance within the setting of breast cancer screening, as it helps to determine if a patient needs to be recalled, allowing an increase of specificity.

A feature to keep in mind when analysing the contour of nodular lesions is the halo sign, defined as a thin hyperlucent ring that surrounds >50% of the margin of the nodule and is detected

Figure 2. (a) Craniocaudal view of synthesized 20 mammogram and (b) ultrasound, in patient from screening with newly merging nodular lesion presenting microlobular margin and in complete halo sign. See [Supplementary Video 2](#).

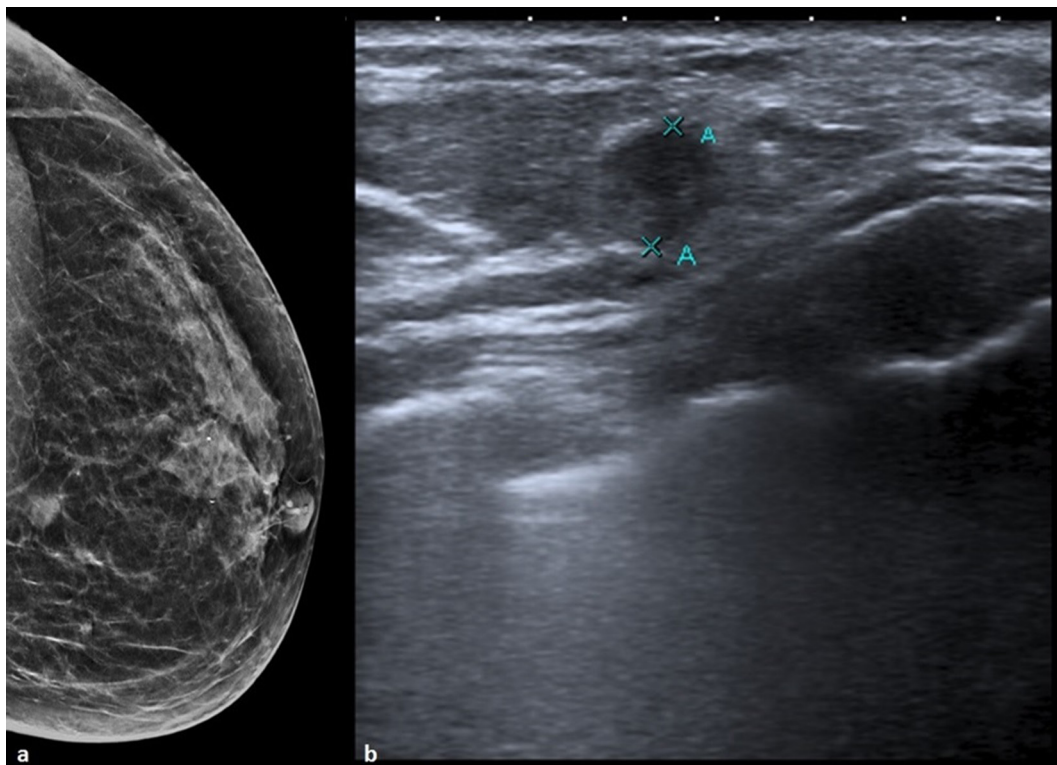
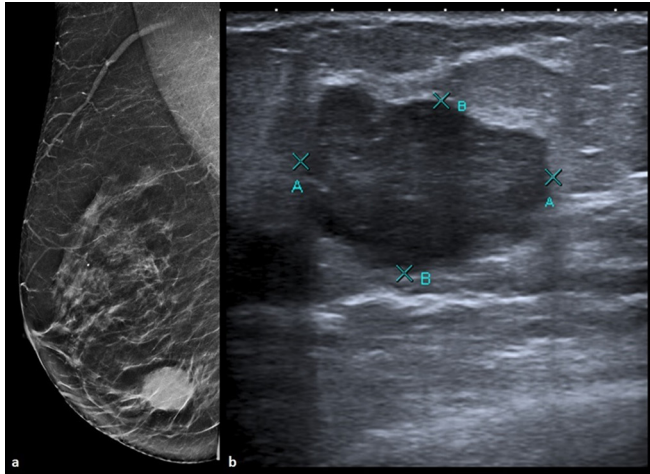


Figure 3. (a) Medium lateral oblique view of synthesized 2D mammogram and (b) ultrasound, in patient from screening with newly emerging nodular lesion presenting microlobular margins and in complete halo sign. See [Supplementary Video 3](#).



in at least one mammographic view.⁷ On the other hand, the mechanism and significance of the halo sign have changed in line with the development of mammography systems. Wolfe⁹ suggested that the halo sign results from the compression of fat by the circumscribing lesions. Moskowitz¹⁰ and Gordenne et al¹¹ challenged this theory, suggesting that the halo was a perceptual illusion (Mach band), associated with the principle of lateral inhibition: the eye is disturbed by adjacent structures with markedly different optical densities and seen not only around localized tumours in a fatty environment, but frequently also around fibroglandular tissue. Cupples et al¹² went a step further. They used an optical magnification method (magnifying glass or binocular microscope) and suggested that a halo is not always a perceptual illusion seen around benign and malignant lesions. Nakashima et al⁷ suspected that halo signs in digital mammography are magnified due to the contour highlight effect of image processing. Furthermore, in tomosynthesis, this contour highlight effect overlaps due to the reconstruction of a limited number of data samples with a narrow angular range of X-ray emissions.¹³ Although the cause of the halo sign has not yet been established, the presence of this sign is useful as an indicator of a smooth margin of the lesion at a macroscopic level and contributes to increase the contrast between a circumscribing mass and the surrounding breast tissue.⁷

In a study developed in Japan,⁷ the halo sign was recognized in three benign lesions in 2D mammograms; however, when tomosynthesis was used it was shown in 41 lesions, 30 benign and 11 malignant ($p = 0.988$). The authors concluded that, although tomosynthesis was superior in detecting circumscribed lesions, it was not possible to assure if they were benign. The limitation of this study is that the age of the subjects was not considered.

In our series of cases, we did take into account the age of the females recalled in the screening; two age groups were considered, 45 to 49 and 50 to 69 years. In our autonomous community screening is initiated at 45 years, unlike in the others (starting at 50). In females under 50 years, we detected halo signs in 79.3% benign lesions and their presence is a reliable marker (positive predictive value 100%) of benign lesions. In females ≥ 50 years, the halo sign identifies 81.8% of benign lesions and its presence implies slightly over half (69.2%) of the probability of a benign lesion. Regardless of the age, the presence of a halo sign identifies 80% of benign lesions and if a halo sign is seen, there is an 88.9% of probability that the patient has a benign lesion. In both age groups, and in the general population, the halo sign is a significant marker of benign lesion (in all cases with $p < 0.001$).

In our study, only four lesions with positive halo sign were malignant, found in the 50 to 69 age group, which could be influenced by the higher incidence of breast cancer in females aged ≥ 50 .^{14,15} Three of the lesions were medullary carcinomas hormone receptor- and HER2-negative, and with a Ki-67 higher than 45%. Histologically, this tumour shows well-defined borders, a lymphoplasmacytic infiltrate, and high-grade cells with sheet-like growth, without glandular or fibrosis formation.¹⁶ The histological features of this type of tumour do not explain its favourable prognosis.¹⁷ In 1989, Meyer et al¹⁸ described the mammography findings and ultrasonography of medullary carcinomas. The lesion commonly mimics a benign tumour, round or oval shaped with a well-defined lobulated contour. In ultrasound, the most common presentation is a hypoechoic lesion, generally with no attenuation of the sound and occasional cystic areas, similar to what we found in our series.

Concerning this aspect, the radiological description of the border of the malignant neoplasm could direct us to the histological type, as also reflected in one of our series,¹⁹ in which we characterize hidden breast cancers in tomosynthesis. These

Table 3. Accuracy of positive halo sign (and 95% confidence interval) as predictor of benign lesion on the general population and various age groups

	S	E	PPV	NPV
General population (including risk lesions as malignant)	80% (72%–88%)	91.8% (86%–97%)	88.9% (83%–95%)	85% (78%–92%)
Females aged 45 to 49 years	79.3% (71%–87%)	100% (95%–100%)	100% (95%–100%)	60% (50%–69%)
Females aged 50 to 69 years (including risk lesions as malignant)	81.8% (74%–89%)	90% (84%–96%)	69.2% (60%–78%)	94.7% (90%–99%)

E, specificity; NPV, negative predictive values; PPV, positive predictive values; S, sensitivity; PPV, positive predictive values.

neoplasms were invasive ductal carcinomas, poorly or moderately differentiated, most luminal B, with a worse prognostic outcome. Histologically, a mixture of non-neoplastic ducts and lobules characterizes these neoplasms.

There are several limitations in this study. First, the study was done with one center that uses only one tomosynthesis system. There is no assurance that the same results will apply to other tomosynthesis systems. Second, larger series are needed to confirm these findings and establish a larger number of subgroups with better diagnostic use.

From our findings, we conclude that the trend of a halo sign is to act as a marker of benign lesion in females < 50 years. In females \geq 50 years, other breast imaging techniques should

be considered, with or without histological studies, to rule out malignancy.

ACKNOWLEDGEMENTS

The scientific guarantor of this publication is Cristina Romero Castellano.

ETHICS APPROVAL

Institutional Review Board approval was not required because no new technology was used. Methodology: retrospective, case-control study, performed at one institution.

INFORMED CONSENT

Written informed consent was obtained from all subjects (patients) in this study.

REFERENCES

- Skaane P, Bandos AI, Gullien R, Eben EB, Ekseth U, Haakenaasen U, et al. Comparison of digital mammography alone and digital mammography plus tomosynthesis in a population-based screening program. *Radiology* 2013; **267**: 47–56. doi: <https://doi.org/10.1148/radiol.12121373>
- Mammography Quality Standards Act Regulations, Part 900.12(e)(5)(vi). Effective April 28, 1999. Amended February 6, 2002.
- U.S. Food and Drug Administration. Meeting of the radiological devices advisory panel. P080003/S001 hologic selenia dimensions 3D system FDA executive summary. Published October 24, 2012. 2016. Available from: https://www.accessdata.fda.gov/cdrh_docs/pdf8/P080003S001B.pdf [Accessed September 9, 2016].
- Aujero MP, Gavenonis SC, Benjamin R, Zhang Z, Holt JS. Clinical performance of synthesized two-dimensional mammography combined with tomosynthesis in a large screening population. *Radiology* 2017; **283**: 70–6. doi: <https://doi.org/10.1148/radiol.2017162674>
- Zuckerman SP, Maidment ADA, Weinstein SP, McDonald ES, Conant EF. Imaging with synthesized 2D mammography: differences, advantages, and pitfalls compared with digital mammography. *AJR Am J Roentgenol* 2017; **209**: 222–9. doi: <https://doi.org/10.2214/AJR.16.17476>
- Sickles EA. Nonpalpable, circumscribed, noncalcified solid breast masses: likelihood of malignancy based on lesion size and age of patient. *Radiology* 1994; **192**: 439–42. doi: <https://doi.org/10.1148/radiology.192.2.8029411>
- Nakashima K, Uematsu T, Itoh T, Takahashi K, Nishimura S, Hayashi T, et al. Comparison of visibility of circumscribed masses on Digital Breast Tomosynthesis (DBT) and 2D mammography: are circumscribed masses better visualized and assured of being benign on DBT? *Eur Radiol* 2017; **27**: 570–7. doi: <https://doi.org/10.1007/s00330-016-4420-5>
- American College of Radiology. *ACR BI-RADS Atlas: breast imaging reporting and data system*. 5th ed; 2013.
- Wolfe JN. Benign breast conditions. In: Wolfe JN, ed. *Xeroradiography of the breast*. 59. Springfield, III: Thomas; 1972.
- Moskowitz M. Minimal breast cancer redux. *Radiol Clin North Am* 1983; **21**: 93–113.
- Gordenne WH, Malchair FL. Mach bands in mammography. *Radiology* 1988; **169**: 55–8. doi: <https://doi.org/10.1148/radiology.169.1.2843941>
- Cupples TE, Eklund GW, Cardenosa G. Mammographic halo sign revisited. *Radiology* 1996; **199**: 105–8. doi: <https://doi.org/10.1148/radiology.199.1.8633130>
- Sechopoulos I. A review of breast tomosynthesis. Part II. Image reconstruction, processing and analysis, and advanced applications. *Med Phys* 2013; **40**: 014302. doi: <https://doi.org/10.1118/1.4770281>
- Zornoza G, Alberro JA, Sabadell MD, et al. Cáncer de mama en España: algunos resultados de una encuesta multicéntrica. *Rev Senol Patol Mamar* 2003; **16**: 90–6.
- Winters S, Martin C, Murphy D, Shokar NK. Breast cancer epidemiology, prevention, and screening. *Prog Mol Biol Transl Sci* 2017; **151**: 1–32. doi: <https://doi.org/10.1016/bs.pmbts.2017.07.002>
- Sewell CW. Pathology of benign and malignant breast disorders. *Radiol Clin North Am* 1995; **33**: 1067–80.
- Rubens JR, Lewandrowski KB, Kopans DB, Koerner FC, Hall DA, McCarthy KA. Medullary carcinoma of the breast. Overdiagnosis of a prognostically favorable neoplasm. *Arch Surg* 1990; **125**: 601–4.
- Meyer JE, Amin E, Lindfors KK, Lipman JC, Stomper PC, Genest D. Medullary carcinoma of the breast: mammographic and US appearance. *Radiology* 1989; **170**: 79–82. doi: <https://doi.org/10.1148/radiology.170.1.2642350>
- Aguilar Angulo PM, Romero Castellano C, Ruiz Martín J, Sánchez-Camacho González-Carrato MP, Cruz Hernández LM. Characterization of invisible breast cancers in digital mammography and tomosynthesis: radio-pathological correlation. *Radiologia* 2017; **59**: 511–5. doi: <https://doi.org/10.1016/j.rx.2017.08.002>

Received:
17 August 2017

Revised:
30 January 2018

Accepted:
13 February 2018

<https://doi.org/10.1259/bjr.20170605>

Cite this article as:

Deng C-Y, Juan Y-H, Cheung Y-C, Lin Y-C, Lo Y-F, Lin GG, et al. Quantitative analysis of enhanced malignant and benign lesions on contrast-enhanced spectral mammography. *Br J Radiol* 2018; **91**: 20170605.

FULL PAPER

Quantitative analysis of enhanced malignant and benign lesions on contrast-enhanced spectral mammography

¹CHIH-YING DENG, MD, ^{1,2}YU-HSIANG JUAN, MD, ^{1,2}YUN-CHUNG CHEUNG, MD, ^{1,2}YU-CHING LIN, MD, ³YUNG-FENG LO, MD, PhD, ^{1,2}GIGIN LIN, MD, PhD, ^{2,3}SHIN-CHEH CHEN, MD and ^{1,2}SHU-HANG NG, MD

¹Department of Medical Imaging and Intervention, Chang Gung Memorial Hospital, Linkou and Taoyuan, Taiwan

²Department of Medical Imaging and Radiological Sciences, Medical College of Chang Gung University, Taoyuan, Taiwan

³Department of Surgery, Chang Gung Memorial Hospital at Linkou, Taoyuan, Taiwan

Address correspondence to: Dr Yun-Chung Cheung

E-mail: alex2143@cgmh.org.tw

Objective: To retrospectively analyze the quantitative measurement and kinetic enhancement among pathologically proven benign and malignant lesions using contrast-enhanced spectral mammography (CESM).

Methods: We investigated the differences in enhancement between 44 benign and 108 malignant breast lesions in CESM, quantifying the extent of enhancements and the relative enhancements between early (between 2–3 min after contrast medium injection) and late (3–6 min) phases.

Results: The enhancement was statistically stronger in malignancies compared to benign lesions, with good performance by the receiver operating characteristic curve [0.877, 95% confidence interval (0.813–0.941)]. Using optimal cut-off value at 220.94 according to Youden index, the sensitivity was 75.9%, specificity 88.6%, positive likelihood ratio 6.681, negative likelihood

ratio 0.272 and accuracy 82.3%. The relative enhancement patterns of benign and malignant lesions, showing 29.92 vs 73.08% in the elevated pattern, 7.14 vs 92.86% in the steady pattern, 5.71 vs 94.29% in the depressed pattern, and 80.00 vs 20.00% in non-enhanced lesions ($p < 0.0001$), respectively.

Conclusion: Despite variations in the degree of tumour angiogenesis, quantitative analysis of the breast lesions on CESM documented the malignancies had distinctive stronger enhancement and depressed relative enhancement patterns than benign lesions.

Advances in knowledge: To our knowledge, this is the first study evaluating the feasibility of quantifying lesion enhancement on CESM. The quantities of enhancement were informative for assessing breast lesions in which the malignancies had stronger enhancement and more relative depressed enhancement than the benign lesions.

INTRODUCTION

Mammography remains an important breast-imaging technique for both screening and diagnostic purposes, although the variable density of breast tissue can influence the sensitivity and increase the susceptibility of breast cancer.^{1,2} Recently, technical advances in digital imaging have facilitated the development of advanced mammographic imaging techniques including tomosynthesis and dual energy contrast-enhanced spectral mammography (CESM). These modalities have been found to improve the cancer detection rate by resolving the superimposition of breast tissue on conventional mammography in tomosynthesis³ or enhancing cancers secondary to tumour angiogenesis in CESM.^{4–9} While tomosynthesis is suited for breast cancer detection, CESM is preferable for differentiating cancers from benign lesions. The characterisation of breast lesions in these two techniques is crucial for prompt and effective patient management.

CESM can provide low-energy mammograms and additional contrast-enhanced subtracted mammograms within the same examination. The low-energy mammogram has been proven to be qualitatively equivalent to conventional mammograms.^{10–12} Under the suppressed background of normal breast tissue, breast cancers characterized by hyperangiogenesis can easily be displayed on CESM due to the presence of iodine uptake. This result indicates the increased possibility of malignancy rather than non-malignancy. However, 6–28% of enhanced lesions have also been documented in certain precancerous or benign diseases^{4–7} including atypical ductal hyperplasia, flat epithelial atypia, intraductal papilloma, fibroadenoma, hamartoma, radial scar, or adenosis.^{4–7} Furthermore, additional information of associate enhancement could help to assess the probably malignant microcalcifications.⁵ In order to better understand the differentiation capability of CESM, we

retrospectively analyzed the quantitative measurement and relative enhancement at early and late phases among pathologically proven benign and malignant lesions. To our knowledge, the feasibility of quantifying lesion enhancement on CESM has not been reported before.

METHODS AND MATERIALS

Patient population and imaging protocol

Approval for this study was obtained from Chang Gung Memorial Hospital's Institutional Review Board. We retrospectively reviewed the cases that had undergone CESM from January 2012 to December 2015 in our hospital. The inclusion criteria were: (1) suspicious malignant breast lesions determined either by mammography or sonography; (2) breast lesions pathologically proven either by image-guided biopsy or surgery; (3) cases where CESM was performed according to our standardized protocol: performing craniocaudal (CC) views first and mediolateral oblique (MLO) views later to quantify the difference of enhancement for the same lesion; and (4) lesions with a clinical follow up of at least 1 year. One male patient was excluded due to the indigent difficulty of obtaining adequate CC view image on man.

CESM was performed using a commercial mammography apparatus (Senographe Essential CESM; GE Healthcare, Buc, France) using molybdenum or rhodium with automatic cooperation of copper filter. A single-bolus injection of a non-ionic contrast medium (Omnipaque 350 mg I ml⁻¹; GE Healthcare, Dublin, Ireland) was administered, with injection rate of 3 ml s⁻¹, followed by saline chase via an intravenous catheter that was inserted into the forearm prior to the examination. To successfully recombine the image for subtraction, the patients received repeated exposure from low and high energy in 1 to 2 s alterations during each breast-compressed position, resulting in two images below and above the iodine k-edge at 33.2 keV. Image subtractions can be obtained by diminishing the attenuation differences between the low- and high-energy images and reduction of the noise of non-enhancing image. Enhancement secondary to the iodine uptake was measured by the residual net attenuation.

All mammogram acquisitions were sequentially performed with breast holding during imaging. The bilateral breasts compressed in the CC view were first performed, followed by the MLO view. The imaging procedure takes about 2 to 6 min. Due to the longer positioning time of the MLO view compared to the CC view, we designed the acquisition order such that the CC view was performed first, followed by the MLO view. This was to allow post-contrast CC views of the bilateral breasts to be completed within 3 min after the injection of the contrast medium, while the post-contrast MLO views could be accomplished within 6 min after contrast medium injection. The average time interval between the CC and MLO views of our series was 102 s (range from 72 to 156 s). Low- and high-energy acquisitions were almost simultaneously captured during each single view study and then recombined to obtain a subtracted mammogram. Therefore, the imaging procedure provided a total of eight mammography images, including the low-energy image, used as a substitute to the conventional mammogram, and the CESM images.

Imaging analysis

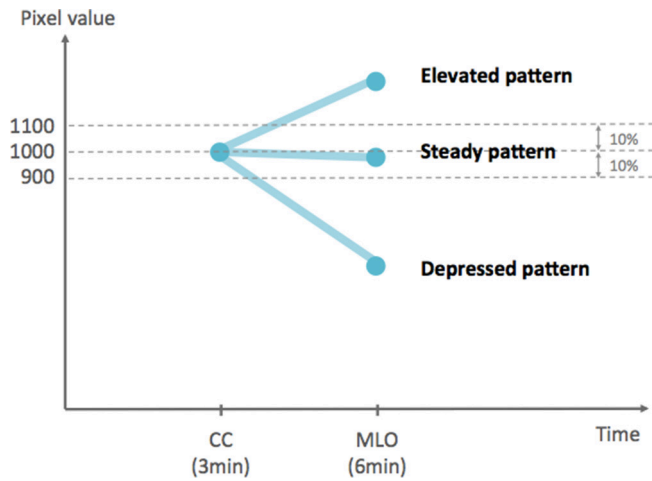
All enhanced breast lesions, including masses, architectural distortions and microcalcifications, were processed using a semi-automatic segmentation programme in MATLAB R2014a (MathWorks, Natick, MA). Semi-automatic segmentation was performed by automatic selection of the region of interest (ROI) of the breast lesions, followed by manually adjustment by a single radiologist with 3 years of experience in breast imaging. The algorithm is mainly based on edge-based segmentation to delineate the contour of breast lesions. This method process included ameliorating the image quality, obtaining energy texture image and detecting the edges,¹³ followed by manual correction of the region of interest of the enhanced lesions manually with a free-hand dragging tool. Lesion without identifiable enhancement from both the automatic segmentation and the radiologist was defined as non-enhanced lesions.

The pixel values of enhanced lesions were determined by the semi-automatic segmentation described in the Supplementary Material 1 (Supplementary material available online). After applying volume of interest LUT transformation using non-linear sigmoid function, the pixel values were obtained. The basic equation sigmoid volume of interest look-up table transformation of window centre and window width is $\bar{I}(x, y) = \frac{\text{output_range}}{1 + e^{-4 \frac{I(x,y) - Wc}{Ww}}}$. The

descriptive statistics of enhanced lesions was calculated using the maximum, 95th percentile, 75th percentile, mean, skewness, and kurtosis. The enhancement values from either the CC or MLO views were used for analysis. We measured the pixel values from the bounded lesions that were not affected from the shape of lesions. Since we could not separately obtain the exact pixel values of the normal glandular tissue superimposed over the enhanced lesions, the results of enhancement were simply based on the bounded lesions. Otherwise, the enhancement pattern was evaluated at two relative points between the early phase (2 min after the injection of the contrast medium on CC views) and delayed phase (4 min after contrast medium injection on MLO views) of enhancement, respectively. Unlike dynamic contrast-enhanced MRI (DCE-MRI), the relative enhancement on CESM was not ever published previously. In our report, we grouped in three patterns including: (1) elevated pattern (the enhancement increased more than 10% from the early phase to the late phase), (2) steady pattern (the enhancement changed within 10%), and (3) depressed pattern (the enhancement decreased more than 10%) (Figure 1).

Colour-coded map was used for visual demonstration of the enhancement pattern of the same lesion. On the colour-coded map, the reference for colour-coding was based on the average pixel of the whole breast on CESM. Generally, the average pixel had a baseline of zero. A net pixel value greater than the average pixel was counted as a positive value, with all pixel values below the average recorded were counted as zero. The background was set to black and the cancers increased brightness with the net pixel values. Pixel values below the average pixel of the whole breast were coloured blue as a baseline, and the maximum pixel of the whole image was coloured red using a jet colour-coded map; the sequence used was red, yellow, green, cyan, and blue (colour figures were provided on online version only).

Figure 1. Relative enhancement patterns of early and late phases. Elevated pattern: the interval enhancement increased more than 10%. Steady pattern: the interval enhancement changed within 10%. Depressed pattern: the interval enhancement decreased more than 10%.



Statistical analysis

The diagnostic accuracy of CESM in the discrimination of benign and malignant lesions was statistically analyzed by Pearson's X^2 test, logistic regression analysis, and receiver operating characteristic (ROC) curve analysis. The best cut-off value was determined using the Youden index, with $Y = sensitivity$ (1 specificity). The sensitivity, specificity, positive likelihood ratio, negative likelihood ratio, and accuracy were then calculated. A p -value < 0.001 was considered to indicate statistical significance. All statistical analyses were performed using the SPSS statistical software (IBM Corp., Armonk, NY).

RESULTS

A total of 152 breast lesions fulfilled the study criteria and were included in the analysis. Of these, all were presented in females,

with a mean age of 48.01 years (range, 25–84 years). Of the 152 lesions, 108 were malignancies and 44 were benignities (Table 1).

After applying semi-automatic segmentation to CESM, there were 104 mass lesions (98 of which enhanced), 44 microcalcifications (10 of which enhanced) and 4 architectural distortions (all of which enhanced). Of all the 152 lesions, 100 of the 108 malignancies (92.59%) and 12 of the 44 non-malignancies (27.27%) exhibited enhancement, while 8 (7.4%) of the malignant lesions and 32 (72.73%) of the non-malignant lesions did not observed enhancement. The eight non-enhancing malignancies all presented with microcalcification only were diagnosed to ductal carcinoma *in situ* (DCIS) in seven (87.5%) and invasive ductal carcinoma (IDC) in one (12.5%). Of these seven DCIS, three were low grade and four were intermediate grade. The only one IDC was Grade 2.

All enhanced lesions were identified and processed using the semi-automatic segmentation programme mentioned above. The non-enhanced lesions were counted as zero. The degree of enhancement was statistically higher in malignancies than in benign diseases in terms of the mean, 75th percentile, 95th percentile, and the maximum (Table 2). The ROC curve revealed good differentiation between malignancies and non-malignancies, and the area under the ROC curve (AUC) was 0.875 [95% confidence interval (CI) 0.811–0.940, $p < 0.0001$]. The optimal cut-off value was 220.94 according to the Youden index, with a sensitivity of 75.5%, specificity of 88.6%, positive likelihood ratio of 6.642, negative likelihood ratio 0.277, and accuracy of 82.1% (Table 3). Compared to human observers in our study, 24 of 44 benign lesions were initially categorized into Breast Imaging Reporting and Data System 4 due to presence of enhancement. 5 of 24 (20.8%) benign lesions had enhancement degree greater than the optimal cut-off value of 220.94, which indicates the possibility of false positive. In the contrary, 4 DCIS of 108 malignant lesions without enhancement were initially categorized into Breast Imaging Reporting and Data System 2 or 3. However, only one of four (25%) malignant lesions had enhancement greater than 220.94.

Table 1. Patient pathological characteristics

Malignant (n = 108)		Benign (n = 44)	
Ductal carcinoma <i>in situ</i>	24	Flat epithelial atypia	22
Invasive ductal carcinoma	74	Proliferative breast disease ^a	7
Invasive lobular carcinoma	3	Intraductal papilloma	2
Squamous cell carcinoma	2	Fibroadenoma	5
Metastatic serous adenoma	1	Adenosis	5
Mucinous carcinoma	1	Fibrosis	1
Angiosarcoma	1	Non-proliferative breast disease ^b	2
Adenoid cystic carcinoma	1		
Liposarcoma	1		

^aProliferative breast disease other than FEA.

^bNon-proliferative breast disease other than fibroadenoma, adenosis, fibrosis

There were two lesions only identified on MLO view, therefore two lesions were excluded in the enhancement pattern study. Of the 150 lesions, 106 were malignancies and 44 were benignity. Among the enhancement patterns, the incidence of benign disease and malignancy, respectively, was 26.92% (7/26) and 73.08% (19/26) in the elevated pattern, 7.14% (1/14) and 92.86% (13/14) in the steady pattern, 5.71% (4/70) and 94.29% (66/70) in the depressed pattern, and 80.00% (8/40) and 20.0% (32/40) in non-enhanced lesions. Of the 106 malignant lesions, 62.26% were depressed (Figure 2), 17.92% were elevated (Figure 3), 12.26% were steady (Figure 4), and 7.55% were indeterminate due to non-enhancement (Table 4). The enhancement pattern was found to be statistically significant between the benign and malignant lesions ($p < 0.0001$).

We separately exploited the CC views (at early phase) and MLO views (at late phase) to evaluate the relative contrast enhancement patterns. In considering to the different degree of compression

Table 2. Enhancement degree: malignant vs benign tumours

	Benign	Malignant	p-value	OR	95% CI
Mean	85.79	476.05	<0.0001 ^a	1.008	1.005–1.010
75th percentile	114.74	588.78	<0.0001 ^a	1.006	1.004–1.008
95th percentile	159.72	744.57	<0.0001 ^a	1.005	1.003–1.006
Maximum	261.25	1022.20	<0.0001 ^a	1.003	1.002–1.004
Kurtosis	1.46	2.99	<0.0001 ^a	1.717	1.317–2.237
Skewness	0.11	0.17	0.487	0.457	0.504–4.217

95% CI, 95% confidence interval; OR, odds ratio.

The table illustrates the degree of enhancement of both malignant and benign lesions, including the mean, 75th percentile, 95th percentile, maximum, kurtosis, and skewness. The p-value was determined by logistic regression.

^aA p-value < 0.001 is considered to be statistically significant.

and force in the individual positioning, we recorded the breast thickness and compression force of our all cases. The average breast thickness of CC and MLO view of right and left breasts were 52.72, 53.87, 53.41, 53.69 mm and the average compression forces were 135.92, 142.43, 140.53 and 142.43 Newtons respectively. We believed that the standard requirement for quality control acquired steady pressure and breast thickness that had been published by O'Leary's study.¹⁴ Additionally, the correlation coefficient (intraclass correlation coefficient) of breast thicknesses on the CC view to MLO view of right breast was 0.963 [95% CI (0.948–0.973)] and 0.963 for left breast [95% CI (0.950–0.973)], indicating the excellent consistency. The Bland–Altman plot is shown in Figure 5a,b.

DISCUSSION

CESM is a recently developed breast imaging technique that facilitates the detection and size measurement of cancer by mammographic morphology and angiogenic enhancement. Technical and clinical experiences of CESM have been published elsewhere.^{6,7} Many blinded interobserver studies have reported that CESM can improve the diagnosis of breast cancer with increased sensitivity, specificity, positive-predictive value, negative-predictive value, and accuracy.^{12,15,16} Otherwise, CESM can assist clinical decision making by identifying potential multifocal, multicentric or bilateral breast cancer before surgery,

leading to a change treatment strategy in 19% patients after detection of additional malignant lesions.¹⁷ Our study showed similar findings in which among the 152 breast lesions in 141 patients (11 patients with bilateral lateral lesions), showing 7 of the 108 malignancies and 4 of the 44 non-malignancies.

The enhancement technique is an important way of displaying angiogenic lesions. Malignant lesions are mostly hypervascular with immature tumour vessels. As shown in our results, the degree of enhancement of malignant tumours is frequently greater than that of benign lesions. The additional information gained via this method is important for diagnostic consideration. The optimal cut-off value of malignant lesions was calculated to prove the power of the test, although the value was not applied to all cases universally. From our results, we found out that using a cut-off value of 220.94, we can yield a positive likelihood ratio of 6.642, indicating that higher enhancement probably relates to malignancy.

As for other related diagnostic tools, both CESM and DCE-MRI can evaluate suspicious breast lesions using kinetic enhancement. Although CESM has lower sensitivity but better specificity than DCE-MRI, both CESM and DCE-MRI are superior to mammography, especially in dense breast.¹⁸ DCE-MRI is a sensitive imaging modality for the detection of cancer and the interpretation of lesions.^{19,20} The continuous acquisition of the enhancement of lesions provides kinetic information for cancer diagnosis with documented diagnostic value.²¹ The DCE-MRI lexicon of enhancement curves has been classified into three types according to the change in their signal intensity over time after the injection of a contrast medium, and include persistent enhancement (Type I), plateau (Type II), and washout (Type III) patterns.²¹ Kuhl et al²¹ reported 101 malignant lesions distributed as follows: Type I, 8.9%; Type II, 33.6%; and Type III, 57.4%. They also reported 165 benign lesions distributed as follows: Type I, 83.0%; Type II, 11.5%; and Type III, 5.5%. These results had an overall diagnostic accuracy of 86.0%, sensitivity of 91.0%, and specificity of 83.0%. Meanwhile, uncertainty remains as to whether iodine would play a role in CESM similar to that of gadolinium in DCE-MRI. Nevertheless, the main concern is the radiation dose administered during the treatment time in order to obtain a continuous time-enhancement curve.

Table 3. Areas under receiver operating characteristic curve of the degree of enhancement

	AUC	p-value	95% CI
Mean	0.877	<0.0001 ^a	0.813–0.941
75th percentile	0.877	<0.0001 ^a	0.813–0.941
95th percentile	0.875	<0.0001 ^a	0.810–0.940
Maximum	0.858	<0.0001 ^a	0.787–0.929
Skewness	0.691	<0.0001 ^a	0.597–0.785
Kurtosis	0.784	<0.0001 ^a	0.687–0.881

95% CI, 95% confidence interval; AUC, area under the curve; Q75, 75 percentile; Q95, 95 percentile; ROC, receiver operating characteristic curve; 95% CI, 95% confidence interval.

The ROC curves of the degree of enhancement including the mean, 75th percentile, 95th percentile, and maximum.

^aA p-value <0.001 is considered to be statistically significant.

Figure 2. Case of depressed relative enhancement of a 61-year-old female with pathologically proven right breast invasive ductal carcinoma. Mammography CC (a) and MLO views (b) of the right breast revealed a mass lesion in the upper outer quadrant. Colour-coded map CC (c) and MLO views (d) of the right breast revealed depressed relative enhancement. CC, craniocaudal; MLO, mediolateral oblique.

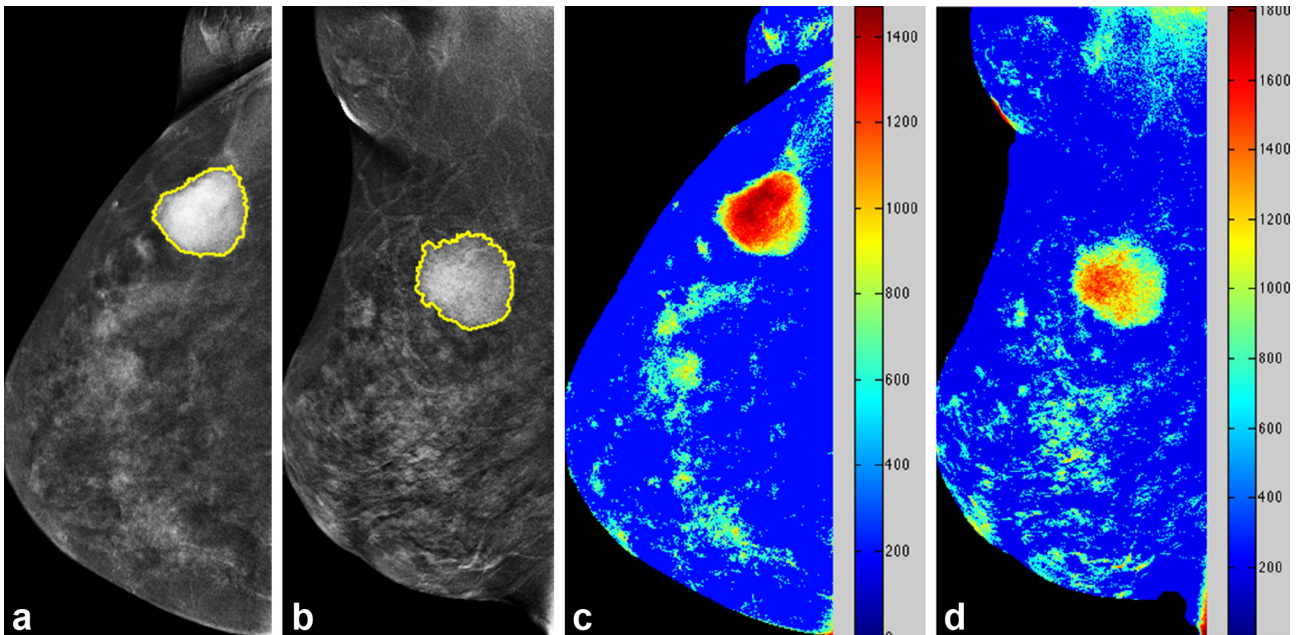


Figure 3. Case of elevated relative enhancement of a 39-year-old female with pathologically proven right breast invasive ductal carcinoma. Mammography CC (a) and MLO views (b) of the right breast revealed a speculated mass lesion in the lower outer quadrant. Colour-coded map CC (c) and MLO views (d) of the right breast revealed elevated relative enhancement. CC, craniocaudal; MLO, mediolateraloblique.

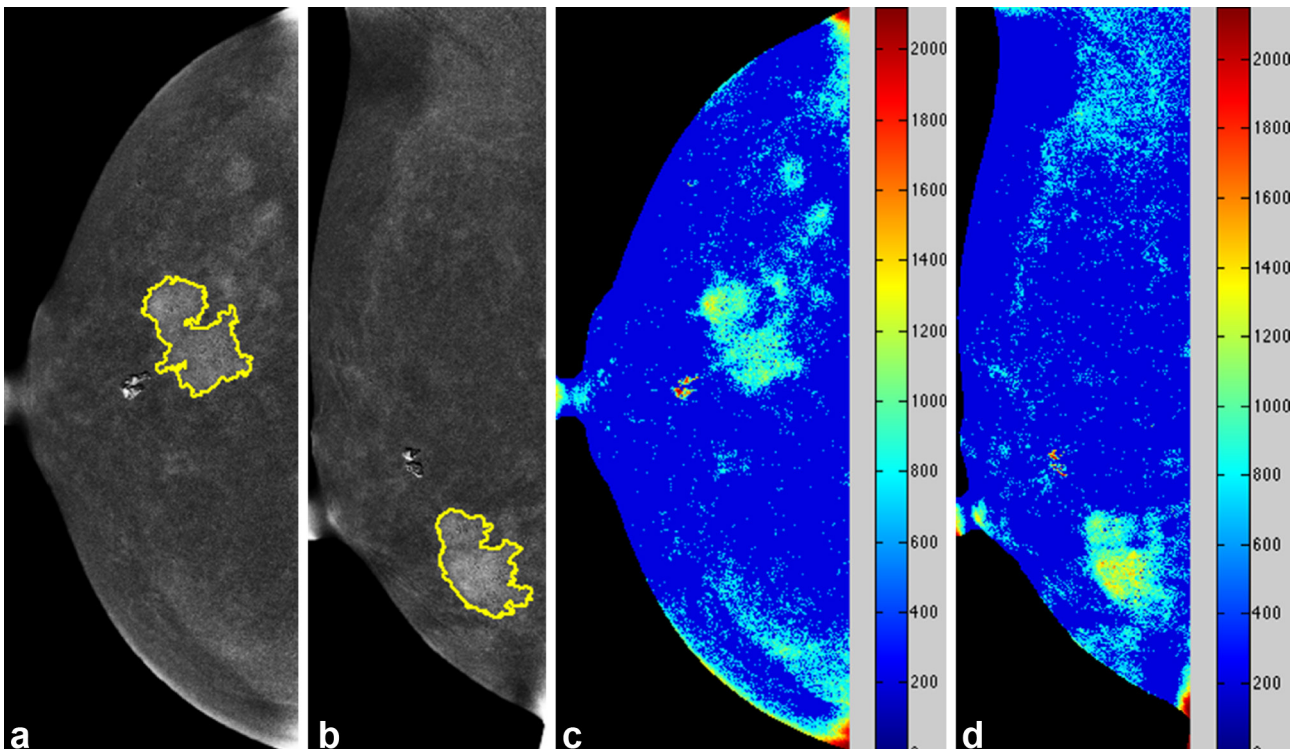
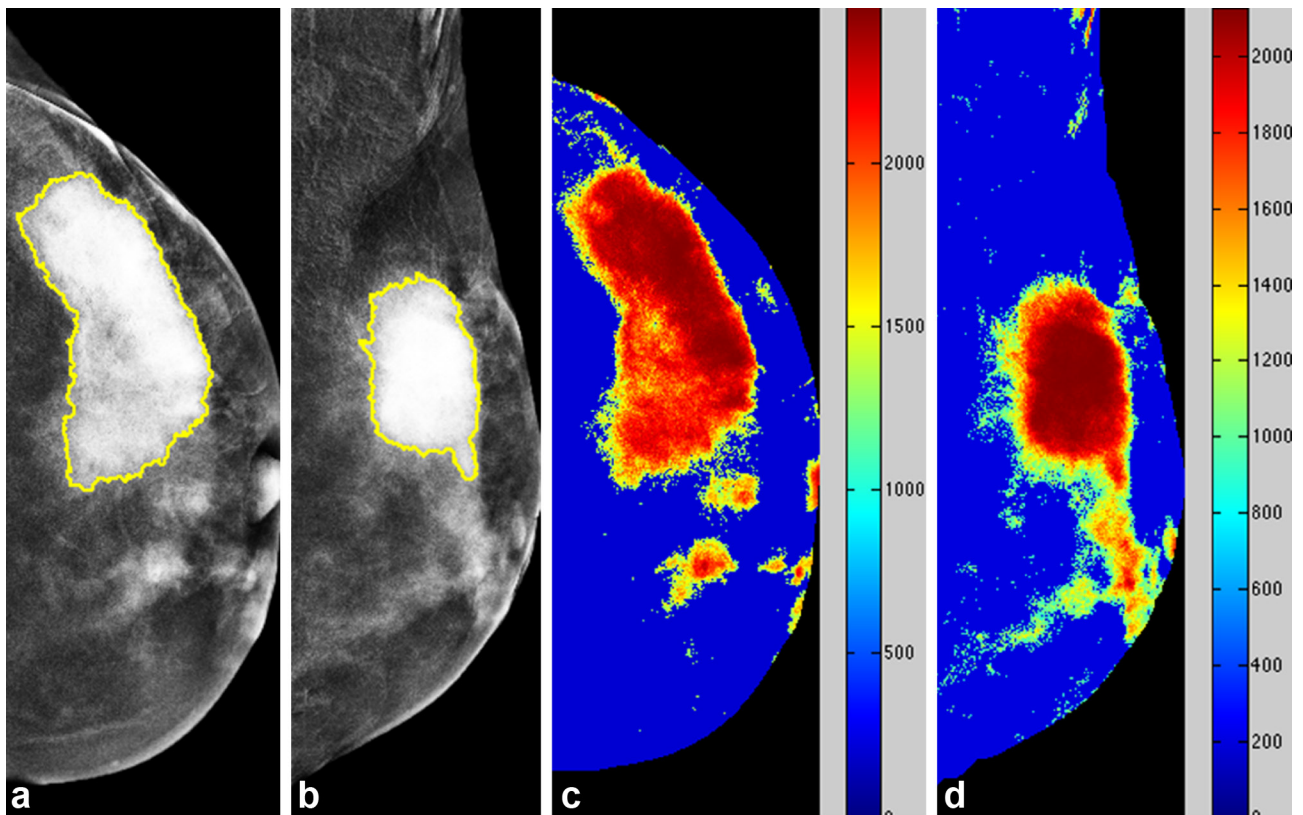


Figure 4. Case of steady relative enhancement of a 39-year-old female with pathologically proven left breast invasive ductal carcinoma. Mammography CC (a) and MLO views (b) of the left breast revealed a strongly enhanced mass lesion in the upper outer quadrant. Colour-coded map CC (c) and MLO views (d) of the right breast revealed steady relative enhancement. CC, craniocaudal; MLO, mediolateral oblique.



In the past, digital subtraction angiography revealed that the majority of breast cancers had rapid and strong enhancement with washout due to their hypervascularities.^{22–24} However, digital subtraction angiography is seldom used due to the invasive nature of the procedure. Similar to breast DCE-MRI, the investigation of tumour enhancement secondary to leakage of the contrast medium into the interstitial spaces is a topic of interest. To our best knowledge, there was no similar CESM report to investigate the enhancement patterns of cancers as compared to our study. Only a CESM study with a different protocol of performance using sequential exposure at 3rd, 5th, 7th and 10th

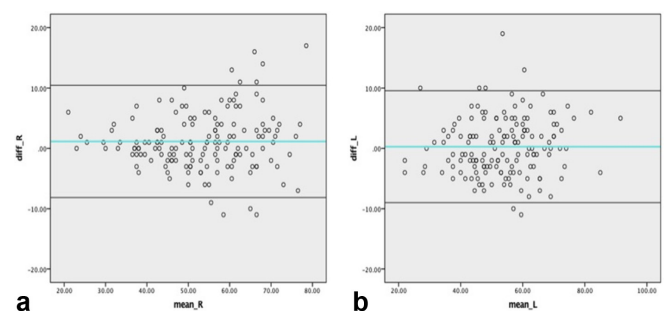
minutes after contrast injection in single to analyze the enhancement patterns of cancers. Their few cases revealed that 3 of 10 (30%) malignant lesions with decreased pattern, 4 of 10 (40%) with plateau pattern, 1 of 10 (10%) with increased pattern and 2 of 10 (20%) without enhancement.²⁵ A recent advanced study demonstrated a significant correlation of kinetic curves between DCE-MRI with gadolinium and contrast-enhanced digital breast tomosynthesis with iodine.²⁶ These results indicated that iodine might display enhancement comparable to that of gadolinium

Table 4. Relative early and late enhancements of malignant and benign breast lesions

	Benign (n = 44)	Malignant (n = 106)	Total (n = 150)
Age	49 (33–84)	47.8 (25–73)	47.9 (25–84)
Dynamic kinetic curve			
Elevated	7 (15.91%)	19 (17.92%)	26
Steady	1 (2.27%)	13 (12.26%)	14
Depressed	4 (9.09%)	66 (62.26%)	70
Non-enhanced	32 (72.73%)	8 (7.55%)	40

Pearson's chi-squared test $\chi^2(3) = 223.972$, $p < 0.0001$.

Figure 5. Bland-Altman plot of breast thickness of bilateral breasts. (a) Bland-Altman plot of breast thickness of right CC view and MLO view. (b) Bland-Altman plot of breast thickness of left CC view and MLO view. CC, craniocaudal; MLO, mediolateral oblique.



in DCE-MRI. Unfortunately, a high dose of multiexposure radiation was needed to trace the degree of lesion enhancement at subsequent time points in order to plot an enhancement curve.

In contrast to the previous study, we utilized the time interval between the CC views and MLO views to estimate the contrast enhancement characteristics of breast lesions and quantitatively analyze pathologically proven breast lesions using original CESM images. The plotting of enhancement curves requires at least three different time points from DCE-MRI. Additional exposures would, therefore, be in excess of the normal performance of CESM. From our designed analysis using the two image acquisition time points, the relative enhancement at early (CC view) and late (MLO view) net enhancements on CESM is adequate to classify the enhancement as elevated, steady, or depressed.

With regard to DEC-MRI, malignancies typically exhibit maximal enhancement within 2–3 min after the injection of gadolinium either with or without washout. In Kuhl's DCE-MRI study, washout was observed in 57.4% of malignancies.²¹ In our CESM study, depressed, steady, and elevated enhancement patterns may correspond to the washout, plateau, and persistent rising enhancement patterns of DCE-MRI, respectively. Approximately, 62.26% of our malignant lesions (66 of 106) exhibited depressed relative enhancements, similar to the washout curve of DCE-MRI by Kuhl's study (57.4%) However, up to 17.92% (19 of 106) of malignant lesions had elevated enhancement that might overlap with benign lesions.

There are several limitations in our study. First, this study was a retrospective analysis on the clinical cases that was performed

sequentially with CC views first followed by MLO views for examining bilateral breasts in a same session. We could only document the relative enhancement between early and late phases rather than dynamic kinetic enhancement. Second, CESM was not routinely performed for all cases of malignancy because it is not currently a compulsory modality for clinical management. However, our analyzed cases were consecutively performed without specific histological selection. Third, the thickness of a large breast might delay image acquisitions by more than 6 min after contrast medium injection due to the expenditure of a greater amount of energy. Fortunately, we noticed no such case in our series. Fourth, the reference for the enhancement measurements was based on the average enhancement of the whole breast including normal and abnormal enhancements. This might induce a technical error whereby mild enhanced lesions are masked on the colour-coded map. In our study, seven DCIS and one IDC were observed to have subtle enhancement on the original CESM, but were invisible on the colour-coded map. A correlation with the original CESM could resolve this pitfall. Fifth, the shape and density of the lesions in different views might influence the enhancement results. However, we assume that this effect was limited due to the residual iodine concentration only after the subtraction of high-to-low-energy mammograms.

CONCLUSION

Despite variations in the degree of tumoral angiogenesis, quantitative analysis of the breast lesions on CESM documented distinctive enhancement and relative enhancement patterns among the malignant and benign lesions.

REFERENCES

- Cheung YC, Lin YC, Wan YL, Yeow KM, Huang PC, Lo YF, et al. Diagnostic performance of dual-energy contrast-enhanced subtracted mammography in dense breasts compared to mammography alone: interobserver blind-reading analysis. *Eur Radiol* 2014; **24**: 2394–403. doi: <https://doi.org/10.1007/s00330-014-3271-1>
- Boyd NF, Martin LJ, Bronskill M, Yaffe MJ, Duric N, Minkin S. Breast tissue composition and susceptibility to breast cancer. *J Natl Cancer Inst* 2010; **102**: 1224–37. doi: <https://doi.org/10.1093/jnci/djq239>
- Kopans DB. Digital breast tomosynthesis from concept to clinical care. *AJR Am J Roentgenol* 2014; **202**: 299–308. doi: <https://doi.org/10.2214/AJR.13.11520>
- Lewin JM, Isaacs PK, Vance V, Larke FJ. Dual-energy contrast-enhanced digital subtraction mammography: feasibility. *Radiology* 2003; **229**: 261–8. doi: <https://doi.org/10.1148/radiol.2291021276>
- Cheung YC, Tsai HP, Lo YF, Ueng SH, Huang PC, Chen SC. Clinical utility of dual-energy contrast-enhanced spectral mammography for breast microcalcifications without associated mass: a preliminary analysis. *Eur Radiol* 2016; **26**: 1082–9. doi: <https://doi.org/10.1007/s00330-015-3904-z>
- Dromain C, Thibault F, Diekmann F, Fallenberg EM, Jong RA, Koomen M, et al. Dual-energy contrast-enhanced digital mammography: initial clinical results of a multireader, multicase study. *Breast Cancer Res* 2012; **14**: R94. doi: <https://doi.org/10.1186/bcr3210>
- Dromain C, Thibault F, Muller S, Rimareix F, Delaloge S, Tardivon A, et al. Dual-energy contrast-enhanced digital mammography: initial clinical results. *Eur Radiol* 2011; **21**: 565–74. doi: <https://doi.org/10.1007/s00330-010-1944-y>
- Dromain C, Balleyguier C, Muller S, Mathieu MC, Rochard F, Opolon P, et al. Evaluation of tumor angiogenesis of breast carcinoma using contrast-enhanced digital mammography. *AJR Am J Roentgenol* 2006; **187**: W528–W537. doi: <https://doi.org/10.2214/AJR.05.1944>
- Diekmann F, Diekmann S, Jeunehomme F, Muller S, Hamm B, Bick U. Digital mammography using iodine-based contrast media. *Invest Radiol* 2005; **40**: 397–404. doi: <https://doi.org/10.1097/01.ri.0000167421.83203.4e>
- Francescone MA, Jochelson MS, Dershaw DD, Sung JS, Hughes MC, Zheng J, et al. Low energy mammogram obtained in contrast-enhanced digital mammography (CEDM) is comparable to routine full-field digital mammography (FFDM). *Eur J Radiol* 2014; **83**: 1350–5. doi: <https://doi.org/10.1016/j.ejrad.2014.05.015>
- Lalji UC, Jeukens CR, Houben I, Nelemans PJ, van Engen RE, van Wylick E, et al. Evaluation of low-energy contrast-enhanced spectral mammography images by comparing them to full-field digital

- mammography using EUREF image quality criteria. *Eur Radiol* 2015; **25**: 2813–20. doi: <https://doi.org/10.1007/s00330-015-3695-2>
12. Luczyńska E, Heinze-Paluchowska S, Dyczek S, Blecharz P, Rys J, Reinfuss M. Contrast-enhanced spectral mammography: comparison with conventional mammography and histopathology in 152 women. *Korean J Radiol* 2014; **15**: 689–96. doi: <https://doi.org/10.3348/kjr.2014.15.6.689>
 13. Zhang Y, Tomuro N, Furst J, Stan Raicu D. Image enhancement and edge-based mass segmentation in mammogram. In: Dawant BM, Haynor DR, eds. *Medical imaging 2010: image processing*. vol. **7623**. San Diego, CL, USA: SPIE; 2010. pp. 72634.
 14. O'Leary D, Grant T, Rainford L. Image quality and compression force: the forgotten link in optimisation of digital mammography? *Breast Cancer Research* 2011; **13**(Suppl 1): P10. doi: <https://doi.org/10.1186/bcr2962>
 15. Blum KS, Antoch G, Mohrmann S, Obenauer S. Use of low-energy contrast-enhanced spectral mammography (CESM) as diagnostic mammography—proof of concept. *Radiography* 2015; **21**: 352–8. doi: <https://doi.org/10.1016/j.radi.2015.02.005>
 16. Wang Q, Li K, Wang L, Zhang J, Zhou Z, Feng Y. Preclinical study of diagnostic performances of contrast-enhanced spectral mammography versus MRI for breast diseases in China. *Springerplus* 2016; **5**: 763. doi: <https://doi.org/10.1186/s40064-016-2385-0>
 17. Tardivel AM, Balleyguier C, Dunant A, Delaloge S, Mazouni C, Mathieu MC, et al. Added value of contrast-enhanced spectral mammography in postscreening assessment. *Breast J* 2016; **22**: 520–8. doi: <https://doi.org/10.1111/tbj.12627>
 18. Fallenberg EM, Schmitzberger FF, Amer H, Ingold-Heppner B, Balleyguier C, Diekmann F, et al. Contrast-enhanced spectral mammography vs. mammography and MRI – clinical performance in a multi-reader evaluation. *Eur Radiol* 2017; **27**: 2752–64. doi: <https://doi.org/10.1007/s00330-016-4650-6>
 19. Kuhl C. The current status of breast MR imaging. Part I. Choice of technique, image interpretation, diagnostic accuracy, and transfer to clinical practice. *Radiology* 2007; **244**: 356–78. doi: <https://doi.org/10.1148/radiol.2442051620>
 20. Kuhl CK. Current status of breast MR imaging. Part 2. Clinical applications. *Radiology* 2007; **244**: 672–91. doi: <https://doi.org/10.1148/radiol.2443051661>
 21. Kuhl CK, Mielcareck P, Klaschik S, Leutner C, Wardelmann E, Gieseke J, et al. Dynamic breast MR imaging: are signal intensity time course data useful for differential diagnosis of enhancing lesions? *Radiology* 1999; **211**: 101–10. doi: <https://doi.org/10.1148/radiology.211.1.r99ap38101>
 22. Watt AC, Ackerman LV, Windham JP, Shetty PC, Burke MW, Flynn MJ, et al. Breast lesions: differential diagnosis using digital subtraction angiography. *Radiology* 1986; **159**: 39–42. doi: <https://doi.org/10.1148/radiology.159.1.3513251>
 23. Ackerman LV, Watt AC, Shetty P, Flynn MJ, Burke M, Kambouris A, et al. Breast lesions examined by digital angiography. Work in progress. *Radiology* 1985; **155**: 65–8. doi: <https://doi.org/10.1148/radiology.155.1.3883425>
 24. Watt AC, Ackerman LV, Windham JP, Shetty PC, Burke MW, Flynn MJ, et al. Breast lesions: differential diagnosis using digital subtraction angiography. *Radiology* 1986; **159**: 39–42. doi: <https://doi.org/10.1148/radiology.159.1.3513251>
 25. Jong RA, Yaffe MJ, Skarpathiotakis M, Shumak RS, Danjoux NM, Gunesevara A, et al. Contrast-enhanced digital mammography: initial clinical experience. *Radiology* 2003; **228**: 842–50. doi: <https://doi.org/10.1148/radiol.2283020961>
 26. Froeling V, Diekmann F, Renz DM, Fallenberg EM, Steffen IG, Diekmann S, et al. Correlation of contrast agent kinetics between iodinated contrast-enhanced spectral tomosynthesis and gadolinium-enhanced MRI of breast lesions. *Eur Radiol* 2013; **23**: 1528–36. doi: <https://doi.org/10.1007/s00330-012-2742-5>

Cite this article as:

Warren LM, Dance DR, Young KC. Radiation risk of breast screening in England with digital mammography. *Br J Radiol* 2016; **89**: 20150897.

FULL PAPER

Radiation risk of breast screening in England with digital mammography

¹LUCY M WARREN, PhD, ^{1,2}DAVID R DANCE, PhD, MD and ^{1,2}KENNETH C YOUNG, PhD

¹National Coordinating Centre for the Physics of Mammography, Royal Surrey County Hospital NHS Foundation Trust, Guildford, UK

²Department of Physics, University of Surrey, Guildford, UK

Address correspondence to: Dr Lucy Mae Warren

E-mail: lucy.warren@nhs.net

Objective: To estimate the risks and benefits of breast screening in terms of number of deaths due to radiation-induced cancers and the number of lives saved owing to modern screening in the National Health Service Breast Screening Programme (NHSBSP) in England.

Methods: Radiation risk model, patient dose data and data from national screening statistics were used to estimate the number of deaths due to radiation-induced breast cancers in the NHSBSP in England. Dose and dose effectiveness factors (DDREFs) equal to one and two were assumed. The breast cancer mortality reduction in the invited population due to screening and the percentage of females diagnosed with symptomatic breast cancer, who die from breast cancer, were collated from the literature. The number of lives saved owing to screening was calculated.

Results: Assuming, a total of 1,770,436 females between the ages of 50–70 years were screened each year, and a breast cancer mortality reduction of 20% due to screening in the invited population, the number of screen-detected

cancers were 14,872 annually, resulting in 1071 lives saved. Conversely, for the same mortality reduction, the number of radiation-induced cancers was 36 and 18 for DDREFs of 1 and 2, respectively. This resulted in seven and three deaths due to radiation-induced cancers annually for DDREFs of 1 and 2, respectively. The ratios of lives saved owing to screening to radiation-induced cancers were 30:1 and 60:1 for DDREFs of 1 and 2. The ratios of lives saved owing to screening to deaths due to radiation-induced cancers were 156:1 and 312:1 for DDREFs of 1 and 2. For the 1.8% of the screening population with very thick breasts, the latter ratios decrease to 94:1 and 187:1 for DDREFs of 1 and 2.

Conclusion: The breast cancer mortality reduction due to screening greatly outweighs the risk of death due to radiation-induced cancers.

Advances in knowledge: Estimation of the radiation risk for modern breast screening in England using digital mammography.

INTRODUCTION

In the National Health Service Breast Screening Programme (NHSBSP) in England, females are invited for screening every 3 years between the ages of 50 and 70 years. During the screening examination, two views of both breasts are acquired using a mammography system. An ongoing randomized control trial (RCT) is investigating the use of an age extension to 47–73 years.¹ This would result in each female receiving two extra screening invitations during her lifetime.

During a mammography screening examination, the breast is exposed to ionizing radiation. There have been a number of publications estimating the radiation risks of screening programmes worldwide.^{2–5} These studies consider different screening regimes and age ranges than those in the NHSBSP. Studies relating to the breast screening programme in the UK include the NHSBSP Report 54,⁶ Berrington de González and Reeves⁷ and the Report of the

Independent Advisory Group on Ionizing Radiation.⁸ Berrington de González and Reeves⁷ compared the radiation risk with the mortality benefits of screening females under the age of 50 years, outside the current screening age range in the NHSBSP. A review of the radiation risks of breast screening was published in NHSBSP Report 54.⁶ There are several differences between the assumptions made in that report and current practice. At the time of the report, only two-view mammography was performed at the prevalent screen and one-view mammography was performed thereafter. In modern screening, two-view mammography is performed at all screening rounds. In addition, since the time of this report, mammography systems have transitioned from using film-screen mammography to digital mammography and use different X-ray target and filter materials, causing changes in the average breast dose per examination. In addition, recent publications have provided updated radiation risk coefficients from those used in NHSBSP Report 54.⁶ Finally,

assumptions about mortality due to breast cancer outside screening have also changed owing to improved treatments.

The Report of the Independent Advisory Group on Ionising Radiation⁸ estimates the radiation risk and benefit of screening in the UK breast screening programme. Two-view examinations were assumed as performed in current screening and an extended age range of 47–73 years was considered. However, the mean glandular dose (MGD) used was based on data using film-screen mammography,^{9,10} and the description of the calculations and assumptions is very brief.

In this report, the radiation risk has been compared with the lives saved owing to screening for the current imaging protocol used in the breast screening programme in the UK and taking account of the new information discussed above. There are additional harms of screening such as false positives, pain and psychological distress from procedures and overdiagnosis.¹¹ These harms are not considered in this article. This is not because they are unimportant but because the risk associated with the use of radiation in screening is the focus of this work.

METHODS AND MATERIALS

Published risk factors for risk of radiation-induced cancers

There is an extensive literature estimating the lifetime risk of breast cancer from X-ray exposure.^{12–17}

Preston *et al*^{12,13} conducted a pooled analysis of eight cohorts using follow-up data for each cohort. They developed equations for the excess absolute risk (EAR) and the excess relative risk (ERR) of breast cancer induction from which risk factors can be calculated for any given age or population. In the ERR model, the increased risk is taken to be proportional to the natural underlying incidence of the cancer concerned, whereas in the EAR model, the increase is taken to depend on dose and age at exposure but to be independent of the underlying incidence.¹⁴

Three international advisory bodies^{15–17} have calculated the lifetime attributable risk of breast cancer incidence and mortality using EAR and ERR models. Both the International Commission of Radiological Protection (ICRP) 103¹⁶ and Biologic Effects of Ionizing Radiation VII (BEIR VII)¹⁵ use the Life Span Study incidence data from Preston *et al*¹² and an EAR model. The Environment Protection Agency (EPA) report¹⁸ states that the ICRP 103 model and EPA model (based on the BEIR VII model) are essentially the same (although they are applied to estimate the risk in different populations). The United Nations Scientific Committee on Effects of Atomic Radiation (UNSCEAR) 2006 Report¹⁷ has alternative ERR and EAR models which could be used to calculate the risk of radiation-induced cancers, although the report does not conclude which of the ERR or EAR models (or a mixture) is appropriate.

The choice of EAR or ERR model is open to discussion. The Committee on the Biologic Effects of Ionizing Radiation VII¹⁵ suggests that theoretically the preferred transportation model between populations for breast cancer should be based on a multiplicative (relative) risk model. However, observations by Land *et al*¹⁹ found that risks calculated using the absolute risk

model were comparable for Japanese A-bomb survivors, patients undergoing tuberculosis fluoroscopy in Massachusetts and New York females treated with radiation for mastitis, whereas risks were much larger in the Japanese cohort when a relative risk model was used. However, BEIR VII authors suggest this finding may have been due to the fractionated exposures and lower energy photons in the latter two cohorts compared with the A-bomb exposure. Preston *et al*¹² confirmed the finding by Land *et al*¹⁹ that the risks calculated using the absolute model were similar for the Caucasian cohorts and A-bomb survivors, whereas the relative model results in much higher risks for the A-bomb survivors. Based on this finding by Preston *et al*,¹² ICRP based their model solely on the absolute model.

For a particular data set, it does not matter whether the risk is expressed in terms of ERR or EAR. What is important is how the excess risk is transferred between populations with different background risks. The absolute model has been used in this work because it is considered to be more stable when applied to populations other than those from which the model was developed.² For this purpose, the ICRP 103 model¹⁶ has been used, since this model is backed by a large international agency. The data used for the lifetime risk of cancer incidence over the range of ages seen in breast screening have been taken from Health Protection Agency the Centre for Radiation, Chemicals and Environmental Hazards Report 28 (HPA CRCE-028) report.²⁰

As with choice between EAR and ERR, the choice of dose and dose rate effectiveness factor (DDREF) is a topic of much discussion and research. Some authors suggest a DDREF of 1.0.^{2,7,21,22} They argue that a reduction factor does not apply in cases where fractionated high-dose rate radiation is received. Some suggest a DDREF of 1.5¹⁵ based on estimates of curvature of the dose–response curve from experimental animal data and from the latest Life Span Study data on solid cancer incidence. Others suggest a DDREF of 2.0^{16,17} on the basis of observations in various epidemiologic data sets. In this report, results are given for DDREFs of 1.0 and 2.0, since the appropriate choice of DDREF is uncertain.

Calculation of the number of lives saved and lost owing to radiation-induced cancers in the National Health Service Breast Screening Programme in England

In this section, the numbers of lives saved owing to screening and lost owing to radiation-induced breast cancers are calculated for the age range 50–70 years (current regime in NHSBSP) and also for the age extension being piloted in an RCT of 47–73 years.¹

In order to calculate the number of radiation-induced cancers, it was assumed that all screening examinations included two views. For the age range 50–70 years, it was assumed that females attended seven screening rounds at ages 51, 54, 57, 60, 63, 66 and 69 years. For the age range 47–73 years, it was assumed females attended two extra screening rounds, one at age 48 years and a second at age 72 years. The attendance rate and the number of females in each screening round were calculated using data from the NHSBSP statistics for the year 2013–14 for England.²³ Summed over all screening rounds, the total number of females screened was 1,770,436 for the age range 50–70

years and would be 2,312,525 if the age range was extended to 47–73 years. The number of females who would be screened in the screening rounds at ages 48 and 72 years was estimated by extrapolating the number of females in the standard age range to this wider age range.

HPA CRCE-028²⁰ provides ICRP risk factors for radiation-induced breast cancer for age bands of 10 years, between the ages of 0 and 99 years. In order to determine the risk factor at the age for each screening round (Table 1), a Gaussian curve was fitted to the data, from which the risk factor at the age for each screening round was interpolated.

Three different dose situations were investigated. First, the whole screening population was considered. The MGD was assumed to be equal to 3 mGy for a two-view examination. This is based on average doses of 1.5 mGy per view for digital mammography systems in the NHSBSP between 2010 and 2012.²⁴

The second situation considered was for a subgroup of the population with larger breasts, who are therefore likely to receive higher doses without an increase in cancer detection. From a dose survey of breast screening centres in the UK over the period of 2010–12,²⁴ for breasts with thickness above 90 mm, imaged on digital radiography systems, the average MGD was 2.3 mGy for the craniocaudal view and 2.7 mGy for the mediolateral oblique view. Therefore, an average MGD of 5.0 mGy for a two-view examination has been assumed. Only a small proportion of females will have breasts thicker than 90 mm (1.8%).

The final dose situation assumed that females with largest breasts may have multiple images per view. For the worst-case scenario that the females with largest breasts have two images per view, such that the entire breast is imaged twice, the resultant MGD would be 10 mGy. However, it is likely females would actually receive an MGD in between 5 and 10 mGy, since usually only part of the breast is exposed twice. In a dose survey of breast screening centres in the UK over the period of 2010–12, <0.1% of females had two images per view and received an MGD of >5 mGy (personal communication, Young and Oduko, 2016).

The number of induced cancers (I) for 1 year of screening was calculated using the following equation for each dose situation and age range of screening:

$$I = \sum_{j=1}^m DR_j S_j, \quad (1)$$

where D is the MGD (in milligray) of a screening examination, j is the screening round, m is the total number of the screening rounds attended by the females, R_j is the lifetime risk of radiation-induced cancer (per million females per milligray) for the age of females in screening round j and S_j is the number of females screened in screening round j per year (expressed in millions).

Next, the total number of detected cancers was calculated. The average detection rate in England per screening visit was 8.4 per 1000 females, taken from the NHSBSP statistics for the year 2013–14 for England.²³ The average detection rates were the same for the age ranges 50–70 and 47–73 years.²³ Using the detection rates and the total number of females screened, the number of screen-detected cancers were calculated for each age range.

Overdiagnosed cancers will not be detected in the absence of screening; so, the number of cancers must be reduced accordingly before calculating the number of lives saved owing to screening.

There is no uniform method of estimation of overdiagnosis, and estimates vary considerably from <5 to around 50%.²⁵ The independent review of the UK NHSBSP¹¹ suggests that 19% of diagnosed cancers in the screened population (screen detected and interval) are overdiagnosed. They also note that although this is calculated from old RCTs and therefore may not reflect current screening programmes, there is no clear evidence to suggest that the current rate of overdiagnosis would be lower or higher than that in the original trials. Therefore, it has been assumed here that the overdiagnosis has not changed since the RCTs.

Table 1. Lifetime risk of radiation-induced breast cancer for UK females for dose and dose effectiveness factors (DDREFs) of 1 and 2

Age (years)	Radiation risk factor (per million per mGy)	
	DDREF = 1	DDREF = 2
48	13.8	6.9
51	11.4	5.7
54	9.3	4.7
57	7.5	3.8
60	6.0	3.0
63	4.7	2.4
66	3.6	1.8
69	2.8	1.4
72	2.1	1.0

Using detection rates from the NHSBSP interval cancer review,²⁶ it was calculated that 25% of cancers in the population who attended screening were interval cancers. Screening 1,770,436 females per year, at a detection rate of 8.4 per 1000 females screened, results in 14,872 screen-detected cancers per year and 4957 ($1/3 \times 14,872$) interval cancers (T_I). Therefore, there are 3768 overdiagnosed cancers [$0.19 \times (14,872 + 4957)$] and 16,061 non-overdiagnosed cancers. By definition, an interval cancer cannot be overdiagnosed, so there are 11,104 ($14,872 - 3768$) screen-detected cancers which are not overdiagnosed (T_{SC}).

Lead time describes the amount of time a diagnosis of cancer is brought forward owing to screening and is estimated to be around 40 months.²⁷ Although the cancers are detected earlier with screening, they would still be detected in the absence of a screening programme (unlike overdiagnosed cancers). Therefore, there has been no reduction in the number of cancers detected owing to lead time when calculating the number of lives saved.

The final two pieces of information required to calculate the total number of lives saved owing to screening are the breast cancer mortality reduction in the population invited for screening and the probability of females with a symptomatic cancer dying from the disease.

There are several publications^{11,28–37} which have estimated mortality reduction due to breast screening, which are summarized in Table 2. Since the mortality reduction in the population invited to screening found in the literature was mainly 20% with a range of 15–30% in the invited population, this value and range have been used in this work.

The total number of lives saved (L_s) for 1 year of screening was found from the following equation:

$$L_s = M_{NS} r \frac{T_{SC} + T_I}{f}. \quad (2)$$

Here, T_{SC} and T_I are the number of screen-detected cancers which are not overdiagnosed and the number of interval cancers, r is the breast cancer mortality reduction in the invited population, M_{NS} is the probability of a female with a symptomatic cancer dying of the disease and f is the attendance rate for breast screening. The derivation of this equation is given in Appendix A.

The attendance rate was assumed to be 72%, based on national screening statistics for 2013–14 for England.²³ Mook et al³⁸ found that 24% of females diagnosed with symptomatic cancer died from the disease (based on 10-year survival). However, the study by Mook et al³⁸ included only invasive cancer. From NHSBSP statistics for England during 2013–14, 22% of screen-detected cancers are *in situ*. It has been assumed that the overdiagnosed cancers are primarily *in situ* and that the cancers which are not overdiagnosed have a mortality rate of 24% found by Mook et al.³⁸ This is reduced from a mortality rate of 50% used in NHSBSP Report 54,⁶ taking account of the improvement in treatment over time.

The number of lives lost owing to radiation-induced cancers (L_L) for 1 year of screening was estimated by multiplying the number of radiation-induced cancers by the fraction of females with a radiation-induced breast cancer, who later die from the radiation-induced cancer. If the radiation-induced cancers are detected whilst the females are participating in the screening programme, the survival of the females from radiation-induced breast cancer would be the same as that from screen-detected cancers. However, owing to the long delay in the appearance of these breast cancers, some radiation-induced cancers will occur at ages beyond the screening programme and will therefore have the same survival as symptomatic cancers. Therefore, the fraction of females with a radiation-induced breast cancer, who later die from the radiation-induced cancer, has been assumed to be the average of the fraction for screen-detected and symptomatic cancers. The effect of this assumption on the results is considered in the Discussion section of this article.

Table 2. Mortality benefit to the invited population found in previous publications

Publication	Mortality benefit to invited population
Marmot et al ¹¹	20%
Gotzche et al ²⁸	15%
US Task Force ²⁹	19%
Canadian Task Force ³⁰	21%
Demissie et al ³¹	30%
Tabar et al ³²	27%
Broeders et al ³³	25%
Weedon-Fekjaer et al ³⁴	28%
Lauby-Secretan et al ³⁵	23%
Duffy et al ³⁷	21%
Nyström et al ³⁶	15%

Finally, from the number of lives saved owing to screening and the number of lives lost owing to radiation-induced cancers, it was possible to calculate the number of females who must be screened (NNS) regularly over their lifetime to save a life:^{3,39}

$$\text{NNS} = \frac{S}{n(L_s - L_L)}, \quad (3)$$

where n is the number of screening rounds attended by the females over their lifetime and S is the total number of females screened per year (*i.e.* summed over all screening rounds).

In addition, the number of females screened over their lifetime, which results in one radiation-induced breast cancer death (NSD), was calculated using:

$$\text{NSD} = \frac{S}{nL_L}. \quad (4)$$

RESULTS

For the age range 50–70 years, and a 20% breast cancer mortality reduction in the population invited to screening, a total of 1,700,436 females were screened per year, resulting in the detection of 14,872 cancers and 1071 lives saved. For the average MGD of 3 mGy, this corresponds to 36 radiation-induced breast cancers and 7 radiation-induced cancer deaths for a DDREF of 1 and 18 radiation-induced breast cancers and 3 radiation-induced breast cancer deaths for a DDREF of 2. The ratios of the number of lives saved owing to screening to the number of radiation-induced cancers were therefore 30 : 1 for a DDREF of 1 and 60 : 1 for a DDREF of 2. For the assumed mortality reduction of 20%, the ratios of the number of lives saved owing to screening to the number of lives lost owing to radiation-induced breast cancer were 156 : 1 for a DDREF of 1 and 312 : 1 for a DDREF of 2.

There is some uncertainty over the breast cancer mortality reduction in the population invited to screening, with the range in

the literature covering 15–30%. The ratio of the number of lives saved owing to screening to the number of lives lost owing to radiation-induced breast cancer for this range of breast cancer mortality reductions ranges from 110 to 268 for a DDREF of 1 and 220–535 for a DDREF of 2.

The ratios of the number of lives saved owing to screening to the number of radiation-induced breast cancers and to the number of radiation-induced breast cancer deaths have also been investigated for different subgroups of the screening population and different age ranges (Table 3). It was found that the calculated values of these ratios for the extended age range of 47–73 years are very similar to the values of the ratios for the age range 50–70 years.

Table 3 also shows that for the small subgroup of the population (1.8%) with breasts of thickness 90 mm and above, the ratios of the lives saved owing to screening to the number of radiation-induced breast cancers and to the number of lives lost owing to radiation-induced breast cancers decreased, compared with the corresponding ratios for the entire screening population. The ratio of the number of lives saved owing to screening to the number of radiation-induced cancers was 18 : 1 for a DDREF of 1 and 36 : 1 for a DDREF of 2. The ratio of the number of lives saved owing to screening to the number of deaths owing to radiation-induced breast cancers was 94 : 1 for a DDREF of 1 and 187 : 1 for a DDREF of 2.

Finally, for the even smaller subgroup of the population (<0.1%) who receive an MGD of 10 mGy, the ratio of the number of lives saved owing to screening to the number of radiation-induced cancers was 9 : 1 for a DDREF of 1 and 18 : 1 for a DDREF of 2. For this subgroup, the ratio of number of lives saved owing to screening to the number of deaths owing to radiation-induced breast cancers was 47 : 1 for a DDREF of 1 and 94 : 1 for a DDREF of 2.

The number of females who must be screened in all screening rounds to save a life and the number of females attending all screening rounds per radiation-induced breast cancer and radiation-induced breast cancer death are given in Table 4 for

Table 3. Ratio of lives saved owing to screening to number of radiation-induced cancers and to the number of lives lost owing to radiation-induced breast cancer

DDREF	MGD (mGy)	Lives saved/induced cancers		Lives saved/lives lost	
		Age range = 50–70 years	Age range = 47–73 years	Age range = 50–70 years	Age range = 47–73 years
1	3 ^a	30 (22–45)	28 (21–42)	156 (110–268)	145 (102–249)
	5 ^b	18 (13–27)	17 (13–25)	94 (66–161)	87 (61–149)
	10 ^c	9 (7–13)	8 (6–13)	47 (33–80)	43 (31–75)
2	3 ^a	60 (45–90)	56 (42–83)	312 (220–535)	290 (205–497)
	5 ^b	36 (27–54)	33 (25–50)	187 (132–321)	174 (123–298)
	10 ^c	18 (13–27)	17 (13–25)	94 (66–161)	87 (61–149)

DDREF, dose and dose effectiveness factor; MGD, mean glandular dose.

The ratios are given for the age ranges 50–70 years and 47–73 years, DDREFs of 1 and 2, three MGDs and a 20% reduction in breast cancer mortality in the invited population. The bracketed values show results for 15–30% reductions in breast cancer mortality.

^aAverage MGD for all thicknesses.

^bAverage MGD for breasts of thickness 90 mm or greater (1.8% of females with breasts of thickness 90 mm or greater).

^cMGD assuming females with breasts 90 mm or greater have two images per view of the entire breast (<0.1% of females).

Table 4. Number of females screened to save a life, number of females screened per radiation-induced-breast cancer death and number of females screened per radiation-induced breast cancers

DDREF	Age range (years)	Screening rounds attended	Females screened to save a life	Females screened per radiation-induced breast cancer death	Females screened per radiation-induced breast cancer
1	50–70	7	238 (158–318)	36,856	7068
	47–73	9	185 (123–247)	26,634	5108
2	50–70	7	238 (158–318)	73,712	14,137
	47–73	9	185 (123–247)	53,268	10,216

DDREF, dose and dose effectiveness factor.

Data are given for the age ranges 50–70 years and 47–73 years, for DDREFs of 1 and 2, for MGD of 3 mGy and a 20% reduction in breast cancer mortality in the invited population. The bracketed values show results for 15–30% reductions in breast cancer mortality.

the DDREFs, MGDs and breast cancer mortality benefits to the invited population considered.

DISCUSSION

The number of cancers detected per radiation-induced cancer was found to be five times larger in this work compared with NHSBSP Report 54.⁶ This is due to several differences in the analyses performed, which have competing impacts on the number of cancers detected per radiation-induced cancer. Firstly, the radiation risk factors used in this work provided in the HPA CRCE-028 report,²⁰ using the ICRP 103 model,¹⁶ are lower for the age range used in this work compared with the National Radiological Protection Board (NRPB) model⁴⁰ used in NHSBSP Report 54.⁶ For the age range 50–70 years, on an average, the risk factors are three times lower in this work compared with NHSBSP Report 54⁶ (for the same value of DDREF), causing a proportionate increase in the ratio of the number of cancers detected to the number of radiation-induced cancers.

Secondly, the cancer detection rates in this work are 1.05 times higher in this work than that in the NHSBSP Report 54.⁶

Finally, the MGD used is lower in the presented work than that in NHSBSP Report 54,⁶ causing a decrease in the number of radiation-induced cancers, and therefore an increase in the ratio of the number of detected cancers to radiation-induced cancers. In NHSBSP Report 54,⁶ an MGD of 4.5 mGy was assumed for the whole population and an MGD of 7 mGy was assumed for the subgroup of the population with breasts of thicknesses of 90 mm and above. This compares with 3 and 5 mGy for the whole population and the subgroup with the largest breasts in the present work. This is due to the switch from film-screen to digital mammography systems and due to the adoption of higher energy X-ray spectra. Young and Oduko²⁴ found that the average MGD for a two-view examination using digital radiography mammography systems is about 25% lower than that for film screen. It should be noted that specific manufacturer designs can lead to consistently higher or lower doses than this average.

Some females require multiple images per breast. Young and Oduko²⁴ estimated that 1.6% of females had one extra image per view and 0.4% of females had two extra images per view. This may be due to repositioning, reacquisition owing to the quality

of the image or “tiling” to image the entire breast. The additional dose will depend on the area of overlap of the images of the breast. As a worst-case scenario, one could assume that these females who have two extra images per view have the largest breasts (>90 mm) and the entire breast is imaged twice, doubling the dose. As seen in Table 3, this causes the ratio of lives saved owing to screening to lives lost owing to radiation-induced breast cancers for this group of females to reduce from 94 : 1 to 47 : 1. In reality, it is unlikely that the entire breast will be imaged twice, only part of it and therefore, the ratio for these females will be somewhere between these two values.

It is assumed in this work that the survival of a female from radiation-induced breast cancer was the same as that of a female with the average of screen-detected and symptomatic cancers. If instead the survival of a female from radiation-induced breast cancer was the same as that of a female with a screen-detected cancer or symptomatic cancer, the ratio of the lives saved to lived lost ranges from 125 : 1 to 208 : 1 for a DDREF of 1. In reality, the ratio will be somewhere between these two values, because for some females, the radiation-induced cancers will be detected whilst they are still participating in the screening programme and for others, the cancer will be detected at ages beyond the screening programme.

For the results presented, the average breast cancer detection rates from national breast screening statistics for 2013–14²³ were used for the age ranges considered. Alternatively, the detection rate at the age for each screening round has also been used, found by interpolating the data given in the 2013–14 breast screening statistics.²³ The calculations have been performed both ways (not presented) and the results did not change between methods. Therefore, the average detection rates were used to improve the readability of the article.

It was found in our analysis that around 240 females needed to be screened in 7 screening rounds between the ages of 50 and 70 years to save a life. Tabar *et al*³² estimated that 414 females would need to be screened every 2–3 years for 7 years to save a life. This corresponds to 145 females screened every 2–3 years for 20 years between the ages of 50 and 70 years to save a life. The difference in estimates is likely to be due to the difference between the mortality rate at the time of the Swedish Two-County Trial and the more recent estimate used in our calculations.

In this work, the number of females who must be screened in all screening rounds to save a life and the number of females attending all screening rounds per radiation-induced breast cancer death were higher for the age range 50–70 years than that for the age range 47–73 years. This is due to the greater number of screening rounds attended in the age range 47–73 years—more cancers were detected, but the total radiation dose received by the females was higher.

Marmot et al¹¹ found that inviting females aged 50–70 every 3 years prevents around 1300 breast cancer deaths a year. This difference is likely to be due to the uncertainty associated with estimating the amount of overdiagnosis and the mortality rate of the symptomatic cancers. If overdiagnosis were 5% rather than 19%, the overdiagnosis would increase from 1071 to 1256 lives saved per year. If the mortality rate were to increase from 24 to 28%, this would increase the number of lives saved per year from 1071 to 1249.

A limitation of this work is that only the number of lives saved owing to screening and lives lost owing to radiation-induced cancers has been considered and not the number of life-years gained or lost. Estimating the number of life-years saved or gained would take into account that deaths due to induced cancers are likely on an average to occur later than the deaths prevented by screening. The ratios of lives saved owing to screening to the number of lives lost owing to radiation-induced cancers can be calculated for each screening round. For the screening rounds at age 48 and 72 years, these ratios are 76 : 1 and 500 : 1, respectively, for a DDREF of 1. However, if life-years gained were to be compared for these two screening ages, this difference is likely to reduce.

An additional limitation of this work is that the additional radiation exposure due to mammography at assessment was not considered. However, the average percentage of females recalled for further imaging in the NHSBSP is only about 4%.²³ Since repeat imaging is usually more limited than the original screening, the increase in the population dose due to assessment mammography is likely to be <4%.

There are several different radiation risk models available. In this work, the EAR model used by ICRP 103 has been used. Analyzing the same data using the EAR model by Berrington de Gonzalez et al⁴¹ instead (adaptations of the BEIR VII model) caused no change to the ratio of lives saved owing to screening to the lives lost owing to radiation-induced breast cancers. A larger difference would be expected if an ERR model were to be used instead of an EAR model. However, the authors feel that the use of an EAR model is more appropriate, as discussed earlier in this article.

UK data indicate that the radiation dose in mammography has decreased significantly with the advent of digital mammography. The benefit of reducing the dose further should be balanced against the possible resultant change in cancer detection when optimizing a mammography system.

CONCLUSION

For a breast cancer mortality reduction of 20% to the population invited to screening in England, the number of deaths caused by radiation-induced cancers is estimated to be around 150 times smaller than the number of lives saved owing to screening.

ACKNOWLEDGMENTS

The authors would like to acknowledge the help of Dr Jennifer Oduko, for her assistance with patient dose data for the article. The authors would like to thank Dr Matthew Wallis for his feedback on the detection rates and mortality rates used in the article and Professor Sue Moss for her feedback and advice on the analysis performed. Finally, the authors would like to thank the associate editor of BJR for his or her suggested improvements to the article.

FUNDING

One of the authors (KCY) was funded by the National Office of the NHS Cancer Screening Programmes (now within the Health and Wellbeing Directorate of Public Health England). The other authors (LMW and DRD) were funded as part of OPTIMAM2 research programme funded by Cancer Research UK.

REFERENCES

1. ISRCTN registry. Nationwide cluster-randomised trial of extending the NHS breast screening age range in England. Available from: <http://www.controlled-trials.com/ISRCTN33292440>
2. Yaffe MJ, Mainprize JG. Risk of radiation-induced breast cancer from mammographic screening. *Radiology* 2011; **258**: 98–105. doi: <http://dx.doi.org/10.1148/radiol.10100655>
3. Hendrick RE, Helvie MA. Mammography screening: a new estimate of number needed to screen to prevent one breast cancer death. *AJR Am J Roentgenol* 2012; **198**: 723–8. doi: <http://dx.doi.org/10.2214/AJR.11.7146>
4. Mattsson A, Leitz W, Rutqvist LE. Radiation risk and mammographic screening of women from 40 to 49 years of age: effect on breast cancer rates and years of life. *Br J Cancer* 2000; **82**: 220–6. doi: <http://dx.doi.org/10.1054/bjoc.1999.0903>
5. Hauge IH, Pedersen K, Olerud HM, Hole EO, Hofvind S. The risk of radiation-induced breast cancers due to biennial mammographic screening in women aged 50–69 years is minimal. *Acta Radiol* 2014; **55**: 1174–9. doi: <http://dx.doi.org/10.1177/0284185113514051>
6. Joint working party of the NHSBSP National Coordinating Group for Physics Quality Assurance and the National Radiological Protection Board. NHSBSP publication no 54: review of radiation risk; 2003. ISBN: 1-871997-99-2.
7. Berrington de González A, Reeves G. Mammographic screening before age 50 years in the UK: comparison of the radiation risks with the mortality benefits. *Br J Cancer* 2005; **93**: 590–6. doi: <http://dx.doi.org/10.1038/sj.bjc.6602683>
8. Independent Advisory Group on Ionising Radiation. *Risk of solid cancers following radiation exposure: estimates for the UK population*: Health Protection Agency; 2011. ISBN: 978-0-85951-705-8.
9. Dance DR, Skinner CL, Young KC, Beckett JR, Kotre CJ. Additional factors for the estimation of mean glandular breast dose using the UK

- mammography dosimetry protocol. *Phys Med Biol* 2000; **45**: 3225–40. doi: <http://dx.doi.org/10.1088/0031-9155/45/11/308>
10. Young KC, Burch A, Oduko JM. Radiation doses received in the UK breast screening programme in 2001 and 2002. *Br J Radiol* 2005; **78**: 207–18. doi: <http://dx.doi.org/10.1259/bjr/41095952>
 11. Marmot MG, Altman DG, Cameron DA, Dewar JA, Thompson SG, Wilcox M and The independent UK panel on Breast Cancer Screening. The benefits and harms of breast cancer screening: an independent review. *Br J Cancer* 2013; **108**: 2205–40. doi: <http://dx.doi.org/10.1038/bjc.2013.177>
 12. Preston DL, Mattsson A, Holmberg E, Shore R, Hildreth NG, Boice JD Jr. Radiation effects on breast cancer risk: a pooled analysis of eight cohorts. *Radiat Res* 2002; **158**: 220–35. doi: [http://dx.doi.org/10.1667/0033-7587\(2002\)158\[0220:REOBCR\]2.0.CO;2](http://dx.doi.org/10.1667/0033-7587(2002)158[0220:REOBCR]2.0.CO;2)
 13. Preston DL, Mattsson A, Holmberg E, Shore R, Hildreth NG, Boice JD Jr. ERRATA: Radiation effects on breast cancer risk: a pooled analysis of eight cohorts. *Radiat Res* 2002; **158**: 666. doi: [http://dx.doi.org/10.1667/0033-7587\(2002\)158\[0666:E\]2.0.CO;2](http://dx.doi.org/10.1667/0033-7587(2002)158[0666:E]2.0.CO;2)
 14. Law J, Faulkner K, Young KC. Risk factors for induction of breast cancer by X-rays and their implications for breast screening. *Br J Radiol* 2007; **80**: 261–6. doi: <http://dx.doi.org/10.1259/bjr/20496795>
 15. Committee to Assess Health Risks from Exposure to Low Levels of Ionizing Radiation. Health Risks from Exposure to Low Levels of Ionizing Radiation: BEIR VII—Phase 2 2006. DOI: 10.17226/11340.
 16. The International Commission on Radiological Protection. Annuals of the ICRP. Publication 103. The 2007 Recommendations of the International Commission on Radiological Protection; 2007. ISBN: 978-0-7020-3048-2.
 17. United Nations Scientific Committee on the Effects of Atomic Radiation. Effects of Ionizing Radiation. 2008. ISBN: 978-92-1-142263-4.
 18. US Environmental Protection Agency. *EPA Radiogenic cancer risk models and projections for the US population*; 2011. EPA 402-R-11-001.
 19. Land CE, Boice JD Jr, Shore RE, Norman JE, Tokunaga M. Breast cancer risk from low-dose exposures to ionizing radiation: results of parallel analysis of three exposed populations of women. *J Natl Cancer Inst* 1980; **65**: 353–76. doi: <http://dx.doi.org/10.1093/jnci/65.2.353>
 20. Wall BF, Haylock R, Jansen JTM, Hillier MC, Hart D, Scrimpton PC. *HPA-CRCE-028: Radiation risks from medical X-ray examinations as a function of the age and sex of the patient*: Health Protection Agency; 2011. ISBN: 978-0-85951-709-6.
 21. Heyes GJ, Mill AJ, Charles MW. Mammography-oncogenecity at low doses. *J Radiol Prot* 2009; **29**: A123–32. doi: <http://dx.doi.org/10.1088/0952-4746/29/2A/S08>
 22. US Environmental Protection Agency. *Estimating radiogenic cancer risks*; 1994. EPA 402-R-93-076.
 23. National Statistics. Breast Screening Programme. England—2013–14; 2014. Available from: <http://www.hscic.gov.uk/catalogue/PUB16803>
 24. Young KC, Oduko JM. Radiation doses received in the United Kingdom breast screening programme in 2010 to 2012. *Br J Radiol* 2016; **89**: 20150831. doi: <http://dx.doi.org/10.1259/bjr.20150831>
 25. Puliti D, Duffy SW, Miccinesi G, de Koning H, Lynge E, Zappa M, et al. Overdiagnosis in mammographic screening for breast cancer in Europe: a literature review. *J Med Screen* 2012; **19**(Suppl. 1): 42–56. doi: <http://dx.doi.org/10.1258/jms.2012.012082>
 26. NHS Cancer Screening Programmes. National collation of breast interval cancer data: screening years 1st April 2003–31st March 2005. NHSBSP Occasional Report 1203; 2005. ISBN: 978-1-84463-089-9.
 27. Duffy SW, Parmar D. Overdiagnosis in breast cancer screening: the importance of length of observation period and lead time. *Breast Cancer Res* 2013; **15**: R41. doi: <http://dx.doi.org/10.1186/bcr3427>
 28. Gotzsche PC, Nielsen M. Screening for breast cancer with mammography. *Cochrane Database Syst Rev* 2011; **1**: CD001877. DOI:<http://dx.doi.org/10.1002/14651858.CD001877.pub5>
 29. Nelson HD, Tyne K, Naik A, Bougatso C, Chan BK, Humphrey L. Screening for breast cancer: an update for the U.S. Preventive Services Task Force. *Ann Intern Med* 2009; **151**: 727–37. doi: <http://dx.doi.org/10.7326/0003-4819-151-10-200911170-00009>
 30. Canadian Task Force on Preventive Health Care; Tonelli M, Connor Gorber S, Joffres M, Dickinson J, Singh H, Lewin G, et al. Recommendations on screening for breast cancer in average-risk women aged 40–74 years. *CMAJ* 2011; **183**: 1991–2001. doi: <http://dx.doi.org/10.1503/cmaj.110334>
 31. Demissie K, Mills OF, Rhoads GG. Empirical comparison of the results of randomized controlled trials and case-control studies in evaluating the effectiveness of screening mammography. *J Clin Epidemiol* 1998; **51**: 81–91. doi: [http://dx.doi.org/10.1016/S0895-4356\(97\)00243-6](http://dx.doi.org/10.1016/S0895-4356(97)00243-6)
 32. Tabár L, Vitak B, Chen TH, Yen AM, Cohen A, Tot T, et al. Swedish two-county trial: impact of mammographic screening on breast cancer mortality during 3 decades. *Radiology* 2011; **260**: 658–63. doi: <http://dx.doi.org/10.1148/radiol.11110469>
 33. Broeders M, Moss S, Nyström L, Njor S, Jonsson H, Paap E, et al; EUROSREEN Working Group. The impact of mammographic screening on breast cancer mortality in Europe: a review of observational studies. *J Med Screen* 2012; **19**: 14–25. doi: <http://dx.doi.org/10.1258/jms.2012.012078>
 34. Weedon-Fekjær H, Romundstad PR, Vatten LJ. Modern mammography screening and breast cancer mortality: population study. *BMJ* 2014; **348**: g3701. doi: <http://dx.doi.org/10.1136/bmj.g3701>
 35. Lauby-Secretan B, Scoccianti C, Loomis D, Benbrahim-Tallaa L, Bouvard V, Bianchini F, et al. Breast cancer screening—Viewpoint of the IARC working group. *N Engl J Med* 2015; **373**: 2353–8. doi: <http://dx.doi.org/10.1056/NEJMs1504363>
 36. Nyström L, Bjurstram N, Jonsson H, Zackrisson S, Frisell J. Reduced breast cancer mortality after 20+ years of follow-up in the Swedish randomized controlled mammography trials in Malmö, Stockholm, and Göteborg. *J Med Screen* 2016. DOI: <http://dx.doi.org/10.1177/0969141316648987>, (<http://msc.sagepub.com/content/early/2016/06/15/0969141316648987.abstract>)
 37. Duffy SW, Yen Ming-Fang A, Chen TH, Chen SL, Chui SY, Fan JJ, et al. Long-term benefits of breast screening. *Breast Cancer Manage* 2012; **1**: 31–8. doi: <http://dx.doi.org/10.2217/bmt.12.8>
 38. Mook S, Van't Veer LJ, Rutgers EJ, Ravdin PM, van de Velde AO, van Leeuwen FE, et al. Independent prognostic value of screen detection in invasive breast cancer. *J Natl Cancer Inst* 2011; **103**: 585–97. doi: <http://dx.doi.org/10.1093/jnci/djr043>
 39. Duffy SW, Tabar L, Olsen AH, Vitak B, Allgood PC, Chen TH, et al. Absolute numbers of lives saved and overdiagnosis in breast cancer screening, from a randomized trial and from the Breast Screening Programme in England. *J Med Screen* 2010; **17**: 25–30. doi: <http://dx.doi.org/10.1258/jms.2009.009094>
 40. National Radiological Protection Board. Estimates of late radiation risks to the UK population. Doc NRPB 1993; **4**: 15–157.
 41. Berrington de Gonzalez A, Iulian Apostoaei A, Veiga LH, Rajaraman P, Thomas BA, Owen Hoffman F, et al. RadRAT: a radiation risk assessment tool for lifetime cancer risk projection. *J Radiol Prot* 2012; **32**: 205–22. doi: <http://dx.doi.org/10.1088/0952-4746/32/3/205>

APPENDIX A

Derivation of number of lives saved owing to screening per year

The number of cancers in the invited population is given by:

$$T_T = T_{SC} + T_{SOD} + T_I + T_{NS}, \quad (A1)$$

where T_{SC} is the number of screen-detected cancers, which are not overdiagnosed, T_{SOD} is the number of screen-detected cancers, which are overdiagnosed, T_I is the number of interval cancers and T_{NS} is the number of cancers detected in non-attendees.

The number of cancers detected in the non-attendees is related to the proportion of females accepting the screening invitation f according to:

$$T_{NS} = (T_{SC} + T_I) \frac{(1-f)}{f}. \quad (A2)$$

The number of deaths in the invited population ($D_{Invited}$) and the number of deaths in the same population when not invited to screening ($D_{NotInvited}$) are given in Equations (A3) and (A4), where M_{SC} and M_{NS} are the mortality rates for females with screen-detected and symptomatic cancers.

$$D_{Invited} = M_{SC}T_{SC} + M_{NS}(T_I + T_{NS}), \quad (A3)$$

$$D_{NotInvited} = M_{NS}(T_{SC} + T_I + T_{NS}). \quad (A4)$$

The mortality reduction to the invited population (r) is given by:

$$r = 1 - \frac{D_{Invited}}{D_{NotInvited}}. \quad (A5)$$

Substituting (A3) and (A4) into (A5) and rearranging gives:

$$M_{SC} = \frac{M_{NS}}{T_{SC}} [(1-r)T_{SC} - r(T_I + T_{NS})]. \quad (A6)$$

The number of lives saved is given by the following equation:

$$\text{Lives saved} = (M_{NS} - M_{SC})T_{SC}. \quad (A7)$$

Substituting (A2) and (A6) into (A7) gives:

$$\text{Lives saved} = M_{NS}r \frac{(T_{SC} + T_I)}{f}.$$



Mobile Digital Mammography takes to the road

In collaboration with Lamboo Mobile Medical we are offering the MAMMOMAT Revelation on a mobile medical trailer

50° Wide-Angle Tomosynthesis

Detect even the smallest lesions that are no longer hidden by overlying breast tissue.

50° Wide-Angle Biopsy

Target accuracy of ± 1 mm based on 50° wide-angle tomosynthesis.

Personalised Soft Compression

Increase patient comfort and achieve consistent image quality.

Breast Density Assessment

100% objective, volumetric breast density assessment for instant risk stratification directly at the acquisition workstation before the patient leaves.

InSpect – Integrated Specimen Imaging

Get your specimen scan within just 20 seconds on the mammography system. Allowing you to stay with your patient during the entire examination and decompress your patient sooner.

For further information contact

joanne.barry@siemens-healthineers.com

[siemens-healthineers.co.uk/revelation](https://www.siemens-healthineers.co.uk/revelation)

